

Higher order QCD corrections to the transverse and longitudinal fragmentation functions in electron-positron annihilation

P.J. Rijken and W.L. van Neerven

Instituut-Lorentz
University of Leiden
P.O. Box 9506
2300 RA Leiden
The Netherlands

September 1996

Abstract

We present the calculation of the order α_s^2 corrections to the coefficient functions contributing to the longitudinal ($F_L(x, Q^2)$) and transverse fragmentation functions ($F_T(x, Q^2)$) measured in electron-positron annihilation. The effect of these higher order QCD corrections on the behaviour of the fragmentation functions and the corresponding longitudinal ($d\sigma_L(x, Q^2)/dx$) and transverse cross sections ($d\sigma_T(x, Q^2)/dx$) are studied. In particular we investigate the dependence of the above quantities on the mass factorization scale (M) and the various parameterizations chosen for the parton fragmentation densities $D_p^H(x, M^2)$ ($p = q, g; H = \pi^\pm, K^\pm, P, \bar{P}$). Our analysis reveals that the order α_s^2 contributions to $F_L(x, Q^2)$ are large whereas these contributions to $F_T(x, Q^2)$ are small. From the above fragmentation functions one can also compute the integrated cross sections σ_L and σ_T in an independent way. The

sum $\sigma_{\text{tot}} = \sigma_L + \sigma_T$, corrected up to order α_s^2 , agrees with the well known result in the literature providing us with an independent check on our calculations.

1 Introduction

Semi-leptonic processes represented by electron-positron annihilation into hadrons, deep inelastic lepton-hadron scattering and the Drell-Yan process have provided us with the most valuable testing grounds for perturbative quantum chromodynamics (QCD). Perturbative calculations in next-to-leading order, and in some cases even to higher order, give a good explanation of numerous quantities measured in various experiments [1]. The reason for these successes originates from the experimental as well as theoretical characteristics of the above reactions. From the experimental viewpoint semi-leptonic reactions provide us with an overwhelming amount of data and in the case of electron-positron annihilation into hadrons and deep inelastic lepton-hadron scattering the background is fully under control. Therefore the systematical and statistical errors are very small. From the theoretical viewpoint we want to mention the following features. First, the Born approximation to semi-leptonic cross sections is of purely electroweak origin so that it is independent of the strong coupling constant α_s . Since the electroweak standard model is tested up to about a few promille by the LEP1-experiments [2] each deviation from the Born approximation is due to the strong interactions. Second, if one limits oneself to the computation of semi-inclusive or inclusive quantities, like structure functions or total cross sections, the final hadronic state is completely integrated over and we do not have to care about problems as jet definition or hadronization effects. The third feature is that it is possible to extend the calculation of the QCD corrections to the above integrated quantities beyond next-to-leading order. Examples are the order α_s^2 contributions to the coefficient functions corresponding to the Drell-Yan cross section $d\sigma/dQ^2$ [3] and the deep inelastic structure functions $F_k(x, Q^2)$ [6] where Q^2 denotes the virtuality of the electroweak vector bosons γ, Z, W . Order α_s^3 corrections are even known for sum rules $\int_0^1 dx x^{n-1} F_k(x, Q^2)$ ($n \leq 10$) [8] and the total cross section $\sigma_{\text{tot}}(e^+e^- \rightarrow \text{“hadrons”})$ [11]. The reason that these higher order corrections are much easier to compute than those encountered in e.g. hadron-hadron collisions (except for the Drell-Yan process) can be attributed to the simplicity of the phase space integrals and the virtual corrections appearing in semi-leptonic processes. Moreover if one integrates in the latter processes over the total hadronic state one can use alternative methods to evaluate the Feynman diagrams (see e.g. [16]), which are not applicable to hadron-hadron reactions or to more exclusive semi-leptonic processes. In the past the order α_s^2 contributions to the coefficient functions have been calculated for the Drell-Yan cross section $d\sigma/dQ^2$ [3] and the deep inelastic structure functions $F_k(x, Q^2)$ [6]. However the same corrections were not computed for the fragmentation functions showing up in the process $e^+e^- \rightarrow H + \text{“X”}$ where H is the detected hadron ($H = \pi^\pm, K^\pm, P, \bar{P}$) and “X” stands for any inclusive hadronic state. These corrections are needed because of the large amount of data which have collected over the past ten years. The above process has been studied over a wide range of energies of many different e^+e^- -colliders. Data have been collected from DASP ($\sqrt{s} = 5.2$ GeV) [18], ARGUS ($\sqrt{s} = 10$ GeV) [19], TASSO ($\sqrt{s} = 22, 35, 45$ GeV) [20], MARK II [22] and TPC/ 2γ ($\sqrt{s} = 29$ GeV) [23], CELLO ($\sqrt{s} = 35$ GeV) [24], AMY ($\sqrt{s} = 55$ GeV) [25] and the LEP experiments DELPHI [27], ALEPH [28],

OPAL [30, 32] ($\sqrt{s} = 91.2$ GeV). In particular the last two experiments found a discrepancy between the measured longitudinal fragmentation function $F_L(x, Q^2)$ and its theoretical prediction computed up to order α_s . We want to fill in this gap in our knowledge by presenting the order α_s^2 contributions to the longitudinal ($F_L(x, Q^2)$) and transverse fragmentation ($F_T(x, Q^2)$) functions and discuss their phenomenological implications. The coefficient functions corrected up to order α_s^2 are already computed for $F_L(x, Q^2)$ and can be found in recent work [33]. Here we want to add the order α_s^2 contributions to the coefficient functions corresponding to $F_T(x, Q^2)$ which are much more complicate. The order α_s^2 corrections to the asymmetric fragmentation function will be postponed to a future publication. Although a complete next-to-next-to-leading (NNLO) order analysis of the transverse (and also asymmetric) fragmentation function is not possible, since we do not know the three-loop order timelike DGLAP [34] splitting functions, one can still study the effect of the order α_s^2 corrected coefficient functions. Furthermore one can obtain the transverse cross section σ_T for which analysis the DGLAP splitting functions are not needed so that the former is factorization scheme independent. The sum of the transverse (σ_T) and the longitudinal (σ_L) cross sections yield $\sigma_{\text{tot}}(e^+e^- \rightarrow \text{“hadrons”})$. It turns out that the σ_{tot} presented in this paper is in agreement with the order α_s^2 corrected result quoted in the literature [37] providing us with a very strong check on our calculations. This paper will be organized as follows. In section 2 we introduce our notations of the fragmentation functions and the corresponding cross sections. In section 3 we give an outline of the calculations of the parton subprocesses contributing to the process $e^+e^- \rightarrow H + \text{“X”}$ up to order α_s^2 . In section 4 we perform the renormalization and mass factorization of the partonic quantities providing us with the longitudinal and transverse coefficient functions. The discussion of our results will be presented in section 5 and a comparison with data coming from recent and past experiments on electron-positron annihilation will be made. The long expressions obtained for the order α_s^2 corrected coefficient functions are presented in the $\overline{\text{MS}}$ -scheme and the A-(annihilation) scheme in appendix A and appendix B respectively.

2 Single particle inclusive cross sections

In this paper we want to study the QCD corrections to the single particle inclusive process

$$e^+ + e^- \rightarrow \gamma, Z \rightarrow H + \text{“}X\text{”}, \quad (2.1)$$

where “ X ” denotes any inclusive final hadronic state and H represents either a specific charged outgoing hadron or a sum over all charged hadron species. The unpolarized differential cross section of the above process is given by [40, 41]

$$\frac{d^2\sigma^H}{dx d\cos\theta} = \frac{3}{8}(1 + \cos^2\theta)\frac{d\sigma_T^H}{dx} + \frac{3}{4}\sin^2\theta\frac{d\sigma_L^H}{dx} + \frac{3}{4}\cos\theta\frac{d\sigma_A^H}{dx}. \quad (2.2)$$

The Björken scaling variable x is defined by

$$x = \frac{2pq}{Q^2}, \quad q^2 = Q^2 > 0, \quad 0 < x \leq 1, \quad (2.3)$$

where p and q are the four-momenta of the produced particle H and the virtual vector boson (γ, Z) respectively. In the centre of mass (CM) frame of the electron-positron pair the variable x can be interpreted as a fraction of the total CM energy carried away by the hadron H . The variable θ denotes the angle of emission of particle H with respect to the electron beam direction in the CM frame. The transverse, longitudinal and asymmetric cross sections in (2.2) are defined by σ_T^H , σ_L^H , and σ_A^H respectively. The latter only shows up if the intermediate vector boson is given by the Z -boson and is absent in purely electromagnetic annihilation.

In the QCD improved parton model which describes the production of the parton denoted by p and its subsequent fragmentation into hadron H , the cross sections σ_k^H ($k = T, L, A$) can be expressed as follows

$$\begin{aligned} \frac{d\sigma_k^H}{dx} = \int_x^1 \frac{dz}{z} \left[\sigma_{\text{tot}}^{(0)}(Q^2) \left\{ D_S^H\left(\frac{x}{z}, M^2\right) \mathbb{C}_{k,q}^S(z, Q^2/M^2) + D_g^H\left(\frac{x}{z}, M^2\right) \right. \right. \\ \left. \left. \cdot \mathbb{C}_{k,g}^S(z, Q^2/M^2) \right\} + \sum_{p=1}^{n_f} \sigma_p^{(0)}(Q^2) D_{\text{NS},p}^H\left(\frac{x}{z}, M^2\right) \mathbb{C}_{k,q}^{\text{NS}}(z, Q^2/M^2) \right], \quad (2.4) \end{aligned}$$

for $k = T, L$. In the case of the asymmetric cross section we have

$$\frac{d\sigma_A^H}{dx} = \int_x^1 \frac{dz}{z} \left[\sum_{p=1}^{n_f} A_p^{(0)}(Q^2) D_{A,p}^H\left(\frac{x}{z}, M^2\right) \mathbb{C}_{A,q}^{\text{NS}}(z, Q^2/M^2) \right]. \quad (2.5)$$

In the formulae (2.4) and (2.5) we have introduced the following notations. The function $D_g^H(z, M^2)$ denotes the gluon fragmentation density corresponding to the hadron of species H . The same notation holds for the quark and anti-quark fragmentation densities which are given by $D_p^H(z, M^2)$ and $D_{\bar{p}}^H(z, M^2)$ respectively. Further we have

defined the singlet (S) and non-singlet (NS, A) combinations of quark fragmentation densities. They are given by

$$D_S^H(z, M^2) = \frac{1}{n_f} \sum_{p=1}^{n_f} (D_p^H(z, M^2) + D_{\bar{p}}^H(z, M^2)), \quad (2.6)$$

$$D_{\text{NS},p}^H(z, M^2) = D_p^H(z, M^2) + D_{\bar{p}}^H(z, M^2) - D_S^H(z, M^2), \quad (2.7)$$

$$D_{\text{A},p}^H(z, M^2) = D_p^H(z, M^2) - D_{\bar{p}}^H(z, M^2). \quad (2.8)$$

The index p stands for the quark species and n_f denotes the number of light flavours. Assuming that the charm and the bottom quark can be treated as massless we can put $n_f = 5$ and the indices $p = 1, 2, 3, 4, 5$ stand for $p = u, d, s, c, b$. Further the variable M appearing in $D_p^H(z, M^2)$ stands for the mass factorization scale which for convenience has been put equal to the renormalization scale. The pointlike cross section of the process

$$e^+ + e^- \rightarrow p + \bar{p}, \quad (2.9)$$

which shows up in (2.4) is equal to

$$\begin{aligned} \sigma_p^{(0)}(Q^2) = \frac{4\pi\alpha^2}{3Q^2} N \left[e_\ell^2 e_p^2 + \frac{2Q^2(Q^2 - M_Z^2)}{|Z(Q^2)|^2} e_\ell e_p C_{V,\ell} C_{V,p} + \frac{(Q^2)^2}{|Z(Q^2)|^2} \right. \\ \left. \cdot (C_{V,\ell}^2 + C_{A,\ell}^2)(C_{V,p}^2 + C_{A,p}^2) \right], \quad (2.10) \end{aligned}$$

$$\sigma_{\text{tot}}^{(0)}(Q^2) = \sum_{p=1}^{n_f} \sigma_p^{(0)}(Q^2), \quad (2.11)$$

with

$$Z(Q^2) = Q^2 - M_Z^2 + iM_Z\Gamma_Z. \quad (2.12)$$

Here N stands for the number of colours ($N = 3$) and M_Z, Γ_Z denote the mass and width of the Z -boson respectively. For the latter we have used the narrow width approximation. Furthermore we have neglected all quark masses in (2.10). The charges of the lepton and the up and down quarks are given by

$$e_\ell = -1, \quad e_u = \frac{2}{3}, \quad e_d = -\frac{1}{3}. \quad (2.13)$$

The vector- and axial-vector coupling constants of the Z -boson to the lepton and quarks are equal to

$$\begin{aligned} C_{A,\ell} &= \frac{1}{2 \sin 2\theta_W}, & C_{V,\ell} &= -C_{A,\ell} (1 - 4 \sin^2 \theta_W), \\ C_{A,u} &= -C_{A,d} = -C_{A,\ell}, & & \\ C_{V,u} &= C_{A,\ell} (1 - \frac{8}{3} \sin^2 \theta_W), & C_{V,d} &= -C_{A,\ell} (1 - \frac{4}{3} \sin^2 \theta_W), \end{aligned} \quad (2.14)$$

where θ_W denotes the Weinberg angle.

The electroweak coupling constants also appear in the asymmetry factor $A_p^{(0)}$ (2.5) which is given by

$$A_p^{(0)} = \frac{4\pi\alpha^2}{3Q^2} N \left[\frac{2Q^2(Q^2 - M_Z^2)}{|Z(Q^2)|^2} e_\ell e_p C_{A,\ell} C_{A,p} + 4 \frac{(Q^2)^2}{|Z(Q^2)|^2} C_{A,\ell} C_{A,p} C_{V,\ell} C_{V,p} \right]. \quad (2.15)$$

The QCD corrections in (2.4), (2.5) are described by the coefficient functions $\mathbb{C}_{k,\ell}^r$ ($k = T, L, A$; $\ell = q, g$) which can be distinguished with respect to the flavour group $SU(n_f)$ in a singlet ($r = S$) and a non-singlet part ($r = NS$). They depend on the factorization scale M and in order α_s^2 on the number of flavours n_f . As will be shown later on the gluonic coefficient function only receives contributions from flavour singlet channel partonic subprocesses so that we can drop the superscript S on \mathbb{C}_g . However the quark coefficient functions can be of flavour singlet as well as flavour non-singlet origin. Up to first order in the strong coupling constant α_s it turns out that $\mathbb{C}_{k,q}^{NS} = \mathbb{C}_{k,q}^S$. However in higher order both quantities start to deviate from each other. Hence we define the purely singlet coefficient function $\mathbb{C}_{k,q}^{PS}$ via

$$\mathbb{C}_{k,q}^S = \mathbb{C}_{k,q}^{NS} + \mathbb{C}_{k,q}^{PS}. \quad (2.16)$$

Like $\mathbb{C}_{k,g}$ the purely singlet coefficient function only receives contributions from the flavour singlet channel partonic subprocesses which for the first time show up in order α_s^2 .

Using charge conjugation invariance of the strong interactions one can show that $\mathbb{C}_{A,q}^{NS} = -\mathbb{C}_{A,\bar{q}}^{NS}$ and $\mathbb{C}_{A,q}^{PS} = \mathbb{C}_{A,g} = 0$. This implies that to σ_A^H (2.5) only non-singlet channel partonic subprocesses can contribute. Another important property of the coefficient function is that they do not depend on the probe γ or Z or on the electroweak couplings given in (2.13), (2.14) so that one can extract the overall pointlike cross section $\sigma_p^{(0)}$ (2.10) or the asymmetry factor $A_p^{(0)}$ (2.15). However this is only true if all quark masses are equal to zero and if one sums over all quark members in one family provided the latter appear in the inclusive state of the partonic subprocess (see section 4).

From (2.2) we can derive the total hadronic cross section

$$\sigma_{\text{tot}}(Q^2) = \frac{1}{2} \sum_H \int_0^1 dx \int_{-1}^1 d\cos\theta \left(x \frac{d^2\sigma^H}{dx d\cos\theta} \right) = \sigma_T(Q^2) + \sigma_L(Q^2), \quad (2.17)$$

with

$$\sigma_k(Q^2) = \frac{1}{2} \sum_H \int_0^1 dx x \frac{d\sigma_k^H}{dx}, \quad (k = T, L, A), \quad (2.18)$$

where one has summed over all types of outgoing hadrons H . Hence we obtain the result

$$\sigma_{\text{tot}}(Q^2) = R_{ee} \sigma_{\text{tot}}^{(0)}(Q^2), \quad (2.19)$$

where R_{ee} represents the QCD corrections to the pointlike total cross section $\sigma_{\text{tot}}^{(0)}(Q^2)$. At this moment the perturbation series of R_{ee} is already known up to order α_s^3 [11]. Up to order α_s^2 it reads [37]

$$R_{ee} = 1 + \frac{\alpha_s}{4\pi} C_F [3] + \left(\frac{\alpha_s}{4\pi}\right)^2 \left[C_F^2 \left\{ -\frac{3}{2} \right\} + C_A C_F \left\{ -11 \ln \frac{Q^2}{M^2} - 44\zeta(3) \right. \right. \\ \left. \left. + \frac{123}{2} \right\} + n_f C_F T_f \left\{ 4 \ln \frac{Q^2}{M^2} + 16\zeta(3) - 22 \right\} \right]. \quad (2.20)$$

In section 4 we also want to present the coefficient functions $\mathbb{C}_{k,\ell}$ up to order α_s^2 and show that they lead to the same R_{ee} as calculated in the literature (see section 5). Finally we also define the transverse, longitudinal and asymmetric fragmentation functions $F_k^H(x, Q^2)^*$

$$F_k^H(x, Q^2) = \frac{1}{\sigma_{\text{tot}}^{(0)}(Q^2)} \frac{d\sigma_k^H}{dx}, \quad k = (T, L, A). \quad (2.21)$$

Further the total fragmentation function is given by

$$F^H(x, Q^2) = F_L^H(x, Q^2) + F_T^H(x, Q^2). \quad (2.22)$$

In the case the virtual photon dominates the annihilation process (2.1) one observes that, apart from the charge squared e_p^2 in (2.10) ($p = u, d$), the above structure functions are just the timelike photon analogues of the ones measured in deep inelastic electron-proton scattering. When the Z -boson contributes we will define in section 4 for each combination of the electroweak coupling constants in (2.10) a separate structure function. However for the discussion of our results in section 5 this distinction will not be needed.

*Notice that we make a distinction in nomenclature between the fragmentation densities D_p^H and the fragmentation functions F_k^H .

3 Fragmentation coefficient functions in $e^+ e^-$ annihilation up to order α_s^2

In this section we will give an outline of the calculation of the order α_s^2 corrections to the fragmentation coefficient functions. The procedure is analogous to the one presented for the calculation of the Drell-Yan process in [3] and the deep inelastic lepton-hadron reaction in [6]. The coefficient functions originate from the following reaction

$$V(q) \rightarrow "p(k_0)" + p_1(k_1) + p_2(k_2) + \dots + p_\ell(k_\ell), \quad (3.1)$$

where $V = \gamma, Z$ and "p" denotes the detected parton which fragments into the hadron H . The process (3.1) is inclusive with respect to the partons p_i ($i = 1, 2, \dots, \ell$) so that one has to integrate over all momenta indicated by k_i . Notice that the first part of reaction (2.1) i.e. $e^+ e^- \rightarrow V$ is not relevant for the determination of the coefficient function.

Up to order α_s^2 all parton subprocesses represented by (3.1) are listed in table 1. From the amplitude $M_\mu(\ell)$ describing process (3.1) one obtains the parton structure tensor (indicated by a hat)

$$\hat{W}_{\mu\nu}^{(V,V')}(p, q) = \frac{z^{n-3}}{4\pi} \sum_{\ell=1}^{\infty} \int \text{dPS}^{(\ell)} M_\mu^V(\ell) M_\nu^{V'}(\ell)^*. \quad (3.2)$$

Here $\int \text{dPS}^{(k)}$ denotes the k -body phase space integral defined by

$$\int \text{dPS}^{(\ell)} = \left\{ \prod_{j=1}^{\ell} \int \frac{d^n k_j}{(2\pi)^{n-1}} \delta^+(k_j^2) \right\} (2\pi)^n \delta^{(n)}(q - k_0 - \prod_{i=1}^{\ell} k_i), \quad (3.3)$$

$$\delta^+(k_j^2) = \theta(k_j^0) \delta(k_j^2), \quad (3.4)$$

and μ and ν stand for the Lorentz indices of the vector bosons V and V' respectively with $V = \gamma, Z$ and $V' = \gamma, Z$. Further we have defined the partonic scaling variable

$$z = \frac{2k_0 q}{Q^2}, \quad (3.5)$$

and the factor z^{n-3} in (3.2) originates from the n -dimensional phase space of the detected parton p (3.1). It appears in the definition of the cross sections $d\hat{\sigma}_{k,p}/dz$ which are the partonic analogues of the hadronic cross sections in (2.2). The former are proportional to the functions $\hat{\mathcal{F}}_{k,p}$ defined below.

To regularize the ultraviolet (U), infrared(IR) and collinear (C) divergences showing up in expression (3.2) we have chosen the method of n -dimensional regularization. Therefore the phase space integral in (3.3) is generalized to n dimensions so that the above divergences show up as pole terms of the type $(1/\varepsilon)^m$ with $\varepsilon = n - 4$. The calculation of the matrix elements $M_\mu(k) M_\nu(k)^*$ was performed in n dimensions using the algebraic manipulation program FORM [42]. After having computed the traces we have to integrate the matrix elements over all internal loop and final state

momenta where the momentum k_0 of the detected parton is kept fixed. In this paper we take all partons to be massless. The case of massive quarks is discussed in [40] where their contributions are presented up to order α_s .

The parton structure tensor in (3.2) can be also written as

$$\hat{W}_{\mu\nu}^{(V,V')}(k_0, q) = \frac{1}{4\pi} \sum_{\ell=1}^{\infty} \int \text{dPS}^{(\ell)} \langle 0 | \hat{J}_\mu^{(V)}(0) | p, \{p_\ell\} \rangle \langle p, \{p_\ell\} | \hat{J}_\nu^{(V')}(0) | 0 \rangle, \quad (3.6)$$

where $\hat{J}_\mu^{(V)}$ is the electroweak partonic current corresponding to the vector boson V . Using Lorentz covariance and CP invariance (3.6) can be written as follows

$$\begin{aligned} \hat{W}_{\mu\nu}^{(V,V')}(k_0, q) = & (v_{q_1}^{(V)} v_{q_2}^{(V')} + a_{q_1}^{(V)} a_{q_2}^{(V')}) \left[(k_{0\mu} - \frac{k_0 q}{q^2} q_\mu) (k_{0\nu} - \frac{k_0 q}{q^2} q_\nu) \frac{q^4}{(k_0 q)^3} \right. \\ & \cdot \hat{\mathcal{F}}_{L,p}(z, Q^2) - \left(g_{\mu\nu} - \frac{1}{k_0 q} (k_0^\mu q^\nu + q^\mu k_0^\nu) + \frac{q^2}{(k_0 q)^2} k_{0\mu} k_{0\nu} \right) \frac{q^2}{2k_0 q} \\ & \left. \cdot \hat{\mathcal{F}}_{T,p}(z, Q^2) \right] - (v_{q_1}^{(V)} a_{q_2}^{(V')} + a_{q_1}^{(V)} v_{q_2}^{(V')}) i \epsilon_{\mu\nu\alpha\beta} k_0^\alpha q^\beta \frac{q^2}{2(k_0 q)^2} \hat{\mathcal{F}}_{A,p}(z, Q^2). \quad (3.7) \end{aligned}$$

We will call $\hat{\mathcal{F}}_{k,p}(z, Q^2)$ ($p = q, g$) the parton fragmentation functions which describe the Born reaction plus the higher order QCD corrections represented by the parton subprocesses in table 1. The vector and axial-vector couplings of the quark q interacting with the vector boson V are given by $v_q^{(V)}$ and $a_q^{(V)}$ respectively. In the standard model they read

$$\begin{aligned} v_u^{(\gamma)} &= \frac{2}{3}, & a_u^{(\gamma)} &= 0, \\ v_d^{(\gamma)} &= -\frac{1}{3}, & a_d^{(\gamma)} &= 0, \\ v_u^{(Z)} &= \frac{1}{2} - \frac{4}{3} \sin^2 \theta_W, & a_u^{(Z)} &= \frac{1}{2}, \\ v_d^{(Z)} &= -\frac{1}{2} + \frac{2}{3} \sin^2 \theta_W, & a_d^{(Z)} &= -\frac{1}{2}. \end{aligned} \quad (3.8)$$

As we have already mentioned in section 2 below (2.16) in the case of massless quarks the electroweak factors can be completely factorized out of the radiative corrections according to (3.7) so that $\hat{\mathcal{F}}_{k,p}$ ($k = T, L, A$) do not depend on them. Therefore we can also put them all equal to $1/\sqrt{2}$ without affecting the parton fragmentation functions. Hence the latter are obtained via the following projections

$$\hat{\mathcal{F}}_{T,p}(z, Q^2) = \frac{1}{n-2} \left(-\frac{2k_0 q}{q^2} \hat{W}^\mu{}_\mu - \frac{2}{k_0 q} k_0^\mu k_0^\nu \hat{W}_{\mu\nu} \right), \quad (3.9)$$

$$\hat{\mathcal{F}}_{L,p}(z, Q^2) = \frac{1}{k_0 q} k_0^\mu k_0^\nu \hat{W}_{\mu\nu}, \quad (3.10)$$

$$\hat{\mathcal{F}}_{A,p}(z, Q^2) = -\frac{2}{q^2} \frac{1}{(n-2)(n-3)} i \epsilon^{\mu\nu\alpha\beta} k_{0\alpha} q_\beta \hat{W}_{\mu\nu}, \quad (3.11)$$

where according to the prescription in [43] we have contracted the Levi-Civita tensors $\epsilon^{\mu\nu\alpha\beta}$ in n -dimensions. In this paper we will compute the transverse and longitudinal fragmentation functions only and leave the calculation of the asymmetric fragmentation to a future publication. The computation of the latter involves the prescription of the γ_5 -matrix and the Levi-Civita tensor in n -dimensions which is quite intricate. We will now discuss the QCD corrections order by order in perturbation theory. In zeroth order in α_s (see fig. 2) we obtain the simple parton model results

$$\hat{\mathcal{F}}_{T,q}^{(0)} = \delta(1-z), \quad \hat{\mathcal{F}}_{T,g}^{(0)} = 0; \quad \hat{\mathcal{F}}_{L,q}^{(0)} = \hat{\mathcal{F}}_{L,g}^{(0)} = 0. \quad (3.12)$$

The first order corrections denoted by $\hat{\mathcal{F}}_{k,i}^{(1)}$ ($k = T, L; i = q, g$) have been calculated in the literature [44, 45]. In the case of n -dimensional regularization they are computed up to finite terms in the limit $\varepsilon \rightarrow 0$ and can be found in [40, 45]. Since the mass factorization has to be carried out up to order α_s^2 one also needs those terms in $\hat{\mathcal{F}}_{k,i}^{(1)}(z, Q^2, \varepsilon)$ which are proportional to ε . Therefore we have repeated the calculation of the graphs in fig. 3 and 4 and the results can be presented in the following form

$$\hat{\mathcal{F}}_{L,q}^{(1)} = \left(\frac{\hat{\alpha}_s}{4\pi}\right) S_\varepsilon \left(\frac{Q^2}{\mu^2}\right)^{\varepsilon/2} \left[\bar{c}_{L,q}^{(1)} + \varepsilon a_{L,q}^{(1)} \right], \quad (3.13)$$

$$\hat{\mathcal{F}}_{T,q}^{(1)} = \left(\frac{\hat{\alpha}_s}{4\pi}\right) S_\varepsilon \left(\frac{Q^2}{\mu^2}\right)^{\varepsilon/2} \left[P_{qq}^{(0)} \frac{1}{\varepsilon} + \bar{c}_{T,q}^{(1)} + \varepsilon a_{T,q}^{(1)} \right], \quad (3.14)$$

$$\hat{\mathcal{F}}_{L,g}^{(1)} = \left(\frac{\hat{\alpha}_s}{4\pi}\right) S_\varepsilon \left(\frac{Q^2}{\mu^2}\right)^{\varepsilon/2} \left[\bar{c}_{L,g}^{(1)} + \varepsilon a_{L,g}^{(1)} \right], \quad (3.15)$$

$$\hat{\mathcal{F}}_{T,g}^{(1)} = \left(\frac{\hat{\alpha}_s}{4\pi}\right) S_\varepsilon \left(\frac{Q^2}{\mu^2}\right)^{\varepsilon/2} \left[2P_{gq}^{(0)} \frac{1}{\varepsilon} + \bar{c}_{T,g}^{(1)} + \varepsilon a_{T,g}^{(1)} \right]. \quad (3.16)$$

The pole terms $1/\varepsilon$ stand for the collinear divergence in the final state and μ^2 and S_ε are artefacts of n -dimensional regularization. The mass parameter μ originates from the dimensionality of the gauge coupling constant in n dimensions and should not be confused with the renormalization scale R and the mass factorization scale M . The spherical factor S_ε is defined by

$$S_\varepsilon = \exp \left[\frac{1}{2} \varepsilon (\gamma_E - \ln 4\pi) \right]. \quad (3.17)$$

Further $\hat{\alpha}_s$ denotes the bare coupling constant and $P_{ij}^{(0)}$ ($i, j = q, \bar{q}, g$) stand for the lowest order contribution to the DGLAP splitting functions [34]. Using our convention they are presented in eqs. (2.13)-(2.16) of [3]. Notice that in lowest order there is no difference in the expressions for $P_{ij}^{(0)}$ found for the deep inelastic structure functions (spacelike process) and those appearing in the fragmentation functions (timelike process). In next-to leading order the DGLAP splitting functions are different for spacelike and timelike processes as will be shown later on.

The coefficients $\bar{c}_{k,i}^{(1)}$, presented in the $\overline{\text{MS}}$ -scheme, are already calculated in the literature [44, 45] (see also appendix A). Furthermore we also have to compute the

coefficients $a_{k,i}^{(1)}$ (proportional to ε), since they are needed for the mass factorization which has to be carried out up to order α_s^2 . The results are

$$a_{L,q}^{(1)} = C_F \{-1 + \ln(1-z) + 2 \ln z\}, \quad (3.18)$$

$$a_{T,q}^{(1)} = C_F \left\{ D_2(z) - \frac{3}{2}D_1(z) + \left(\frac{7}{2} - 3\zeta(2) \right) D_0(z) - \frac{1}{2}(1+z) \ln^2(1-z) \right. \\ \left. + 2\frac{1+z^2}{1-z} \ln z \ln(1-z) + 2\frac{1+z^2}{1-z} \ln^2 z - 3\frac{1}{1-z} \ln z + \frac{3}{2}(1-z) \ln(1-z) \right. \\ \left. + 3(1-z) \ln z - \frac{3}{2} + \frac{5}{2}z + \frac{3}{2}(1+z)\zeta(2) + \delta(1-z)(9 - \frac{33}{4}\zeta(2)) \right\}, \quad (3.19)$$

$$a_{L,g}^{(1)} = C_F \left\{ 4\frac{1-z}{z}(\ln(1-z) + 2 \ln z - 2) \right\}, \quad (3.20)$$

$$a_{T,g}^{(1)} = C_F \left\{ \left(\frac{2}{z} - 2 + z \right) (\ln^2(1-z) + 4 \ln z \ln(1-z) + 4 \ln^2 z - 3\zeta(2)) \right. \\ \left. - 4\frac{1-z}{z}(\ln(1-z) + 2 \ln z - 3) + 4z \right\}. \quad (3.21)$$

The calculation of the order α_s^2 corrections proceeds in the following way. First we have the two-loop corrections to the quark-vector boson vertex represented by the graphs in fig. 5 which only contribute to $\hat{\mathcal{F}}_{T,q}^{(2)}$. The two-loop vertex correction can be found in eq. (2.49) of [46] (see also appendix A of [47]). The result agrees with the one quoted in [48]. Notice that the first graph in fig. 5 does not contribute for $V = \gamma$ because of Furry's theorem. It only plays a role in the case $V = Z$ provided one sums over all flavours in a quark family in order to cancel the anomaly which originates from the triangle fermion sub-loop. Since all quarks are massless the final result for this graph is zero too even in the case of $V = Z$.

Next we have to compute the one-loop virtual corrections to the radiative process in fig. 4 which contribute to $\hat{\mathcal{F}}_{k,q}^{(2)}$ as well as $\hat{\mathcal{F}}_{k,g}^{(2)}$ ($k = T, L$). The corresponding graphs are shown in fig. 6. Notice that we have omitted the diagrams with the self energy insertions on the external quark and gluon legs. Their contributions vanish because of the method of n -dimensional regularization and the on-mass shell conditions $k_0^2 = k_\ell^2 = 0$. Another vanishing contribution happens for the last graph in fig. 6 when $V = \gamma$ because of Furry's theorem. In the case of $V = Z$ it only contributes when the quarks are massive. However here one has to sum over all members of a quark family in order to cancel the anomaly originating from the triangle fermion loop.

The amplitude of the parton subprocesses in fig. 6 will be denoted by $M(2)$ (see (3.1) where $\ell = 2$). The momenta of the incoming vector boson V and the outgoing partons are parameterized like

$$q = \sqrt{s}(1, \mathbf{0}_{n-1}),$$

$$\begin{aligned}
k_0 &= \frac{s - s_{12}}{2\sqrt{s}} (1, 1, \mathbf{0}_{n-2}), \\
k_1 &= \frac{s - s_2}{2\sqrt{s}} (1, \cos \theta_1, \sin \theta_1, \mathbf{0}_{n-3}), \quad k_2 = q - k_0 - k_1,
\end{aligned} \tag{3.22}$$

where $\mathbf{0}_n$ stands for the n -dimensional null vector. The phase space integral in (3.2), (3.3) becomes

$$\begin{aligned}
\int d\text{PS}^{(2)} |M(2)|^2 &= \frac{1}{8\pi} \frac{1}{\Gamma(1 + \frac{1}{2}\varepsilon)} \frac{1}{(4\pi)^{\varepsilon/2}} s^{\varepsilon/2} (1 - z)^{\varepsilon/2} \\
&\cdot \int_0^1 dy y^{\varepsilon/2} (1 - y)^{\varepsilon/2} |M(2)|^2.
\end{aligned} \tag{3.23}$$

$$\tag{3.24}$$

Here we have defined the Lorentz invariants

$$s = Q^2, \quad s_1 = (k_0 + k_1)^2, \quad s_2 = (k_0 + k_2)^2, \quad s_{12} = (k_1 + k_2)^2, \tag{3.25}$$

with $s = s_1 + s_2 + s_{12}$. The parameterization of (3.23) follows from momentum conservation and the on-shell condition $k_0^2 = k_\ell^2 = 0$. Hence we get

$$\cos \theta_1 = \frac{s_2 s_{12} - s_1 s}{(s - s_{12})(s - s_2)}, \quad s_1 = z(1 - y)s, \quad s_{12} = (1 - z)s, \quad s_2 = zys. \tag{3.26}$$

The Feynman integrals corresponding to the one-loop graphs which contribute to $M(2)$ in (3.23) contain loop momenta in the numerator. They can be reduced to scalar one-loop integrals using an n -dimensional extension of the reduction program in [49]. The expressions for these scalar integrals which are valid for all n can be found in appendix D of [47]. The phase space integrals which emerge from the computation of $|M(2)|^2$ are very numerous so that we cannot present them in this paper. They are calculated algebraically using the program FORM [42].

The most difficult and laborious part of the calculation can be attributed to the parton subprocesses (3.1) where one has to integrate over three partons in the final state (see also table 1). These parton subprocesses are depicted in figs. 7, 8 providing us with the amplitude $M(3)$ (see (3.1) where $\ell = 3$). The graphs in fig. 7 determine $\hat{\mathcal{F}}_{k,q}^{(2)}$ as well as $\hat{\mathcal{F}}_{k,g}^{(2)}$ ($k = T, L$) whereas the graphs in fig. 8, which only contain quarks and anti-quarks in the final state, contribute to $\hat{\mathcal{F}}_{k,q}^{(2)}$ only. For the computation of the three body phase space integrals we choose the following parameterization for the momenta of the virtual vector boson V and the outgoing partons (see [48])

$$\begin{aligned}
q &= \sqrt{s} (1, \mathbf{0}_{n-1}), \\
k_0 &= \left(\frac{s_{023} - s_{23}}{2\sqrt{s_{23}}} \right) (1, 1, \mathbf{0}_{n-2}),
\end{aligned}$$

$$\begin{aligned}
k_1 &= \left(\frac{s_{123} - s_{23}}{2\sqrt{s_{23}}} \right) (1, \cos \chi, \sin \chi, \mathbf{0}_{n-3}), \\
k_2 &= \frac{1}{2}\sqrt{s_{23}}(1, \cos \theta_1, \sin \theta_1 \cos \theta_2, \sin \theta_1 \sin \theta_2, \mathbf{0}_{n-4}), \\
k_3 &= \frac{1}{2}\sqrt{s_{23}}(1, -\cos \theta_1, -\sin \theta_1 \cos \theta_2, -\sin \theta_1 \sin \theta_2, \mathbf{0}_{n-4}),
\end{aligned} \tag{3.27}$$

where we have defined the invariants

$$s_{ij} = (k_i + k_j)^2, \quad s_{ijm} = (k_i + k_j + k_m)^2, \quad s = q^2. \tag{3.28}$$

From momentum conservation and the on-mass shell conditions one can derive

$$1 - \cos \chi = \frac{2s_{23}(s + s_{23} - s_{023} - s_{123})}{(s_{023} - s_{23})(s_{123} - s_{23})}. \tag{3.29}$$

The three-body phase space integral in (3.2), (3.3) can be expressed as

$$\begin{aligned}
\int d\text{PS}^{(3)} |M(3)|^2 &= \frac{1}{2^8 \pi^4} \frac{1}{\Gamma(1 + \varepsilon)} \frac{1}{(4\pi)^\varepsilon} s^{1+\varepsilon} z^{1+\varepsilon/2} (1 - z)^{1+\varepsilon} \\
&\cdot \int_0^1 dy_1 \int_0^1 dy_2 y_1^{1+\varepsilon} (1 - y_1)^{\varepsilon/2} y_2^{\varepsilon/2} (1 - y_2)^{\varepsilon/2} (1 - y_2(1 - z))^{-\varepsilon-2} \\
&\cdot \int_0^\pi d\theta_1 (\sin \theta_1)^{1+\varepsilon} \int_0^\pi d\theta_2 (\sin \theta_2)^\varepsilon |M(3)|^2,
\end{aligned} \tag{3.30}$$

where the invariants in (3.28) depend on z , y_1 , and y_2 in the following way

$$\begin{aligned}
s_{023} &= \frac{y_1 z s}{1 - y_2(1 - z)}, \quad s_{123} = (1 - z)s, \quad s_{23} = \frac{z(1 - z)y_1 y_2 s}{1 - y_2(1 - z)}, \\
2k_0 q &= z s, \quad s_{01} = z(1 - y_1)s.
\end{aligned} \tag{3.31}$$

Before we can perform the angular integrations the matrix element $|M(3)|^2$ has to be decomposed via partial fractioning in terms which have the general form

$$\begin{aligned}
T^{n_1 n_2 n_3 n_4} &= (s_{i_1 j_1})^{n_1} (s_{i_2 j_2})^{n_2} (s_{i_3 j_3})^{n_3} (s_{i_4 j_4})^{n_4}, \\
n_i &= \dots, 2, 1, 0, -1, -2, \dots.
\end{aligned} \tag{3.32}$$

The decomposition can be done in such a way that one invariant e.g. $s_{i_1 j_1}$ in the product (3.32) depends on the polar angle θ_1 whereas an other invariant e.g. $s_{i_2 j_2}$ contains the polar angle θ_1 as well as the azimuthal angle θ_2 . The remaining invariants i.e. $s_{i_3 j_3}$ and $s_{i_4 j_4}$ do not depend on the angles.

Sometimes it happens that the azimuthal angle θ_2 also appears in $s_{i_1 j_1}$. In this case one has to rotate the frame in (3.27) so that $s_{i_1 j_1}$ becomes independent of the

azimuthal angle. This is always possible because the phase space integral (3.4) is Lorentz invariant. The angular integrals take the form

$$I_\varepsilon^{(i,j)} = \int_0^\pi d\theta_1 \int_0^\pi d\theta_2 \frac{(\sin \theta_1)^{1+\varepsilon} (\sin \theta_2)^\varepsilon}{(a + b \cos \theta_1)^i (A + B \cos \theta_1 + C \sin \theta_1 \cos \theta_2)^j}, \quad (3.33)$$

where a , b , A , B , and C are functions of the kinematical invariants s , s_{123} , s_{023} , s_{23} (3.31). These integrals can be found in appendix C of [51]. However they have to be extended by including terms which are proportional to ε^k where the degree k has to be larger than the one appearing in the integrals of [51]. This is necessary because these terms contribute due to the appearance of high power singularities $(1/\varepsilon)^k$ in the phase space integral (3.30). The n -dimensional expression for (3.33) becomes very cumbersome if $a^2 \neq b^2$ and $A^2 \neq B^2 + C^2$. Fortunately this situation can be avoided when one chooses the frame presented in (3.27). In this frame the worst case is given by $a^2 \neq b^2$, $A^2 = B^2 + C^2$ or $a^2 = b^2$, $A^2 \neq B^2 + C^2$. These type of integrals have to be partially done by hand before one can algebraically evaluate expression (3.30) using the program FORM [42]. The angular integrals are easy to perform when $a^2 = b^2$ and $A^2 = B^2 + C^2$ because they can be expressed into a hypergeometric function ${}_2F_1(\alpha, \beta; \gamma; x)$ [52]. Inserting the latter in (3.30) the remaining integrations are then again performed using the algebraic manipulation program FORM. Finally we would like to comment on a special type of term appearing in the transverse parton fragmentation function $\hat{\mathcal{F}}_{T,q}(z, Q^2, \varepsilon)$. They only show up in the non-singlet part and the order α_s^m contribution takes the form

$$\hat{\mathcal{F}}_{T,q}^{(m)}(z, Q^2, \varepsilon) = \sum_{\ell=-1}^{2m-1} (1-z)^{\frac{m}{2}\varepsilon-1} \frac{f_\ell(z)}{\varepsilon^\ell}, \quad (3.34)$$

where $f_\ell(1)$ is finite. These type of terms originate from gluon bremsstrahlung (figs. 4,6,7) and gluon splitting into a quark-anti-quark pair (fig. 8). In the limit $z \rightarrow 1$ all gluons become soft and the angle between the quark and anti-quark pair goes to zero (collinear emission). In the next section expression (3.34) has to be convoluted with the so-called bare fragmentation densities $\hat{D}_q^H(z)$ (for the definition see section 4) which yields the integral

$$\sum_{\ell=-1}^{2m-1} \int_x^1 dz \hat{D}_q^H\left(\frac{x}{z}\right) (1-z)^{\frac{m}{2}\varepsilon-1} \frac{f_\ell(z)}{\varepsilon^\ell}. \quad (3.35)$$

Inspection of the above integral reveals that at $z = 1$ one gets an additional pole term which means that we also have to compute $f_{-1}(1)$. Therefore for $z = 1$ the phase space integrals (3.30) have to be computed even up to one order higher in powers of ε than is needed for those which are integrable at $z = 1$. Since $f_\ell(z) - f_\ell(1)$ is integrable at $z = 1$ we can replace in (3.34) $f_\ell(z)$ by $f_\ell(1)$ and one only has to consider the integral

$$\hat{\mathcal{F}}_{T,q}^{(m)} = \sum_{\ell=-1}^{2m-1} \int_x^1 dz \hat{D}_q^H\left(\frac{x}{z}\right) (1-z)^{\frac{m}{2}\varepsilon-1} \frac{f_\ell(1)}{\varepsilon^\ell}, \quad (3.36)$$

which can be written as

$$\begin{aligned} \hat{\mathcal{F}}_{T,q}^{(m)} &= \sum_{\ell=-1}^{2m-1} \left[\int_x^1 dz (1-z)^{\frac{m}{2}\varepsilon-1} \frac{f_\ell(1)}{\varepsilon^\ell} \left\{ \hat{D}_q^H\left(\frac{x}{z}\right) - \hat{D}_q^H(x) \right\} \right. \\ &\quad \left. + \frac{2}{m} \varepsilon^{-\ell-1} \hat{D}_q^H(x) f_\ell(1) (1-x)^{\frac{m}{2}\varepsilon-1} \right]. \end{aligned} \quad (3.37)$$

If we define the distribution (see [53])

$$\mathcal{D}_i(z) = \left(\frac{\ln^i(1-z)}{1-z} \right)_+, \quad (3.38)$$

by

$$\int_0^1 dz \mathcal{D}_i(z) g(z) = \int_0^1 dz \frac{\ln^i(1-z)}{1-z} (g(z) - g(1)), \quad (3.39)$$

one can rewrite (3.37) in the following way

$$\begin{aligned} \hat{\mathcal{F}}_{T,q}^{(m)} &= \int_x^1 dz \left[\left\{ \sum_{\ell=0}^{2m-1} \frac{f_\ell(1)}{\varepsilon^\ell} \hat{D}_q^H\left(\frac{x}{z}\right) \sum_{i=0}^{\ell} \frac{1}{i!} \left(\frac{1}{2}m\varepsilon\right)^i \mathcal{D}_i(z) \right\} \right. \\ &\quad \left. + \hat{D}_q^H\left(\frac{x}{z}\right) \hat{\mathcal{F}}_{T,q}^{(m),\text{soft}}(z) \right], \end{aligned} \quad (3.40)$$

where $\hat{\mathcal{F}}_{T,q}^{\text{soft}}$ stands for the soft gluon bremsstrahlung contribution which is given by (see the definition in [54])

$$\hat{\mathcal{F}}_{T,q}^{(m),\text{soft}} = \delta(1-z) \sum_{\ell=-1}^{2m-1} \frac{2}{m} \varepsilon^{-\ell-1} f_\ell(1). \quad (3.41)$$

In order α_s^2 ($m=2$) the highest order pole term which can occur in (3.41) is represented by $1/\varepsilon^4$. The latter is cancelled by similar terms originating from the virtual gluon contributions given by the two-loop vertex corrections in fig. 5. Finally we want to emphasize that the type of singular terms in (3.34) only occur in $\hat{\mathcal{F}}_{T,q}^{\text{NS}}$ and $\hat{\mathcal{F}}_{A,q}^{\text{NS}}$ and are absent in $\hat{\mathcal{F}}_{L,p}^{\text{PS}}$ ($p=q, g$) or $\hat{\mathcal{F}}_{k,g}^\dagger$ ($k=T, L$).

Adding all virtual-, soft- and hard-gluon contributions, the IR divergences cancel while computing the parton structure functions $\hat{\mathcal{F}}_{k,p}(z, Q^2, \varepsilon)$ which is in agreement with the Bloch-Nordsieck theorem. The left-over divergences are removed by coupling constant renormalization and the C-divergences are factorized out of $\hat{\mathcal{F}}_{k,p}(z, Q^2, \varepsilon)$ leaving us with the coefficient functions which are finite in the limit $\varepsilon \rightarrow 0$. These two procedures will be carried out in the next section.

[†]Notice that $\hat{\mathcal{F}}_{A,q}^{\text{PS}} = \hat{\mathcal{F}}_{A,g} = 0$ because of charge conjugation invariance of the strong interactions.

4 Determination of the coefficient functions in the $\overline{\text{MS}}$ - and the annihilation scheme (A-scheme)

In this section we determine the coefficient functions of the process (2.1) by applying coupling constant renormalization and mass factorization to the parton fragmentation functions $\hat{\mathcal{F}}_{k,p}$ ($p = q, g$) which are computed up to order α_s^2 in the last section. These coefficient functions have to satisfy renormalization group equations. One can formally solve these equations order by order in α_s by writing the renormalization group functions like the beta-function $\beta(\alpha_s)$ and the anomalous dimension $\gamma_{ij}(\alpha_s)$ ($i, j = q, g$) as a power series in α_s . In this way one can algebraically express the coefficient functions into the coefficients of the power series. Using the mass factorization theorem which holds in every renormalizable field theory for all leading twist two contributions, one can also express the parton fragmentation functions $\hat{\mathcal{F}}_{k,p}$ into the same coefficients. Our calculations described in the last section have to satisfy the algebraic expressions of $\hat{\mathcal{F}}_{k,p}$ at least up to pole terms $(1/\varepsilon)^m$ which is a minimal requirement for the correctness of our results.

Before presenting the algebraic expressions for $\hat{\mathcal{F}}_{k,p}$ we have to decompose them according to the flavour symmetry group. Convoluting the parton structure tensor $\hat{W}_{\mu\nu}^{(V,V')}$ (3.7) with the bare parton fragmentation densities $\hat{D}_p^H(z)$ we obtain the following functions

$$F_k^{H,(V,V')}(x, Q^2) = \sum_{p=q,\bar{q},g} \sum_{q_1, q_2=1}^{n_f} (v_{q_1}^{(V)} v_{q_2}^{(V')} + a_{q_1}^{(V)} a_{q_2}^{(V')}) \cdot \int_0^1 \frac{dz}{z} \hat{D}_p^H\left(\frac{x}{z}\right) \hat{\mathcal{F}}_{k,p}(z, Q^2, \varepsilon), \quad (k = T, L), \quad (4.1)$$

$$F_A^{H,(V,V')}(x, Q^2) = \sum_{p=q,\bar{q}} \sum_{q_1, q_2=1}^{n_f} (v_{q_1}^{(V)} a_{q_2}^{(V')} + a_{q_1}^{(V)} v_{q_2}^{(V')}) \cdot \int_0^1 \frac{dz}{z} \hat{D}_p^H\left(\frac{x}{z}\right) \hat{\mathcal{F}}_{A,p}(z, Q^2, \varepsilon). \quad (4.2)$$

The reason that we call \hat{D}_p^H ‘bare’, originates from the fact that the C-divergence which are removed from $\hat{\mathcal{F}}_{k,p}$ via mass factorization will be absorbed by \hat{D}_p^H so that the latter are dressed up to the phenomenological fragmentation densities defined in (2.4), (2.5). The hadronic fragmentation functions defined in (2.21) are obtained by contracting the parton structure tensor $\hat{W}_{\mu\nu}^{(V,V')}$ (3.7), after convolution by \hat{D}_p^H , with the leptonic tensor due to the subprocess $e^+ + e^- \rightarrow V(V')$ where one also has to include the vector boson propagators given by $Z(Q^2)^{-1}$ in (2.12).

The contributions to $\hat{\mathcal{F}}_{k,p}$ ($p = q, g$) can be distinguished in a flavour singlet (S) and a flavour non-singlet (NS) part. Equations (4.1), (4.2) can then be written as

$$F_k^{H,(V,V')}(x, Q^2) = \int_x^1 \frac{dz}{z} \left[\sum_{p=1}^{n_f} (v_p^{(V)} v_p^{(V')} + a_p^{(V)} a_p^{(V')}) (\hat{D}_p^H\left(\frac{x}{z}\right) + \hat{D}_{\bar{p}}^H\left(\frac{x}{z}\right)) \right].$$

$$\begin{aligned}
& \cdot \hat{\mathcal{F}}_{k,q}^{\text{NS}}(z, Q^2, \varepsilon) + \left(\sum_{q_1=1}^{n_f} a_{q_1}^{(V')} \sum_{p=1}^{n_f} a_p^{(V)} + \sum_{q_1=1}^{n_f} a_{q_1}^{(V)} \sum_{p=1}^{n_f} a_p^{(V')} \right) (\hat{D}_p^H \left(\frac{x}{z} \right) \\
& + \hat{D}_{\bar{p}}^H \left(\frac{x}{z} \right)) \hat{\mathcal{F}}_{k,q}'^{\text{NS}}(z, Q^2, \varepsilon) + \sum_{q_1=1}^{n_f} (v_{q_1}^{(V)} v_{q_1}^{(V')} + a_{q_1}^{(V)} a_{q_1}^{(V')}) \left\{ \frac{1}{n_f} \sum_{p=1}^{n_f} (\hat{D}_p^H \left(\frac{x}{z} \right) \right. \\
& \left. + \hat{D}_{\bar{p}}^H \left(\frac{x}{z} \right)) \hat{\mathcal{F}}_{k,q}^{\text{PS}}(z, Q^2, \varepsilon) + \hat{D}_g^H \left(\frac{x}{z} \right) \hat{\mathcal{F}}_{k,g}(z, Q^2, \varepsilon) \right\}, \quad (k = T, L), \quad (4.3)
\end{aligned}$$

$$\begin{aligned}
F_A^{H,(V,V')}(x, Q^2) &= \int_x^1 \frac{dz}{z} \left[\sum_{p=1}^{n_f} (v_p^{(V)} a_p^{(V')} + a_p^{(V)} v_p^{(V')}) (\hat{D}_p^H \left(\frac{x}{z} \right) - \hat{D}_{\bar{p}}^H \left(\frac{x}{z} \right)) \cdot \right. \\
& \cdot \hat{\mathcal{F}}_{A,q}^{\text{NS}}(z, Q^2, \varepsilon) + \left(\sum_{q_1=1}^{n_f} a_{q_1}^{(V')} \sum_{p=1}^{n_f} v_p^{(V)} + \sum_{q_1=1}^{n_f} a_{q_1}^{(V)} \sum_{p=1}^{n_f} v_p^{(V')} \right) (\hat{D}_p^H \left(\frac{x}{z} \right) \\
& \left. - \hat{D}_{\bar{p}}^H \left(\frac{x}{z} \right)) \hat{\mathcal{F}}_{A,q}'^{\text{NS}}(z, Q^2, \varepsilon) \right]. \quad (4.4)
\end{aligned}$$

Here we use the same notation as introduced above (2.9) where $p = 1, 2, \dots, n_f$ stands for $p = u, d, \dots$. Further we have the relations

$$\hat{\mathcal{F}}_{k,q}^{(r)} = \hat{\mathcal{F}}_{k,\bar{q}}^{(r)}, \quad (k = T, L; r = \text{NS}, \text{PS}), \quad (4.5)$$

$$\hat{\mathcal{F}}_{A,q}^{\text{NS}} = -\hat{\mathcal{F}}_{A,\bar{q}}^{\text{NS}}, \quad \hat{\mathcal{F}}_{A,q}^{\text{PS}} = \hat{\mathcal{F}}_{A,\bar{q}}^{\text{PS}} = 0, \quad \hat{\mathcal{F}}_{A,g} = 0. \quad (4.6)$$

Relations (4.5), (4.6) follow from charge conjugation invariance of the strong interactions. The parton fragmentation function $\hat{\mathcal{F}}_{k,q}^{\text{PS}}$ is called the purely singlet part for reasons we will explain below.

The function $\hat{\mathcal{F}}_{k,g}$ ($k = T, L$), describing process (3.1) where the gluon is detected ($p = g$), receives contributions from the graphs in figs. 4, 6, 7. Since the gluon is a flavour singlet $\hat{\mathcal{F}}_{k,g}$ belongs to the same representation. The quarks q_1 and q_2 in (4.1), which are directly coupled to the vector bosons V and V' respectively, automatically belong to the inclusive state when $p = g$ in reaction (3.1) so that the sums over q_1 , q_2 , and p in (4.1) have to be separately performed.

The non-singlet part $\hat{\mathcal{F}}_{k,q}^{\text{NS}}$ ($k = T, L, A$) describing process (3.1) where the quark or anti-quark is detected ($p = q$ or $p = \bar{q}$), is determined by the graphs in figs. 2-8 except for the combinations C^2 , D^2 and AD , BC (see below). Notice that groups B and D only contribute when the anti-quarks q_1 and q_2 are identical. In the case of the non-singlet contribution the quarks q_1 and q_2 can be identified with p (i.e. $p = q_1 = q_2$) so that the sums over q_1 , q_2 , and p in (4.1) are now connected. The above diagrams also contribute to $\hat{\mathcal{F}}_{k,q}^{\text{S}}$ in the case of $k = T, L$ when they are projected on the singlet channel and the result is the same as the one obtained for $\hat{\mathcal{F}}_{k,q}^{\text{NS}}$ so that we can set $\hat{\mathcal{F}}_{k,q}^{\text{S}} = \hat{\mathcal{F}}_{k,q}^{\text{NS}}$. The groups C^2 and D^2 in fig. 8 only survive if they are projected on the singlet channel. This is because the detected quark p is only connected with the

vector bosons V and V' via the exchange of a gluon which is a flavour singlet. To show this more explicitly we have drawn the cut graphs contributing to the parton structure tensor $\hat{W}_{\mu\nu}^{(V,V')}$ which originate from groups C and D in fig. 9. Because of the purely singlet nature the groups C and D only contribute to $\hat{\mathcal{F}}_{k,q}^S$ and their contribution will be called $\hat{\mathcal{F}}_{k,q}^{\text{PS}}$. Like in the case of $\hat{\mathcal{F}}_{k,q}$ the quarks q_1, q_2 belong to the inclusive state since $p \neq q_1, p \neq q_2$. Therefore one can separately sum over p and q_1, q_2 which determines the factor of $\hat{\mathcal{F}}_{k,q}^{\text{PS}}$ in (4.3). Finally we have a special non-singlet contribution which we will call $\hat{\mathcal{F}}_{k,q}^{\text{NS}}$ (4.3) ($k = T, L$) and $\hat{\mathcal{F}}_{A,q}^{\text{NS}}$ (4.4). The latter originates from the combinations AD and BC in fig. 8 which only appear in the case when the anti-quarks p_1 and p_2 are identical. The corresponding cut graphs are drawn in fig. 10. If one removes the dashed line, which indicates the integration over the momenta cut by that line, one obtains a closed fermion loop. This fermion loop, to which are attached two gluons and one vector boson V (V'), has the same properties as the triangular fermion loops inserted in the virtual diagrams of figs. 5, 6. In fig. 10 we have taken the example that the vector boson V' couples to the cut fermion loop via the quark q_1 whereas V couples to the detected quark p (see also (4.3),(4.4)). Like in the case of the triangle fermion loops in figs. 5,6 only the axial vector current can couple to the cut fermion-loop which rules out $V' = \gamma$ so that only $V' = Z$ remains. Since $a_p^{(\gamma)} = a_{q_1}^{(\gamma)} = 0$ we have in (4.3) $V = Z$ whereas in (4.4) we either can get $V = \gamma$ or $V = Z$. Only when the above condition is satisfied the parton fragmentation functions $\hat{\mathcal{F}}_{k,q}^{\text{NS}}$ ($k = T, L$) and $\hat{\mathcal{F}}_{A,q}^{\text{NS}}$ can contribute to $F_k^{(Z,Z)}$ (4.3) and $F_A^{(V,Z)}$ ($V = \gamma, Z$) respectively. If we now in addition sum in fig. 10 over all quark flavours q_1 belonging to one family one gets $\sum_{q_1=u,d} a_{q_1}^{(Z)} = 0$ (see (3.8)) so that in this case the above contributions due to $\hat{\mathcal{F}}_{k,q}^{\text{NS}}, \hat{\mathcal{F}}_{A,q}^{\text{NS}}$ will vanish. Since one has to sum over all members of one family anyhow in order to cancel the anomaly appearing in the triangle fermion-loops in figs. 5,6 we will do the same for the graphs in fig. 10. Therefore we do not have to calculate $\hat{\mathcal{F}}_{k,q}^{\text{NS}}$ and $\hat{\mathcal{F}}_{k,q}^{\text{NS}}$ and they will not be included in our phenomenological analysis in this paper.

Summarizing the above the singlet fragmentation function $\hat{\mathcal{F}}_{k,q}^S$ ($k = T, L$) receives two kinds of contributions and it can be written as

$$\hat{\mathcal{F}}_{k,q}^S = \hat{\mathcal{F}}_{k,q}^{\text{NS}} + \hat{\mathcal{F}}_{k,q}^{\text{PS}}, \quad (k = T, L). \quad (4.7)$$

After having specified the various parts to the parton fragmentation functions we will now list them below. Starting with the non-singlet part the parton fragmentation function expanded in the bare coupling constant $\hat{\alpha}_s$ read as follows

$$\begin{aligned} \hat{\mathcal{F}}_{L,q}^{\text{NS,(2)}} &= \left(\frac{\hat{\alpha}_s}{4\pi}\right)^2 S_\varepsilon^2 \left(\frac{Q^2}{\mu^2}\right)^2 \left[\frac{1}{\varepsilon} \left\{ -2\beta_0 \bar{c}_{L,q}^{(1)} + P_{qq}^{(0)} \otimes \bar{c}_{L,q}^{(1)} \right\} + \bar{c}_{L,q}^{\text{NS,id,(2)}} \right. \\ &\quad \left. + \bar{c}_{L,q}^{\text{NS,id,(2)}} - 2\beta_0 a_{L,q}^{(1)} + P_{qq}^{(0)} \otimes a_{L,q}^{(1)} \right], \end{aligned} \quad (4.8)$$

$$\hat{\mathcal{F}}_{T,q}^{\text{NS,(2)}} = \left(\frac{\hat{\alpha}_s}{4\pi}\right)^2 S_\varepsilon^2 \left(\frac{Q^2}{\mu^2}\right)^\varepsilon \left[\frac{1}{\varepsilon^2} \left\{ \frac{1}{2} P_{qq}^{(0)} \otimes P_{qq}^{(0)} - \beta_0 P_{qq}^{(0)} \right\} + \frac{1}{\varepsilon} \left\{ \frac{1}{2} (P_{qq}^{(1)})^{\text{NS}} \right. \right.$$

$$\begin{aligned}
& \left. + P_{q\bar{q}}^{(1),\text{NS}}) - 2\beta_0 \bar{c}_{T,q}^{(1)} + P_{qq}^{(0)} \otimes \bar{c}_{T,q}^{(1)} \right\} + \bar{c}_{T,q}^{\text{NS,nid,(2)}} + \bar{c}_{T,q}^{\text{NS,id,(2)}} - 2\beta_0 a_{T,q}^{(1)} \\
& \left. + P_{qq}^{(0)} \otimes a_{T,q}^{(1)} \right]. \tag{4.9}
\end{aligned}$$

The convolution symbol denoted by \otimes is defined by

$$(f \otimes g)(z) = \int_0^1 dz_1 \int_0^1 dz_2 \delta(z - z_1 z_2) f(z_1) g(z_2). \tag{4.10}$$

The second order DGLAP splitting functions denoted by $P_{ij}^{(1)}$ ($i, j = q, g$) are different for deep inelastic structure functions (spacelike process) and fragmentation functions (timelike process). For the latter case they have been calculated in [55, 58]. In order to solve the Altarelli-Parisi equations of the fragmentation densities D_p^H it is convenient to split them into two parts which in the $\overline{\text{MS}}$ -scheme are given by

$$\begin{aligned}
P_{qq}^{\text{NS,(1)}}(z) = n_f C_F T_f & \left[-\frac{160}{9} \mathcal{D}_0(z) - \frac{16}{9} + \frac{176}{9} z - \frac{16}{3} \frac{1+z^2}{1-z} \ln z \right. \\
& \left. - \delta(1-z) \left(\frac{4}{3} + \frac{32}{3} \zeta(2) \right) \right] \\
& + C_F^2 \left[\frac{1+z^2}{1-z} \ln z (12 + 16 \ln(1-z) - 16 \ln z) - 40(1-z) \right. \\
& \left. - (28 + 12z) \ln z + 4(1+z) \ln^2 z + \delta(1-z) (3 - 24\zeta(2) + 48\zeta(3)) \right] \\
& + C_A C_F \left[\left(\frac{536}{9} - 16\zeta(2) \right) \mathcal{D}_0(z) + 8(1+z) \zeta(2) + 8(1+z) \ln z + \frac{212}{9} \right. \\
& \left. - \frac{748}{9} z + \frac{1+z^2}{1-z} \left(4 \ln^2 z + \frac{44}{3} \ln z \right) + \delta(1-z) \left(\frac{17}{3} + \frac{88}{3} \zeta(2) - 24\zeta(3) \right) \right], \tag{4.11}
\end{aligned}$$

$$\begin{aligned}
P_{q\bar{q}}^{\text{NS,(1)}}(z) = (C_F^2 - \frac{1}{2} C_A C_F) & \left[\frac{1+z^2}{1+z} \left(8 \ln^2 z - 32 \ln z \ln(1+z) - 32 \text{Li}_2(-z) \right. \right. \\
& \left. \left. - 16\zeta(2) \right) + 32(1-z) + 16(1+z) \ln z \right], \tag{4.12}
\end{aligned}$$

where $\text{Li}_n(x)$ denote the polylogarithmic functions which can be found in [59]. The splitting function $P_{q\bar{q}}^{\text{NS,(1)}}$ (4.12) arises when the (anti) quarks p_1 and p_2 in reaction (3.1) become identical and it is only determined by the interference terms AB and CD in fig. 8. Like the splitting functions we have also decomposed the second order coefficients $\bar{c}_{k,q}^{\text{NS,(2)}}$ ($k = T, L$) into two parts i.e. $\bar{c}_{k,q}^{\text{NS,nid,(2)}}$ and $\bar{c}_{k,q}^{\text{NS,id,(2)}}$. The latter is

due to identical (anti) quark contributions and like $P_{q\bar{q}}$ it originates from combinations AB and CD in fig. 8. All coefficients $\bar{c}_{k,q}^{(i)}$ ($i = 0, 1$) are computed in the $\overline{\text{MS}}$ -scheme indicated by a bar and they show up in the perturbation series of the coefficient functions as we will see below. The coefficients $a_{k,q}^{(1)}$ are presented in (3.18),(3.19) and β_0 is the lowest order coefficient in the beta-function defined by

$$\beta(\alpha_s) = -2\alpha_s \left[\beta_0 \frac{\alpha_s}{4\pi} + \beta_1 \frac{\alpha_s^2}{4\pi} + \dots \right], \quad \beta_0 = \frac{11}{3}C_A - \frac{4}{3}T_f n_f, \quad (4.13)$$

where α_s now stands for the renormalized coupling (see below). The purely singlet contributions (see (4.7)) are given by

$$\begin{aligned} \hat{\mathcal{F}}_{L,q}^{\text{PS},(2)} = n_f \left(\frac{\hat{\alpha}_s}{4\pi} \right)^2 S_\varepsilon^2 \left(\frac{Q^2}{\mu^2} \right)^\varepsilon \left[\frac{1}{\varepsilon} \left\{ \frac{1}{2} P_{qg}^{(0)} \otimes \bar{c}_{L,g}^{(1)} \right\} + \bar{c}_{L,q}^{\text{PS},(2)} \right. \\ \left. + \frac{1}{2} P_{qg}^{(0)} \otimes a_{L,g}^{(1)} \right], \end{aligned} \quad (4.14)$$

$$\begin{aligned} \hat{\mathcal{F}}_{T,q}^{\text{PS},(2)} = n_f \left(\frac{\hat{\alpha}_s}{4\pi} \right)^2 S_\varepsilon^2 \left(\frac{Q^2}{\mu^2} \right)^\varepsilon \left[\frac{1}{\varepsilon^2} \left\{ \frac{1}{2} P_{gq}^{(0)} \otimes P_{qg}^{(0)} \right\} + \frac{1}{\varepsilon} \left\{ \frac{1}{2} P_{qq}^{\text{PS},(1)} \right. \right. \\ \left. \left. + \frac{1}{2} P_{qg}^{(0)} \otimes \bar{c}_{T,g}^{(1)} \right\} + \bar{c}_{T,q}^{\text{PS},(2)} + \frac{1}{2} P_{qg}^{(0)} \otimes a_{T,g}^{(1)} \right], \end{aligned} \quad (4.15)$$

where $a_{L,g}^{(1)}$ and $a_{T,g}^{(1)}$ are presented in (3.20) and (3.21) respectively. The above expressions are determined by the combinations C^2 (non-identical (anti-) quarks) or C^2 and D^2 (identical (anti-) quarks) in fig. 8. The timelike splitting function $P_{qq}^{\text{PS},(1)}$ can be inferred from [55, 58] and it reads ($\overline{\text{MS}}$ -scheme)

$$\begin{aligned} P_{qq}^{\text{PS},(1)}(z) = C_F T_f \left[-\frac{320}{9z} - 128 + 64z + \frac{896}{9} z^2 + 16(1+z) \ln^2 z - (80 \right. \\ \left. + 144z + \frac{128}{3} z^2) \ln z \right]. \end{aligned} \quad (4.16)$$

From (4.7) we can now also obtain the singlet parton fragmentation function $\hat{\mathcal{F}}_{k,q}^{\text{S},(2)}$ ($k = T, L$). Adding eqs. (4.8) and (4.14) provides us with $\hat{\mathcal{F}}_{L,q}^{\text{S},(2)}$ whereas the sum of eqs. (4.9) and (4.15) leads to $\hat{\mathcal{F}}_{T,q}^{\text{S},(2)}$. In the same way we obtain from (4.11), (4.12) and (4.16) the singlet splitting function

$$P_{qq}^{\text{S},(1)} = P_{qq}^{\text{NS},(1)} + P_{q\bar{q}}^{\text{NS},(1)} + P_{qq}^{\text{PS},(1)}. \quad (4.17)$$

Finally the order α_s^2 contributions to $\hat{\mathcal{F}}_{k,g}$ become

$$\begin{aligned} \hat{\mathcal{F}}_{L,g}^{(2)} = n_f \left(\frac{\hat{\alpha}_s}{4\pi} \right)^2 S_\varepsilon^2 \left(\frac{Q^2}{\mu^2} \right)^\varepsilon \left[\frac{1}{\varepsilon} \left\{ -2\beta_0 \bar{c}_{L,g}^{(1)} + P_{gg}^{(0)} \otimes \bar{c}_{L,g}^{(1)} + 2P_{gq}^{(0)} \otimes \bar{c}_{L,q}^{(1)} \right\} \right. \\ \left. + \bar{c}_{L,g}^{(2)} - 2\beta_0 a_{L,g}^{(1)} + P_{gg}^{(0)} \otimes a_{L,g}^{(1)} + 2P_{gq}^{(0)} \otimes a_{L,q}^{(1)} \right], \end{aligned} \quad (4.18)$$

$$\begin{aligned}
\hat{\mathcal{F}}_{T,g}^{(2)} = n_f & \left(\frac{\hat{\alpha}_s}{4\pi} \right)^2 S_\varepsilon^2 \left(\frac{Q^2}{\mu^2} \right)^\varepsilon \left[\frac{1}{\varepsilon^2} \left\{ P_{gq}^{(0)} \otimes (P_{gg}^{(0)} + P_{qq}^{(0)}) - 2\beta_0 P_{gq}^{(0)} \right\} \right. \\
& + \frac{1}{\varepsilon} \left\{ P_{gq}^{(1)} - 2\beta_0 \bar{c}_{T,g}^{(1)} + P_{gg}^{(0)} \otimes \bar{c}_{T,g}^{(1)} + 2P_{gq}^{(0)} \otimes \bar{c}_{T,q}^{(1)} \right\} + \bar{c}_{T,g}^{(2)} - 2\beta_0 a_{T,g}^{(1)} \\
& \left. + P_{gg}^{(0)} \otimes a_{T,g}^{(1)} + 2P_{gq}^{(0)} \otimes a_{T,g}^{(1)} \right], \tag{4.19}
\end{aligned}$$

where the timelike splitting function $P_{gq}^{(1)}$ in the $\overline{\text{MS}}$ -scheme can be found in [55, 58]. It is given by

$$\begin{aligned}
P_{gq}^{(1)} = C_F^2 & \left[-4 + 36z + (-64 + 4z) \ln z + 16z \ln(1-z) + (8-4z) \ln^2 z \right. \\
& + \left(\frac{16}{z} - 16 + 8z \right) \ln^2(1-z) + \left(\frac{64}{z} - 64 + 32z \right) \ln z \ln(1-z) \\
& \left. + \left(\frac{128}{z} - 128 + 64z \right) \text{Li}_2(1-z) + \left(-\frac{128}{z} + 128 - 64z \right) \zeta(2) \right] \\
& + C_A C_F \left[\frac{136}{9z} + 40 - 8z - \frac{352}{9} z^2 + \left(-\frac{48}{z} + 64 + 72z + \frac{64}{3} z^2 \right) \ln z \right. \\
& - 16z \ln(1-z) - \left(\frac{32}{z} + 16 + 24z \right) \ln^2 z + \left(-\frac{16}{z} + 16 - 8z \right) \ln^2(1-z) \\
& + \left(-\frac{32}{z} + 32 - 16z \right) \ln z \ln(1-z) + \left(-\frac{128}{z} + 128 - 64z \right) \text{Li}_2(1-z) \\
& + \left(\frac{32}{z} + 32 + 16z \right) \text{Li}_2(-z) + \left(\frac{32}{z} + 32 + 16z \right) \ln z \ln(1+z) + \left(\frac{128}{z} \right. \\
& \left. - 96 + 64z \right) \zeta(2) \left. \right]. \tag{4.20}
\end{aligned}$$

The pole terms $(1/\varepsilon)^m$ showing up in the parton fragmentation functions $\hat{\mathcal{F}}_{k,p}$ ($k = T, L$; $p = q, g$) are due to UV and C-divergences. In order to get the coefficient functions corresponding to the fragmentation process (2.1) these singularities have to be removed via coupling constant renormalization and mass factorization.

The coupling constant renormalization can be achieved by replacing the bare (unrenormalized) coupling constant $\hat{\alpha}_s$ by

$$\frac{\hat{\alpha}_s}{4\pi} = \frac{\alpha_s(R^2)}{4\pi} \left(1 + \frac{\alpha_s(R^2)}{4\pi} \frac{2\beta_0}{\varepsilon} S_\varepsilon \left(\frac{R^2}{\mu^2} \right)^{\varepsilon/2} \right), \tag{4.21}$$

where R represents the renormalization scale. After having removed the UV singularities the remaining pole terms can be attributed to final state collinear divergence

only because $\hat{\mathcal{F}}_{k,p}$ is a semi-inclusive quantity. The latter singularities are removed by mass factorization which proceeds in the following way

$$\hat{\mathcal{F}}_{k,q}^{\text{NS}} = \Gamma_{qq}^{\text{NS}} \otimes \mathbb{C}_{k,q}^{\text{NS}}, \quad (4.22)$$

$$\hat{\mathcal{F}}_{k,q}^{\text{S}} = \Gamma_{qq}^{\text{S}} \otimes \mathbb{C}_{k,q}^{\text{S}} + n_f \Gamma_{qg} \otimes \mathbb{C}_{k,g}, \quad (4.23)$$

$$\hat{\mathcal{F}}_{k,g} = 2\Gamma_{gq} \otimes \mathbb{C}_{k,q}^{\text{S}} + \Gamma_{gg} \otimes \mathbb{C}_{k,g}, \quad (4.24)$$

with $\Gamma_{gq} = \Gamma_{g\bar{q}}$, $\Gamma_{qg} = \Gamma_{\bar{q}g}$. The quantities Γ_{ij} are called transition functions in which all C-divergences are absorbed so that the fragmentation coefficient function $\mathbb{C}_{k,p}$ are finite. Both functions are expanded in the renormalized coupling constant $\alpha_s(R^2)$ and depend explicitly on the renormalization scale R and the factorization scale M which implies that they are scheme dependent. If we expand Γ_{ij} in the unrenormalized coupling constant $\hat{\alpha}_s$ the expressions become very simple. Choosing the $\overline{\text{MS}}$ -scheme they take the following form

$$\begin{aligned} \bar{\Gamma}_{qq}^{\text{NS}} = & \mathbb{1} + \frac{\hat{\alpha}_s}{4\pi} S_\varepsilon \left(\frac{M^2}{\mu^2} \right)^{\varepsilon/2} \left[\frac{1}{\varepsilon} P_{qq}^{(0)} \right] + \left(\frac{\hat{\alpha}_s}{4\pi} \right)^2 S_\varepsilon^2 \left(\frac{M^2}{\mu^2} \right)^\varepsilon \left[\frac{1}{\varepsilon^2} \right. \\ & \left. \left\{ \frac{1}{2} P_{qq}^{(0)} \otimes P_{qq}^{(0)} - \beta_0 P_{qq}^{(0)} \right\} + \frac{1}{\varepsilon} \left\{ \frac{1}{2} P_{qq}^{\text{NS},(1)} + \frac{1}{2} P_{q\bar{q}}^{\text{NS},(1)} \right\} \right], \end{aligned} \quad (4.25)$$

$$\bar{\Gamma}_{qq}^{\text{S}} = \bar{\Gamma}_{qq}^{\text{NS}} + 2n_f \bar{\Gamma}_{qq}^{\text{PS}}, \quad (4.26)$$

$$\bar{\Gamma}_{qq}^{\text{PS}} = \left(\frac{\hat{\alpha}_s}{4\pi} \right)^2 S_\varepsilon^2 \left(\frac{M^2}{\mu^2} \right)^\varepsilon \left[\frac{1}{\varepsilon^2} \left\{ \frac{1}{4} P_{gq}^{(0)} \otimes P_{gq}^{(0)} \right\} + \frac{1}{\varepsilon} \left\{ \frac{1}{4} P_{qq}^{\text{PS},(1)} \right\} \right], \quad (4.27)$$

$$\begin{aligned} \bar{\Gamma}_{gq} = & \frac{\hat{\alpha}_s}{4\pi} S_\varepsilon \left(\frac{M^2}{\mu^2} \right)^{\varepsilon/2} \left[\frac{1}{\varepsilon} P_{gq}^{(0)} \right] + \left(\frac{\hat{\alpha}_s}{4\pi} \right)^2 S_\varepsilon^2 \left(\frac{M^2}{\mu^2} \right)^\varepsilon \left[\frac{1}{\varepsilon} \left\{ \frac{1}{2} P_{gq}^{(0)} \otimes \right. \right. \\ & \left. \left. (P_{gq}^{(0)} + P_{q\bar{q}}^{(0)}) - \beta_0 P_{gq}^{(0)} + \frac{1}{\varepsilon} \left\{ \frac{1}{2} P_{gq}^{(1)} \right\} \right\} \right], \end{aligned} \quad (4.28)$$

$$\bar{\Gamma}_{qg} = \frac{\hat{\alpha}_s}{4\pi} S_\varepsilon \left(\frac{M^2}{\mu^2} \right)^{\varepsilon/2} \left[\frac{1}{2\varepsilon} P_{qg}^{(0)} \right], \quad (4.29)$$

$$\bar{\Gamma}_{gg} = \mathbb{1} + \frac{\hat{\alpha}_s}{4\pi} S_\varepsilon \left(\frac{M^2}{\mu^2} \right)^{\varepsilon/2} \left[\frac{1}{\varepsilon} P_{gg}^{(0)} \right], \quad (4.30)$$

where the $\mathbb{1}$ in (4.25) and (4.30) is a shorthand notation for $\delta(1-z)$. Notice that we have expanded the Γ_{ij} above in sufficiently higher order of α_s in order to get the coefficient functions finite. Therefore the computation of $\hat{\mathcal{F}}_{k,p}$ allows us to determine the DGLAP-splitting functions $P_{qq}^{\text{NS},(1)}$, $P_{q\bar{q}}^{\text{NS},(1)}$, $P_{qq}^{\text{PS},(1)}$, and $P_{gq}^{(1)}$ in an alternative way which is different from the method used in [55, 58]. Further the transition functions

satisfy the following relations which originate from energy momentum conservation

$$\int_0^1 dz z (\Gamma_{qq}^S(z) + \Gamma_{gq}(z)) = 1, \quad (4.31)$$

$$\int_0^1 dz z (\Gamma_{gg}(z) + 2n_f \Gamma_{qg}(z)) = 1. \quad (4.32)$$

If we substitute $\hat{\mathcal{F}}_{k,p}$ (4.22) - (4.24) into eq. (4.3) the C-singularities are absorbed by the bare fragmentation densities \hat{D}_p^H as follows

$$D_{\text{NS},p}^H = \Gamma_{qq}^{\text{NS}} \otimes \hat{D}_{\text{NS},p}^H, \quad (4.33)$$

$$D_S^H = \Gamma_{qq}^S \otimes \hat{D}_S^H + 2\Gamma_{gq} \otimes \hat{D}_g^H, \quad (4.34)$$

$$D_g^H = n_f \Gamma_{qg} \otimes \hat{D}_S^H + \Gamma_{gg} \otimes \hat{D}_g^H, \quad (4.35)$$

Here $D_{\text{NS},p}^H$ and D_S^H denote the non-singlet and singlet combinations of the parton fragmentation densities as defined in (2.7), (2.6). The same definition holds for the bare densities $\hat{D}_{\text{NS},p}^H$ and \hat{D}_S^H . The densities $D_{\text{NS},p}^H$, D_S^H , and D_g^H depend on the renormalization scale R and the mass factorization scale M which are usually set to be equal.

Substituting eqs. (4.22)-(4.23), (4.33)-(4.35) in (4.3) and using (4.7) we obtain after rearranging terms the structure function $F_k^{(V,V')}(x, Q^2)$ expressed into the renormalized parton fragmentation densities D_p^H and the fragmentation coefficient functions $\mathbb{C}_{k,p}$ ($p = q, g$).

$$\begin{aligned} F_k^{(V,V')}(x, Q^2) &= \int_x^1 \frac{dz}{z} \left[\sum_{p=1}^{n_f} (v_p^{(V)} v_p^{(V')} + a_p^{(V)} a_p^{(V')}) \left\{ D_S^H \left(\frac{x}{z}, M^2 \right) \right. \right. \\ &\quad \left. \left. \cdot \mathbb{C}_{k,q}^S(z, Q^2/M^2) + D_g^H \left(\frac{x}{z}, M^2 \right) \mathbb{C}_g(z, Q^2/M^2) \right\} \right. \\ &\quad \left. + \sum_{p=1}^{n_f} (v_p^{(V)} v_p^{(V')} + a_p^{(V)} a_p^{(V')}) D_{\text{NS},p}^H \left(\frac{x}{z}, M^2 \right) \mathbb{C}_{k,q}^{\text{NS}}(z, Q^2/M^2) \right], \quad (4.36) \end{aligned}$$

where we have chosen $R = M$.

Like the parton fragmentation functions $\hat{\mathcal{F}}_{k,p}$ in eqs. (4.8)-(4.19) we can express the coefficient functions $\mathbb{C}_{k,p}$ ($p = q, g$) into the renormalization group coefficients. In the $\overline{\text{MS}}$ -scheme they take the following form. The non-singlet coefficient functions become

$$\begin{aligned} \overline{\mathbb{C}}_{L,q}^{\text{NS}} &= \frac{\alpha_s}{4\pi} \left[\bar{c}_{L,q}^{(1)} \right] + \left(\frac{\alpha_s}{4\pi} \right)^2 \left[\left\{ -\beta_0 \bar{c}_{L,q}^{(1)} + \frac{1}{2} P_{qq}^{(0)} \otimes \bar{c}_{L,q}^{(1)} \right\} L_M + \bar{c}_{L,q}^{\text{NS},(2),\text{mid}} \right. \\ &\quad \left. + \bar{c}_{L,q}^{\text{NS},(2),\text{id}} \right], \quad (4.37) \end{aligned}$$

$$\begin{aligned}
\overline{\mathbb{C}}_{T,q}^{\text{NS}} = & \mathbb{1} + \frac{\alpha_s}{4\pi} \left[\frac{1}{2} P_{qq}^{(0)} L_M + \overline{c}_{T,q}^{(1)} \right] + \left(\frac{\alpha_s}{4\pi} \right)^2 \left[\left\{ \frac{1}{8} P_{qq}^{(0)} \otimes P_{qq}^{(0)} \right. \right. \\
& \left. \left. - \frac{1}{4} \beta_0 P_{qq}^{(0)} \right\} L_M^2 + \left\{ \frac{1}{2} (P_{qq}^{(1),\text{NS}} + P_{q\bar{q}}^{(1),\text{NS}}) - \beta_0 \overline{c}_{T,q}^{(1)} + \frac{1}{2} P_{qq}^{(0)} \otimes \overline{c}_{T,q}^{(1)} \right\} L_M \right. \\
& \left. + \overline{c}_{T,q}^{\text{NS,(2),nid}} + \overline{c}_{T,q}^{\text{NS,(2),id}} \right]. \tag{4.38}
\end{aligned}$$

The singlet coefficient functions are given by

$$\overline{\mathbb{C}}_{k,q}^{\text{S}} = \overline{\mathbb{C}}_{k,q}^{\text{NS}} + \overline{\mathbb{C}}_{k,q}^{\text{PS}}, \quad (k = T, L), \tag{4.39}$$

$$\overline{\mathbb{C}}_{L,q}^{\text{PS}} = n_f \left(\frac{\alpha_s}{4\pi} \right)^2 \left[\left\{ \frac{1}{4} P_{qg}^{(0)} \otimes \overline{c}_{L,g}^{(1)} \right\} L_M + \overline{c}_{L,q}^{\text{PS,(2)}} \right], \tag{4.40}$$

$$\begin{aligned}
\overline{\mathbb{C}}_{T,q}^{\text{PS}} = & n_f \left(\frac{\alpha_s}{4\pi} \right)^2 \left[\left\{ \frac{1}{8} P_{gq}^{(0)} \otimes P_{gq}^{(0)} \right\} L_M^2 + \left\{ \frac{1}{2} P_{qq}^{\text{PS,(1)}} + \frac{1}{4} P_{qq}^{(0)} \otimes \overline{c}_{T,g}^{(1)} \right\} L_M \right. \\
& \left. + \overline{c}_{T,q}^{\text{PS,(2)}} \right]. \tag{4.41}
\end{aligned}$$

The gluon coefficient functions become

$$\begin{aligned}
\overline{\mathbb{C}}_{L,g} = & \frac{\alpha_s}{4\pi} \left[\overline{c}_{L,g}^{(1)} \right] + \left(\frac{\alpha_s}{4\pi} \right)^2 \left[\left\{ -\beta_0 \overline{c}_{L,g}^{(1)} + \frac{1}{2} P_{gg}^{(0)} \otimes \overline{c}_{L,g}^{(1)} \right. \right. \\
& \left. \left. + P_{gq}^{(0)} \otimes \overline{c}_{L,q}^{(1)} \right\} L_M + \overline{c}_{L,g}^{(2)} \right], \tag{4.42}
\end{aligned}$$

$$\begin{aligned}
\overline{\mathbb{C}}_{T,g} = & \frac{\alpha_s}{4\pi} \left[P_{gq}^{(0)} L_M + \overline{c}_{T,g}^{(1)} \right] + \left(\frac{\alpha_s}{4\pi} \right)^2 \left[\left\{ \frac{1}{4} P_{gq}^{(0)} \otimes (P_{gg}^{(0)} + P_{q\bar{q}}^{(0)}) \right. \right. \\
& \left. \left. - \frac{1}{2} \beta_0 P_{gq}^{(0)} \right\} L_M^2 + \left\{ P_{gq}^{(1)} - \beta_0 \overline{c}_{T,g}^{(1)} + \frac{1}{2} P_{gg}^{(0)} \otimes \overline{c}_{T,g}^{(1)} + P_{gq}^{(0)} \otimes \overline{c}_{T,q}^{(1)} \right\} L_M \right. \\
& \left. + \overline{c}_{T,g}^{(2)} \right]. \tag{4.43}
\end{aligned}$$

Further we have defined

$$\mathbb{1} \equiv \delta(1-z), \quad L_M = \ln \frac{Q^2}{M^2}, \quad \alpha_s \equiv \alpha_s(M^2). \tag{4.44}$$

In the case $M \neq R$ the resulting coefficient functions can be very easily derived from the above expressions (4.37)-(4.43) by replacing

$$\alpha_s(M^2) = \alpha_s(R^2) \left[1 + \frac{\alpha_s(R^2)}{4\pi} \beta_0 \ln \frac{R^2}{M^2} \right]. \tag{4.45}$$

The explicit expressions for the coefficient functions (4.37)-(4.43) are listed in appendix A.

Besides the $\overline{\text{MS}}$ -scheme one also can compute the coefficient functions in the so called annihilation scheme (A-scheme) [40]. It is defined in such a way that F^H/R_{ee} (see (2.20), (2.22)) does not get any α_s corrections at $M^2 = R^2 = Q^2$. In the A-scheme the transition functions Γ_{ij} are related to the ones in the $\overline{\text{MS}}$ -scheme denoted by $\overline{\Gamma}_{ij}$ (see (4.25)-(4.30)) as follows

$$\Gamma_{qq}^{\text{NS}} = Z_{qq}^{\text{NS}} \overline{\Gamma}_{qq}, \quad \Gamma_{ij} = Z_{ik} \overline{\Gamma}_{kj}, \quad (4.46)$$

where Z_{qq}^{NS} , Z_{ik} are given by (see eqs. (2.61), (2.62) in [40])

$$Z_{qq}^{\text{NS}} = R_{ee}^{-1} \overline{\mathbb{C}}_q^{\text{NS}}, \quad (4.47)$$

$$Z = \begin{pmatrix} R_{ee}^{-1} \overline{\mathbb{C}}_q^{\text{S}} & R_{ee}^{-1} \overline{\mathbb{C}}_g \\ 0 & 1 \end{pmatrix}. \quad (4.48)$$

The coefficient functions $\overline{\mathbb{C}}_\ell^{(r)}$ ($r = \text{NS}, \text{S}$, $\ell = q, g$) correspond to the structure function F^H defined in (2.22) and they are given by

$$\overline{\mathbb{C}}_\ell^{(r)} = \overline{\mathbb{C}}_{T,\ell}^{(r)} + \overline{\mathbb{C}}_{L,\ell}^{(r)}. \quad (4.49)$$

The coefficient functions in the A-scheme, denoted by $\mathbb{C}_{k,p}$, are related to the ones presented in the $\overline{\text{MS}}$ -scheme in the following way ($k = T, L$)

$$\mathbb{C}_{k,q}^{\text{NS}} = (Z_{qq}^{\text{NS}})^{-1} \overline{\mathbb{C}}_{k,q}^{\text{NS}}, \quad (4.50)$$

$$\mathbb{C}_{k,i} = (Z^{-1})_{ji} \overline{\mathbb{C}}_{k,j}. \quad (4.51)$$

Expanding all coefficient functions and R_{ee} in α_s the former take the following form in the A-scheme

$$\begin{aligned} \mathbb{C}_{L,q}^{\text{NS}} &= \frac{\alpha_s}{4\pi} \left[\overline{c}_{L,q}^{(1)} \right] + \left(\frac{\alpha_s}{4\pi} \right)^2 \left[\left\{ -\beta_0 \overline{c}_{L,q}^{(1)} + \frac{1}{2} P_{qq}^{(0)} \otimes \overline{c}_{L,q}^{(1)} \right\} L_M + \overline{c}_{L,q}^{(2),\text{NS,nid}} \right. \\ &\quad \left. + \overline{c}_{L,q}^{(2),\text{NS,id}} + R^{(1)} \overline{c}_{L,q}^{(1)} - \overline{c}_q^{(1)} \otimes \overline{c}_{L,q}^{(1)} \right], \end{aligned} \quad (4.52)$$

$$\begin{aligned} \mathbb{C}_{T,q}^{\text{NS}} &= \mathbb{1} + \frac{\alpha_s}{4\pi} \left[\frac{1}{2} P_{qq}^{(0)} L_M + R^{(1)} \mathbb{1} - \overline{c}_{L,q}^{(1)} \right] + \left(\frac{\alpha_s}{4\pi} \right)^2 \left[\left\{ \frac{1}{8} P_{qq}^{(0)} \otimes P_{qq}^{(0)} \right. \right. \\ &\quad \left. \left. - \frac{1}{4} \beta_0 P_{qq}^{(0)} \right\} L_M^2 + \left\{ \frac{1}{2} (P_{qq}^{\text{NS,(1)}} + P_{q\bar{q}}^{\text{NS,(1)}}) - \beta_0 \overline{c}_{T,q}^{(1)} + \frac{1}{2} R^{(1)} P_{qq}^{(0)} \right. \right. \\ &\quad \left. \left. - \frac{1}{2} P_{qq}^{(0)} \otimes \overline{c}_{L,q}^{(1)} \right\} L_M + R^{(2)} \mathbb{1} - \overline{c}_{L,q}^{\text{NS,(2),nid}} - \overline{c}_{L,q}^{\text{NS,(2),id}} - R^{(1)} \overline{c}_{L,q}^{(1)} \right] \end{aligned}$$

$$+ \bar{c}_q^{(1)} \otimes \bar{c}_{L,q}^{(1)} \Big], \quad (4.53)$$

$$\mathbb{C}_{L,q}^{\text{PS}} = n_f \left(\frac{\alpha_s}{4\pi} \right)^2 \left[\left\{ \frac{1}{4} P_{qg}^{(1)} \otimes \bar{c}_{L,g}^{(1)} \right\} L_M + \bar{c}_{L,q}^{\text{PS},(2)} \right] = \bar{\mathbb{C}}_{L,q}^{\text{PS}}, \quad (4.54)$$

$$\begin{aligned} \mathbb{C}_{T,q}^{\text{PS},(2)} &= n_f \left(\frac{\alpha_s}{4\pi} \right)^2 \left[\left\{ \frac{1}{8} P_{qg}^{(0)} \otimes P_{gq}^{(0)} \right\} L_M^2 + \left\{ \frac{1}{2} P_{qg}^{\text{PS},(1)} + \frac{1}{4} P_{qg}^{(0)} \otimes \bar{c}_{T,g}^{(1)} \right\} L_M \right. \\ &\quad \left. - \bar{c}_{L,q}^{\text{PS},(2)} \right], \end{aligned} \quad (4.55)$$

$$\begin{aligned} \mathbb{C}_{L,g} &= \frac{\alpha_s}{4\pi} \left[\bar{c}_{L,g}^{(1)} \right] + \left(\frac{\alpha_s}{4\pi} \right)^2 \left[\left\{ -\beta_0 \bar{c}_{L,q}^{(1)} + \frac{1}{2} P_{gg}^{(0)} \otimes \bar{c}_{L,g}^{(0)} + P_{gq}^{(0)} \otimes \bar{c}_{L,q}^{(1)} \right\} L_M \right. \\ &\quad \left. + \bar{c}_{L,g}^{(2)} - \bar{c}_g^{(1)} \otimes \bar{c}_{L,q}^{(1)} \right], \end{aligned} \quad (4.56)$$

$$\begin{aligned} \mathbb{C}_{T,g} &= \frac{\alpha_s}{4\pi} \left[P_{gq}^{(0)} L_M - \bar{c}_{L,g}^{(1)} \right] + \left(\frac{\alpha_s}{4\pi} \right)^2 \left[\left\{ \frac{1}{4} P_{gq}^{(0)} \otimes (P_{gg}^{(0)} + P_{qq}^{(0)}) \right. \right. \\ &\quad \left. \left. - \frac{1}{2} \beta_0 P_{gq}^{(0)} \right\} L_M^2 + \left\{ P_{gq}^{(0)} - \beta_0 \bar{c}_{T,g}^{(1)} + \frac{1}{2} P_{gg}^{(0)} \otimes \bar{c}_{T,g}^{(1)} + P_{gq}^{(0)} \otimes \bar{c}_{T,g}^{(1)} \right. \right. \\ &\quad \left. \left. - \frac{1}{2} P_{qq}^{(0)} \otimes \bar{c}_g^{(1)} \right\} L_M - \bar{c}_{L,g}^{(2)} + \bar{c}_g^{(1)} \otimes \bar{c}_{L,q}^{(1)} \right], \end{aligned} \quad (4.57)$$

where $\mathbb{1}$ is given by (4.44) and the coefficients $R^{(i)}$ show up in the perturbation series for R_{ee} (2.20):

$$R_{ee} = 1 + \frac{\alpha_s}{4\pi} R^{(1)} + \left(\frac{\alpha_s}{4\pi} \right)^2 R^{(2)}. \quad (4.58)$$

Notice that we have expressed the above coefficient functions into the renormalization group coefficients $P_{ij}^{(1)}$, $\bar{c}_{k,p}^{(i)}$ presented in the $\overline{\text{MS}}$ -scheme. From (4.52)-(4.57) we infer that at $Q^2 = M^2$ ($L_M = 0$) the coefficient functions in (4.49) become

$$\mathbb{C}_q^{\text{NS}} = \mathbb{1} \cdot R_{ee}, \quad \mathbb{C}_q^{\text{PS}} = 0, \quad \mathbb{C}_g = 0. \quad (4.59)$$

In any scheme the coefficient functions satisfy the renormalization group equations

$$\left[\left\{ M \frac{\partial}{\partial M} + \beta(\alpha_s) \frac{\partial}{\partial \alpha_s} \right\} \delta_{ij} - \gamma_{ij}^{(m)} \right] \tilde{\mathbb{C}}_{k,i}^{(m)} = 0, \quad (4.60)$$

with $k = T, L$ and $i, j = q, g$. Further we have defined the Mellin transforms

$$\mathbb{C}_{k,i}^{(m)}(Q^2/M^2) = \int_0^1 dz z^{m-1} \mathbb{C}_{k,i}(z, Q^2/M^2), \quad (4.61)$$

$$\gamma_{ij}^{(m)} = - \int_0^1 dz z^{m-1} P_{ij}(z), \quad (4.62)$$

and introduced the following the notations

$$\tilde{\mathbb{C}}_{k,q}^{(m)} = \mathbb{C}_{k,q}^{(m)}, \quad \tilde{\mathbb{C}}_{k,g}^{(m)} = \frac{1}{2}\mathbb{C}_{k,g}^{(m)}. \quad (4.63)$$

The quantities $\gamma_{ij}^{(m)}$ are the anomalous dimensions corresponding with the timelike cut vertex operators of spin m . Like the timelike splitting functions P_{ij} they are scheme dependent. The relations between the anomalous dimensions obtained from different schemes can e.g. be found in eqs. (3.82)-(3.86) in [62].

5 Results

In this section we will discuss the order α_s^2 contributions to the longitudinal and transverse cross sections and their corresponding fragmentation functions. In particular we investigate how the leading order (LO) longitudinal quantities, which already exist in the literature [40], [43], [44], are modified by including the order α_s^2 contributions. We will do the same for the transverse quantities for which a next-to-leading order (NLO) result already exists. Further we study the dependence of the above quantities on the mass factorization scale M and the renormalization scale R and show that the sensitivity to these scales becomes less when higher order corrections are included. Before we proceed we want to emphasize that with all higher order QCD corrections at hand it is only possible to perform a full NLO analysis on the cross sections and the fragmentation functions. The order α_s^2 contributions also allow for a next-to-next-to-leading order (NNLO) analysis of the transverse cross section $\sigma_T(Q^2)$ but not for the transverse fragmentation function $F_T(x, Q^2)$. For the latter one also needs the three-loop timelike splitting functions which have not been calculated yet. Therefore the order α_s^2 contributions to $F_T(x, Q^2)$ have to be considered as an estimate of the NNLO result. Nevertheless we will use the notation F_T^{NNLO} to indicate the order α_s^2 corrected transverse structure function.

The longitudinal and transverse cross section $\sigma_k(Q^2)$ ($k = T, L$) defined in (2.18) are obtained from the coefficient functions calculated in the previous sections as follows

$$\sigma_k(Q^2) = \sigma_{\text{tot}}^{(0)}(Q^2) \int_0^1 dz z \left[\mathbb{C}_{k,q}^S(z, Q^2/M^2) + \frac{1}{2} \mathbb{C}_{k,g}(z, Q^2/M^2) \right]. \quad (5.1)$$

The results are

$$\begin{aligned} \sigma_L(Q^2) = \sigma_{\text{tot}}^{(0)}(Q^2) & \left[\frac{\alpha_s(R^2)}{4\pi} C_F[3] + \left(\frac{\alpha_s(R^2)}{4\pi} \right)^2 \left[C_F^2 \left\{ -\frac{15}{2} \right\} + C_A C_F \left\{ \right. \right. \\ & \left. \left. -11 \ln \frac{Q^2}{R^2} - \frac{24}{5} \zeta(3) + \frac{2023}{30} \right\} + n_f C_F T_f \left\{ 4 \ln \frac{Q^2}{R^2} - \frac{74}{3} \right\} \right], \end{aligned} \quad (5.2)$$

$$\begin{aligned} \sigma_T(Q^2) = \sigma_{\text{tot}}^{(0)}(Q^2) & \left[1 + \left(\frac{\alpha_s(R^2)}{4\pi} \right)^2 \left[C_F^2 \{6\} + C_A C_F \left\{ -\frac{196}{5} \zeta(3) - \frac{178}{30} \right\} \right. \right. \\ & \left. \left. + n_f C_F T_f \left\{ 16 \zeta(3) + \frac{8}{3} \right\} \right]. \end{aligned} \quad (5.3)$$

Addition of σ_L and σ_T yields the well known answer $\sigma_{\text{tot}}(Q^2)$ (see (2.19) and (2.20)) which is in agreement with the literature [37] (see also [11]). Hence (5.2) and (5.3) provides us with a check on our calculation of the longitudinal and transverse coefficient functions. Notice that in lowest order $\sigma_{\text{tot}}(Q^2)$ only receives a contribution from the transverse cross section (5.3) whereas the order α_s contribution can be only attributed to the longitudinal part in (5.2). In order α_s^2 both σ_L and σ_T contribute to σ_{tot} .

Because of the high sensitivity of expression (5.2) to the value of α_s , the longitudinal cross section provides us with an excellent tool to measure the running coupling

constant.

To illustrate the dependence of the cross sections on the running coupling constant we have plotted the ratios

$$R_L(Q^2) = \frac{\sigma_L(Q^2)}{\sigma_{\text{tot}}(Q^2)} = \frac{\alpha_s(R^2)}{4\pi} C_F[3] + \left(\frac{\alpha_s(R^2)}{4\pi} \right)^2 \left[C_F^2 \left\{ -\frac{33}{2} \right\} + C_A C_F \left\{ -11 \ln \frac{Q^2}{R^2} - 44\zeta(3) + \frac{123}{2} \right\} + n_f C_F T_f \left\{ 4 \ln \frac{Q^2}{R^2} - \frac{74}{3} \right\} \right], \quad (5.4)$$

and

$$R_T(Q^2) = \frac{\sigma_T(Q^2)}{\sigma_{\text{tot}}(Q^2)} = 1 - \frac{\sigma_L(Q^2)}{\sigma_{\text{tot}}(Q^2)}, \quad (5.5)$$

as a function of Q (CM-energy of the e^+e^- system) in fig. 11 and fig. 12 respectively. In fig. 11 we have shown R_L corrected up to order α_s (R_L^{LO}) and R_L corrected up to order α_s^2 (R_L^{NLO}). For R_L^{LO} we have used as input the leading log running coupling constant $\alpha_s^{LL}(n_f, \Lambda_{LO}^{(n_f)}, R^2)$ with $n_f = 5$ and $\Lambda_{LO}^{(5)} = 108$ MeV ($\alpha_s^{LL}(M_Z) = 0.122$). The input parameters of R_L^{NLO} are given by the next-to-leading log running coupling constant $\alpha_s^{NLL}(n_f, \Lambda_{\overline{\text{MS}}}^{(n_f)}, R^2)$ with $n_f = 5$ and $\Lambda_{\overline{\text{MS}}}^{(5)} = 227$ MeV ($\alpha_s^{NLL}(M_Z) = 0.118$). Further we have shown the variation of R_L on the renormalization scale R by choosing the values $R = Q/2, Q, 2Q$. Fig. 11 reveals that the order α_s^2 corrections are appreciable and they vary from 48% ($Q = 10$ GeV) down to 28% ($Q = 200$ GeV) with respect to the LO result. Furthermore one observes an improvement of the renormalization scale dependence while going from R_L^{LO} to R_L^{NLO} . In fig. 12 we have plotted R_T (5.5) up to first order (R_T^{NLO}) and up to second order (R_T^{NNLO}) in the running coupling constant. As input we have used for R_T^{NLO} and R_T^{NNLO} the coupling constants α_s^{LL} and α_s^{NLL} respectively. The features of fig. 12 are the same as those observed in fig. 11. In particular R_T^{NNLO} becomes less dependent on the renormalization scale as is shown for R^{NLO} . In figs. 11, 12 we have also presented the values R_L and R_T at $Q = M_Z$ measured by the OPAL-experiment [32] which are given by

$$R_L = 0.057 \pm 0.005, \quad (5.6)$$

$$R_T = 0.943 \pm 0.005. \quad (5.7)$$

One observes a considerable improvement in the ratios R_k ($k = T, L$) when the order α_s^2 contributions are included. However there is still a little discrepancy between R_L^{NLO} and R_T^{NNLO} , taken at $R = Q = M_Z$, and the data. This can either be removed by choosing a larger $\Lambda_{\overline{\text{MS}}}$ or by including the masses of the heavy quarks c and b in the calculation of the coefficient functions. Also a contribution of higher twist effects can maybe not neglected (see [40, 41]).

We now want to investigate the effect of the order α_s^2 contributions to the longitudinal and transverse fragmentation functions $F_L(x, Q^2)$ and $F_T(x, Q^2)$ as defined in (2.21). For our analysis we have chosen the fragmentation density sets in [63], [64] which will be called BKK1 and BKK2 respectively. The input parameters for α_s and the QCD scale Λ are the same as given below (5.5) except for BKK1 [63] where one has

chosen $\Lambda_{LO}^{(5)} = \Lambda_{\overline{\text{MS}}}^{(5)} = 190$ MeV. The definitions for F_L^{LO} and F_L^{NLO} are the same as those given above for R_L^{LO} and R_L^{NLO} respectively. However for both F_T^{NLO} (order α_s corrected) and F_T^{NNLO} (order α_s^2 corrected) we use $\alpha_s^{NLL}(5, \Lambda_{\overline{\text{MS}}}^{(5)}, R^2)$. In [63, 64] the fragmentation densities $D_p^H(z, M^2)$ have been determined for $H = \pi^+ + \pi^-$, $K^+ + K^-$ by fitting the total fragmentation function $F(x, Q^2) = \sum_H F^H(x, Q^2)$ (2.22) with $H = \pi^\pm, K^\pm, P, \bar{P}$ to the e^+e^- data in the range $5.2 < Q < 91.2$ GeV. Here the proton and anti-proton contributions to the fragmentation functions have been estimated like

$$F_k^{P+\bar{P}}(x, Q^2) = (1 + f(x)) F_k^{\pi^++\pi^-}(x, Q^2), \quad (5.8)$$

with

$$f(x) = 0.16, \quad \text{in [63]}, \quad (5.9)$$

$$f(x) = 0.195 - 1.35(x - 0.35)^2, \quad \text{in [64]}. \quad (5.10)$$

Further we introduce the notation

$$F_k(x, Q^2) = \sum_H F_k^H(x, Q^2), \quad (5.11)$$

where we sum over $H = \pi^+, \pi^-, K^+, K^-, P, \bar{P}$.

Notice that $f(x)$ in (5.10) becomes negative when $x > 0.73$ so that $F_k^{P+\bar{P}}(x, Q^2)$ ceases to be valid above this x -value. In [63] (BKK1) the fit has been only made to the TPC/2 γ -data [23] ($Q = 29$ GeV) whereas in [64] (BKK2) one also included the data coming from the ALEPH [28] and OPAL [30] collaboration. Since the range of Q -values covered by the BKK2 parametrization is larger than the one given by BKK1 the scale evolution of the fragmentation densities turns out to be better when the BKK2-set [64] is chosen. However this improvement goes at the expense of the description of the longitudinal fragmentation function $F_L(x, Q^2)$ as we will show below. For each set there exists a leading log and a next-to-leading log parametrization of $D_p^H(z, M^2)$ ($p = q, g$). The latter is presented in the $\overline{\text{MS}}$ -scheme so that we have to choose the corresponding coefficient functions in appendix A. Further we set the factorization scale M equal to the renormalization scale R .

In fig. 13 we have plotted $F_L(x, Q^2)$ in LO and NLO at $M = Q = M_Z$ and compared the results with the ALEPH [28] and OPAL [32] data. Here we have chosen the BKK1-set because the BKK2-set leads to a much worse result. The latter already happens in LO as was noticed in [64] where one had to choose a very small factorization scale. Here we have chosen the BKK1-set. We observe that F_L^{LO} is below the data in particular in the small x -region. The agreement with the data becomes better when the order α_s corrections are included although at very small x F_L^{NLO} is still smaller than the values given by experiment. In the case of the BKK2-set (not shown in the figure) one gets a result which is far below the data. This was already noticed in fig. 5 of [64] where one had to choose a very small factorization scale M ($M = 20$ GeV) to bring F_L^{LO} in agreement with experiment. In NLO the discrepancy between F_L^{NLO} , in the case of BKK2, and the data becomes even larger which is due to the kaon contribution. It turns out that the convolution of $D_p^{K^++K^-}(z, M^2)$ with the

order α_s^2 contribution from the coefficient functions given in (2.4), leads to a negative $F_L^{K^+K^-}$. This example illustrates the importance of the measurement of $F_L(x, Q^2)$ and the higher order corrections for the determination of the fragmentation densities. We have also shown the results for F_T^{NLO} and F_T^{NNLO} at $M = Q = M_Z$ in fig. 14 using the BKK1-set. Both fragmentation functions agree with the data except that F_T^{NNLO} gets a little bit worse at very small x . Furthermore F_T^{NLO} and F_T^{NNLO} hardly differ from each other which means that the order α_s^2 corrections are small. We do not expect that this will change when the three-loop splitting functions are included. One also notices that F_L constitutes the smallest part of the total fragmentation function $F = F_T + F_L$ which can be inferred from figs. 13, 14. This in particular holds at large x where $F_T \gg F_L$. Hence a fit of the fragmentation densities to the data of F_T is not sufficient to give a precise prediction for F_L and one has to include the data of the latter to provide us with better fragmentation densities. This in particular holds for $D_g^H(z, M^2)$ in the small z -region. The order α_s^2 contribution to F_L will certainly change the parametrization of the gluon fragmentation density given by ALEPH in [28] and OPAL in [32].

To illustrate the effect of the order α_s^2 contributions to the coefficient functions calculated in this paper at various e^+e^- collider energies we have studied the K -factors

$$K_L^H = \frac{F_L^{H,NLO}(x, Q^2)}{F_L^{H,LO}(x, Q^2)}, \quad (5.12)$$

$$K_T^H = \frac{F_T^{H,NNLO}(x, Q^2)}{F_T^{H,NLO}(x, Q^2)}. \quad (5.13)$$

In fig. 15 we have plotted (5.12) for $H = \pi^+ + \pi^-$ at $Q = 5.2, 10, 29, 35, 55, 91.2$ GeV choosing the BKK2-set since the latter shows a better scale evolution. From fig. 15 one infers that the corrections are large at small x where they vary between 2 ($Q = 5.2$ GeV) and 1.4 ($Q = 91.1$ GeV). The corrections become smaller when x increases. A similar plot is made for $K_T^{\pi^+ + \pi^-}$ in fig. 16. Here the order α_s^2 corrections are much smaller than in the longitudinal case except at large x where they are of the same size. Furthermore at low x the order α_s^2 corrections become negative ($K_T^{\pi^+ + \pi^-} < 1$) which is already revealed by fig. 14 for $Q = M_Z$. Again the largest correction occurs at smallest Q . This can be mainly attributed to the running coupling constant which becomes large when Q gets small. In fig. 17 we investigate the dependence of K_T (5.13) on the specific set of fragmentation densities used. The same was done for K_L (5.12) in [33] where we compared the BKK1-set with the one in [40] which is presented in the A-scheme. It turned out that K_L^H is very sensitive to the chosen parametrization. Choosing the set in [40] and $M = Q = M_Z$ it turns out that K_L is mildly dependent on x . Using the same input a similar observation can be made for K_T which shows a constant behaviour over the whole x -region (see fig. 17). On the other hand K_L (see fig. 2 in [33]) and K_T steeply rise when x tends to one if the BKK1 or BKK2 sets are chosen. Hence we conclude that the K -factors heavily depend on the chosen parametrization for the fragmentation densities.

In the next figures we study the factorization scale dependence of the fragmentation functions and show the decrease in sensitivity on the scale choice for M when higher

order corrections are included.

In fig. 18 we have plotted $F_L^{NLO}(x, Q^2)$ at three different scales $M = Q/2, Q, 2Q$ where $Q = M_Z$. Like in fig. 13 we have chosen the BKK1-set since in this case we get agreement with the data. From fig. 18 one infers that the scale variation of F_L is small and that all scales describe the data rather well. To show the improvement in the scale dependence more clearly it is convenient to plot the following quantity

$$\Delta_k^r(x, Q^2) = \frac{\max(F_k^r(\frac{1}{2}Q), F_k^r(Q), F_k^r(2Q)) - \min(F_k^r(\frac{1}{2}Q), F_k^r(Q), F_k^r(2Q))}{\text{average}(F_k^r(\frac{1}{2}Q), F_k^r(Q), F_k^r(2Q))}, \quad (5.14)$$

for $r = LO, NLO, NNLO$ and $k = T, L$.

In fig. 19 one can see that $\Delta_L^{NLO} < \Delta_L^{LO}$ as long as $x > 0.1$ which implies that F_L^{NLO} is less sensitive to the scale M than F_L^{LO} . The same observation is made for F_T (fig. 20) and Δ_T (fig. 21). In fig. 20 we have plotted F_T^{NLO} at the same scales as above. At all three scales the data are described very well. In addition we also show F_T^{NNLO} for $M = Q = M_Z$. At very small x we found that $F_T^{NNLO} < F_T^{NLO}$ for all three scales and F_T^{NNLO} is also below the data. In fig. 21 we see again an improvement while going from LO to NNLO except when $x < 0.1$. The reason that for $x < 0.1$ the scale dependence of F_k^{NLO} ($k = T, L$) is much larger than the one found in F_k^{LO} can be found in [63] where it is stated that the scale evolution of the fragmentation densities is only reliable in the region $0.1 < x < 0.9$.

Finally we also study the scale dependence of the fragmentation functions at a lower energy. As an example we take the total fragmentation function F^H with $H = \pi^+ + \pi^-$ (2.22) and investigate its behaviour for different choices of the factorization scale M where again $M = Q/2, Q, 2Q$. Contrary to the previous plots we have chosen the BKK2-set which range of validity is bounded by $Q \leq 100$ GeV and $0.1 < x < 0.8$. Further we take $Q = 29$ GeV and compare the theoretical result with the TPC/2 γ -data [23]. In fig. 22 we show $F^{H,NLO}$ at three different scales. The scale variation is small and only noticeable at large x . The data are very well described by $F^{H,NLO}$ at the three different scales except at very small x where the BKK2 parametrization is not reliable anymore. The same holds for $F^{H,NNLO}$ which hardly differs from $F^{H,NLO}$ so that even at lower energies the order α_s^2 corrections are very small. To show the improvement of the scale dependence in a better way we have plotted $\Delta^{H,LO}, \Delta^{H,NLO}$ and $\Delta^{H,NNLO}$ in fig. 23. A comparison with fig. 21 shows that there is essentially no difference between the Δ_k^r ($r = LO, NLO, NNLO, k = T, L$) taken at low ($Q = 29$ GeV) and high energies ($Q = M_Z = 91.2$ GeV).

Summarizing our paper we have computed the order α_s^2 contributions to the longitudinal and transverse coefficient functions. The effect of these contributions to the longitudinal and transverse cross sections are large which allow us for a better determination of the strong coupling constant α_s . The corrections to the longitudinal fragmentation function F_L^H are appreciable too which has important consequences for the determination of the gluon fragmentation density $D_g^H(z, M^2)$.

Furthermore one can now make a full NLO analysis of F_L^H . A NNLO description of the transverse structure function is still not possible because of the missing three-loop

DGLAP splitting functions. However the order α_s^2 contributions from the coefficient functions indicate that probably the NNLO corrections are very small.

Appendix A The coefficient functions in the $\overline{\text{MS}}$ -scheme

In this appendix we will present the explicit expressions for the coefficient functions of the fragmentation process in (2.1) which are calculated in section 4 in the $\overline{\text{MS}}$ -scheme. In order to make the presentation self contained we also give the order α_s contributions $\bar{c}_{k,p}^{(1)}$ (4.37)-(4.43) which have already been presented in the literature [40, 44, 45]. The coefficient functions $\bar{\mathbb{C}}_{k,p}$ ($p = q, g$) will be expanded in the renormalized coupling constant $\alpha_s \equiv \alpha_s(M^2)$ where we have chosen the renormalization scale R to be equal to the factorization scale M . If one wants to chose R different from M , $\alpha_s(M^2)$ has to be expressed into $\alpha_s(R^2)$ following the prescription in (4.45). In this paper we will only present the expressions for the transverse coefficient functions since the longitudinal ones are already shown in [33]. However we will make an exception for the order α_s^2 corrections to the non-singlet part $\mathbb{C}_{L,q}^{\text{NS}}$. For future purposes we want to split it into a part due to identical quark contributions (AB and CD in fig. 8) represented by $\bar{c}_{L,q}^{\text{NS,(2),id}}$ and a remaining part given by $\bar{c}_{L,q}^{\text{NS,(2),nid}}$ (see (4.37) and the discussion below (4.12)). The same will be done for the transverse coefficient $\bar{c}_{T,q}^{\text{NS,(2)}}$ in (4.38). The expression for the non-singlet coefficient is very long and we will split it up to the various contributions. First we have the soft plus virtual gluon contributions which are represented by the distributions $\delta(1-z)$ and $\mathcal{D}_0(z)$ (3.38). They are indicated by $\mathbb{C}_{T,q}^{\text{NS}}|_{S+V}$. The remaining part which is integrable at $z = 1$ will be called $\mathbb{C}_{T,q}^{\text{NS}}|_H$ where H refers to hard gluon contributions although $\mathbb{C}_{T,q}^{\text{NS}}|_H$ also originates from subprocesses with (anti) quarks in the final state (see fig. 8 except for C^2 and D^2). Following this prescription the non-singlet coefficient function is constituted by the following parts

$$\bar{\mathbb{C}}_{T,q}^{\text{NS}} = \bar{\mathbb{C}}_{T,q}^{\text{NS,nid}} + \bar{\mathbb{C}}_{T,q}^{\text{NS,id}}, \quad (\text{A1})$$

$$\bar{\mathbb{C}}_{T,q}^{\text{NS,nid}} = \bar{\mathbb{C}}_{T,q}^{\text{NS,nid}}|_{S+V} + \bar{\mathbb{C}}_{T,q}^{\text{NS,nid}}|_H, \quad (\text{A2})$$

$$\begin{aligned} \bar{\mathbb{C}}_{T,q}^{\text{NS,nid}}|_{S+V} &= \delta(1-z) + C_F \frac{\alpha_s}{4\pi} \left[(4\mathcal{D}_0(z) + 3\delta(1-z))L_M + 4\mathcal{D}_1(z) - 3\mathcal{D}_0(z) \right. \\ &\quad \left. + \delta(1-z)(-9 + 8\zeta(2)) \right] \\ &+ \left(\frac{\alpha_s}{4\pi} \right)^2 \left[C_F^2 \left\{ (16\mathcal{D}_1(z) + 12\mathcal{D}_0(z))L_M^2 + (24\mathcal{D}_2(z) - 12\mathcal{D}_1(z) + (16\zeta(2) \right. \right. \\ &\quad \left. \left. - 45)\mathcal{D}_0(z))L_M + \delta(1-z) \left[\left(\frac{9}{2} - 8\zeta(2) \right)L_M^2 + (40\zeta(3) + 24\zeta(2) \right. \right. \right. \\ &\quad \left. \left. \left. - \frac{51}{2} \right)L_M \right] \right\} \right] \end{aligned}$$

$$\begin{aligned}
& + C_A C_F \left\{ \left(-\frac{22}{3} \mathcal{D}_0(z) \right) L_M^2 + \left(-\frac{44}{3} \mathcal{D}_1(z) + \left(\frac{367}{9} - 8\zeta(2) \right) \mathcal{D}_0(z) \right) L_M \right. \\
& + \delta(1-z) \left[-\frac{11}{2} L_M^2 + \left(-12\zeta(3) - \frac{44}{3} \zeta(2) + \frac{215}{6} \right) L_M \right] \left. \right\} \\
& + n_f C_F T_f \left\{ \left(\frac{8}{3} \mathcal{D}_0(z) \right) L_M^2 + \left(\frac{16}{3} \mathcal{D}_1(z) - \frac{116}{9} \mathcal{D}_0(z) \right) L_M + \delta(1-z) \left[2L_M^2 \right. \right. \\
& + \left. \left. \left(\frac{16}{3} \zeta(2) - \frac{38}{3} \right) L_M \right] \right\} + \bar{c}_{T,q}^{\text{NS,(2),nid}} \Big|_{S+V}, \tag{A3}
\end{aligned}$$

with

$$\begin{aligned}
\bar{c}_{T,q}^{\text{NS,(2),nid}} \Big|_{S+V} & = C_F^2 \left[8\mathcal{D}_3(z) - 18\mathcal{D}_2(z) + (16\zeta(2) - 27)\mathcal{D}_1(z) + (-8\zeta(3) \right. \\
& + \left. \frac{51}{2})\mathcal{D}_0(z) + \delta(1-z) \left(30\zeta(2)^2 - 78\zeta(3) - 39\zeta(2) + \frac{331}{8} \right) \right] \\
& + C_A C_F \left[-\frac{22}{3} \mathcal{D}_2(z) + \left(\frac{367}{9} - 8\zeta(2) \right) \mathcal{D}_1(z) + (40\zeta(3) + \frac{44}{3} \zeta(2) \right. \\
& - \left. \frac{3155}{54})\mathcal{D}_0(z) + \delta(1-z) \left(-\frac{49}{5} \zeta(2)^2 + \frac{140}{3} \zeta(3) + \frac{215}{3} \zeta(2) - \frac{5465}{72} \right) \right] \\
& + n_f C_F T_f \left[\frac{8}{3} \mathcal{D}_2(z) - \frac{116}{9} \mathcal{D}_1(z) + \left(\frac{494}{27} - \frac{16}{3} \zeta(2) \right) \mathcal{D}_0(z) \right. \\
& + \left. \delta(1-z) \left(\frac{8}{3} \zeta(3) - \frac{76}{3} \zeta(2) + \frac{457}{18} \right) \right], \tag{A4}
\end{aligned}$$

$$\begin{aligned}
\bar{\mathbb{C}}_{T,q}^{\text{NS,nid}} \Big|_H & = C_F \frac{\alpha_s}{4\pi} \left[-2(1+z)L_M - 2(1+z)\ln(1-z) + 4\frac{1+z^2}{1-z}\ln z \right. \\
& + \left. 3(1-z) \right] + \left(\frac{\alpha_s}{4\pi} \right)^2 \left[C_F^2 \left\{ \left[-8(1+z)(\ln(1-z) - \frac{3}{4}\ln z) - \frac{8}{1-z}\ln z \right. \right. \right. \\
& - \left. \left. 10 - 2z \right] L_M^2 + \left[4(1+z)(\text{Li}_2(1-z) - 3\ln z \ln(1-z) - 3\ln^2(1-z) \right. \right. \\
& + \left. \left. \frac{11}{2}\ln^2 z - 2\zeta(2) \right) + \frac{32}{1-z}(\ln z \ln(1-z) - \ln^2 z + \frac{3}{2}\ln z) \right. \\
& + \left. \left. 4(1-z)\ln(1-z) - (52+20z)\ln z + 5 + 31z \right] L_M \right\}
\end{aligned}$$

$$\begin{aligned}
& + C_A C_F \left\{ \left[\frac{11}{3}(1+z)L_M^2 + \left[(1+z)(-2\ln^2 z + 4\zeta(2) + \frac{22}{3}\ln(1-z)) \right. \right. \right. \\
& \left. \left. \left. + \frac{34}{3}\ln z + \frac{1}{1-z}(4\ln^2 z - \frac{44}{3}\ln z) + \frac{7}{9} - \frac{275}{9}z \right] L_M \right\} \\
& + n_f C_F T_f \left\{ -\frac{4}{3}(1+z)L_M^2 + \left[-\frac{8}{3}(1+z)(\ln(1-z) + \ln z) \right. \right. \\
& \left. \left. + \frac{16}{3}\frac{1}{1-z}\ln z + \frac{28}{9} + \frac{52}{9}z \right] L_M \right\} + \bar{c}_{T,q}^{\text{NS,(2),mid}} \Big|_H \Big], \tag{A5}
\end{aligned}$$

with

$$\begin{aligned}
\bar{c}_{T,q}^{\text{NS,(2),mid}} \Big|_H & = C_F^2 \left[16(1+2z)(-2\text{Li}_3(-z) + \ln z \text{Li}_2(-z)) + \frac{1}{1-z}(96\text{Li}_3(-z) \right. \\
& + 72\zeta(3) - 48\ln z \text{Li}_2(-z) - 192S_{1,2}(1-z) - 24\text{Li}_3(1-z) + 8\ln(1-z) \cdot \\
& \cdot \text{Li}_2(1-z) - 80\ln z \text{Li}_2(1-z) + 20\ln z \ln^2(1-z) - 4\ln^2 z \ln(1-z) \\
& - \frac{80}{3}\ln^3 z + 120\zeta(2)\ln z + 12\text{Li}_2(1-z) - 12\ln z \ln(1-z) + 33\ln^2 z \\
& - 106\ln z + (1+z)(8\text{Li}_3(1-z) + 52\ln z \text{Li}_2(1-z) - 8\ln z \ln^2(1-z) \\
& + 8\ln^2 z \ln(1-z) - 64\zeta(2)\ln z - 32\zeta(3) + 17\ln^3 z - 4\ln^3(1-z)) \\
& + (100 + 116z)S_{1,2}(1-z) + (-16z)\zeta(2)\ln(1-z) + (-48 + 24z) \cdot \\
& \cdot \text{Li}_2(1-z) - (20 + 4z)\ln z \ln(1-z) + (8 + 4z)\ln^2(1-z) + (-45 \\
& - 23z + 8z^2 + \frac{12}{5}z^3)\ln^2 z + (20 - 36z - 16z^2 - \frac{24}{5}z^3)\zeta(2) + (-\frac{24}{5z^2} \\
& - \frac{16}{z} + 8 + 8z - 16z^2 - \frac{24}{5}z^3)(\text{Li}_2(-z) + \ln z \ln(1+z)) + (-29 + 67z) \cdot \\
& \cdot \ln(1-z) + (\frac{24}{5z} + \frac{218}{5} + \frac{248}{5}z + \frac{24}{5}z^2)\ln z - \frac{24}{5z} + \frac{187}{10} - \frac{187}{10}z + \frac{24}{5}z^2 \Big] \\
& + C_A C_F \left[8(1+2z)(2\text{Li}_3(-z) - \ln z \text{Li}_2(-z)) + \frac{1}{1-z}(-48\text{Li}_3(-z) \right. \\
& - 36\zeta(3) + 24\ln z \text{Li}_2(-z) + 24\text{Li}_3(1-z) - 8\ln(1-z)\text{Li}_2(1-z) \\
& - 8\ln z \text{Li}_2(1-z) + 6\ln^3 z - 24\zeta(2)\ln z - \frac{44}{3}\text{Li}_2(1-z)
\end{aligned}$$

$$\begin{aligned}
& -\frac{44}{3} \ln z \ln(1-z) - \frac{11}{3} \ln^2 z + \frac{206}{3} \ln z + (1+z)(-12\text{Li}_3(1-z)) \\
& + 4 \ln(1-z)\text{Li}_2(1-z) + 4 \ln z \text{Li}_2(1-z) + 12\zeta(2) \ln z - 2\zeta(3) - 3 \ln^2 z \\
& + \frac{34}{3} \text{Li}_2(1-z) + \frac{34}{3} \ln z \ln(1-z) + \frac{11}{3} \ln^2(1-z) + (4-4z)S_{1,2}(1-z) \\
& + (8z)\zeta(2) \ln(1-z) + \left(\frac{47}{6} + \frac{47}{6}z - 4z^2 - \frac{6}{5}z^3\right) \ln^2 z + \left(-\frac{28}{3} - \frac{28}{3}z + 8z^2 \right. \\
& \left. + \frac{12}{5}z^3\right)\zeta(2) + \left(\frac{12}{5z^2} + \frac{8}{z} - 4 - 4z + 8z^2 + \frac{12}{5}z^3\right)(\text{Li}_2(-z) + \ln z \ln(1+z)) \\
& + \left(\frac{97}{9} - \frac{383}{9}z\right) \ln(1-z) - \left(\frac{12}{5z} + \frac{122}{15} + \frac{184}{5}z + \frac{12}{5}z^2\right) \ln z + \frac{12}{5z} \\
& \left. + \frac{2513}{270} + \frac{3587}{270}z - \frac{12}{5}z^2 \right] \\
& + n_f C_F T_f \left[\frac{8}{3} \frac{1+z^2}{1-z} (\text{Li}_2(1-z) + \ln z \ln(1-z)) + \frac{1}{4} \ln^2 z + \frac{4}{3} (1+z) \cdot \right. \\
& \left. \cdot (2\zeta(2) - \ln^2(1-z)) + \left(\frac{28}{9} + \frac{52}{9}z\right) \ln(1-z) + \left(\frac{20}{3} + 12z - \frac{64}{3} \frac{1}{1-z}\right) \ln z \right. \\
& \left. - \frac{118}{27} - \frac{34}{27}z \right], \tag{A6}
\end{aligned}$$

$$\begin{aligned}
\overline{\mathbb{C}}_{T,q}^{\text{NS},(2),\text{id}} &= \left(\frac{\alpha_s}{4\pi}\right)^2 \left[(C_F^2 - \frac{1}{2}C_A C_F) \left\{ \left[4 \frac{1+z^2}{1+z} (-4\text{Li}_2(-z) - 4 \ln z \ln(1+z)) \right. \right. \right. \\
& \left. \left. \left. + \ln^2 z - 2\zeta(2) + 8(1+z) \ln(z) + 16(1-z) \right] L_M \right\} + \overline{c}_{T,q}^{\text{NS},(2),\text{id}} \right], \tag{A7}
\end{aligned}$$

$$\begin{aligned}
\overline{c}_{T,q}^{\text{NS},(2),\text{id}} &= (C_F^2 - \frac{1}{2}C_A C_F) \left[16 \frac{1+z^2}{1+z} (\text{Li}_3\left(\frac{1-z}{1+z}\right) - \text{Li}_3\left(-\frac{1-z}{1+z}\right)) \right. \\
& + \frac{1}{2} S_{1,2}(1-z) - \text{Li}_3(1-z) - S_{1,2}(-z) + \frac{1}{2} \text{Li}_3(-z) + \frac{1}{2} \ln z \text{Li}_2(1-z) \\
& - \ln(1-z)\text{Li}_2(-z) - \ln(1+z)\text{Li}_2(-z) - \ln z \text{Li}_2(-z) - \frac{1}{2} \zeta(2) \ln(1-z) \\
& - \frac{1}{2} \zeta(2) \ln(1+z) - \zeta(2) \ln z - \ln z \ln(1-z) \ln(1+z) + \frac{1}{4} \ln^2 z \ln(1-z) \\
& \left. - \frac{1}{2} \ln z \ln^2(1+z) - \frac{3}{4} \ln^2 z \ln(1+z) + \frac{3}{8} \ln^3 z + \frac{1}{2} \zeta(3) - \frac{1}{2} \ln z \right]
\end{aligned}$$

$$\begin{aligned}
& + 16(1+z)(-S_{1,2}(-z) + \frac{1}{2}\text{Li}_3(-z) - \ln(1+z)\text{Li}_2(-z) - \frac{1}{2}\ln z \ln^2(1+z)) \\
& + \frac{1}{4}\ln^2 z \ln(1+z) - \frac{1}{2}\zeta(2)\ln(1+z) + \frac{1}{2}\zeta(3) + \frac{1}{2}\text{Li}_2(1-z) \\
& + \frac{1}{2}\ln z \ln(1-z) + \left(-\frac{24}{5z^2} + \frac{16}{z} + 16z^2 - \frac{24}{5}z^3\right)(\text{Li}_2(-z)) \\
& + \ln z \ln(1+z) + (-4 + 4z + 16z^2 - \frac{24}{5}z^3)\zeta(2) + (12 + 8z - 8z^2 \\
& + \frac{12}{5}z^3)\ln^2 z + 16(1-z)\ln(1-z) + \left(\frac{24}{5z^2} + \frac{118}{5} - \frac{42}{5}z + \frac{24}{5}z^2\right)\ln z \\
& - \left[\frac{24}{5z} + \frac{46}{5} - \frac{46}{5}z + \frac{24}{5}z^2\right]. \tag{A8}
\end{aligned}$$

Notice that the identical quark contribution in (A7) and (A8) carries the colour factor $C_F^2 - \frac{1}{2}C_A C_F$.

The purely singlet coefficient function becomes

$$\begin{aligned}
\overline{\mathbb{C}}_{T,q}^{\text{PS}} &= \left(\frac{\alpha_s}{4\pi}\right)^2 \left[C_F T_f \left\{ 8(1+z)\ln z + \frac{16}{3z} + 4 - 4z - \frac{16}{3}z^2 \right\} L_M^2 \right. \\
& + C_F T_f \left\{ 16(1+z)(\text{Li}_2(1-z) + \ln z \ln(1-z)) + \frac{3}{2}\ln^2 z + \left(\frac{32}{3z} + 8 - 8z \right. \right. \\
& - \left. \left. \frac{32}{3}z^2\right)\ln(1-z) + \left(\frac{64}{3z} - 8 - 40z - \frac{32}{3}z^2\right)\ln z - \frac{16}{3z} - \frac{184}{3} + \frac{136}{3}z \right. \\
& \left. \left. + \frac{64}{3}z^2 \right\} L_M + \overline{c}_{T,q}^{\text{PS},(2)} \right], \tag{A9}
\end{aligned}$$

$$\begin{aligned}
\overline{c}_{T,q}^{\text{PS},(2)} &= C_F T_f \left[8(1+z)(6S_{1,2}(1-z) - 2\text{Li}_3(1-z) + 2\ln(1-z)\text{Li}_2(1-z)) \right. \\
& + 6\ln z \text{Li}_2(1-z) - 2\zeta(2)\ln z + \ln z \ln^2(1-z) + 3\ln^2 z \ln(1-z) \\
& + \frac{11}{6}\ln^3 z + \left(\frac{64}{3z} - 8 - 40z - \frac{32}{3}z^2\right)(\text{Li}_2(1-z) + \ln z \ln(1-z)) + \left(\frac{16}{3z} + 4 \right. \\
& - \left. 4z - \frac{16}{3}z^2\right)\ln^2(1-z) + \left(\frac{64}{3z} - 14 - 14z + \frac{16}{3}z^2\right)\ln^2 z - \left(\frac{32}{3z} + 32 + 32z \right. \\
& + \left. \frac{32}{3}z^2\right)(\text{Li}_2(-z) + \ln z \ln(1+z)) + \left(-\frac{64}{3z} - 8 - 24z + \frac{32}{3}z^2\right)\zeta(2) + \left(-\frac{16}{3z} \right. \\
& - \left. \frac{184}{3} + \frac{136}{3}z + \frac{64}{3}z^2\right)\ln(1-z) - \left(\frac{32}{3z} + \frac{400}{3} + \frac{208}{3}z + \frac{256}{9}z^2\right)\ln z
\end{aligned}$$

$$\left. -\frac{160}{27z} - \frac{236}{3} + \frac{140}{3}z + \frac{1024}{27}z^2 \right]. \quad (\text{A10})$$

The gluonic coefficient function is equal to

$$\begin{aligned} \overline{\mathbb{C}}_{T,g} = & C_F \frac{\alpha_s}{4\pi} \left[\left\{ \frac{8}{z} - 8 + 4z \right\} L_M + \left(\frac{8}{z} - 8 + 4z \right) (\ln(1-z) + 2 \ln z) - \frac{8}{z} + 8 \right] \\ & + \left(\frac{\alpha_s}{4\pi} \right)^2 \left[C_F^2 \left\{ \left[\left(\frac{16}{z} - 16 + 8z \right) \ln(1-z) + (8-4z) \ln z + 8 - 2z \right] L_M^2 \right. \right. \\ & + \left[\left(\frac{64}{z} - 48 + 24z \right) (\text{Li}_2(1-z) + \ln z \ln(1-z)) + \left(\frac{32}{z} - 32 + 16z \right) \cdot \right. \\ & \cdot (\ln^2(1-z) - 2\zeta(2)) + (24 - 12z) \ln^2 z + \left(-\frac{48}{z} + 64 - 12z \right) \ln(1-z) \\ & \left. \left. + (-16 + 20z) \ln z + \frac{8}{z} - 20 + 8z \right] L_M \right. \\ & + C_A C_F \left\{ \left[\left(\frac{16}{z} - 16 + 8z \right) \ln(1-z) - \left(\frac{16}{z} + 16 + 16z \right) \ln z - \frac{124}{3z} \right. \right. \\ & \left. \left. + 32 + 4z + \frac{16}{3}z^2 \right] L_M^2 + \left[- \left(\frac{64}{z} + 48z \right) \text{Li}_2(1-z) - (64 + 16z) \cdot \right. \right. \\ & \left. \left. \cdot \ln z \ln(1-z) + \left(\frac{32}{z} + 32 + 16z \right) (\text{Li}_2(-z) + \ln z \ln(1+z)) + \left(\frac{96}{z} \right. \right. \right. \\ & \left. \left. - 64 + 48z \right) \zeta(2) + \left(\frac{16}{z} - 16 + 8z \right) \ln^2(1-z) - \left(\frac{64}{z} + 48 + 56z \right) \ln^2 z \right. \\ & \left. \left. + \left(-\frac{344}{3z} + 96 - 8z + \frac{32}{3}z^2 \right) \ln(1-z) + \left(-\frac{400}{3z} + 64 + 40z + \frac{32}{3}z^2 \right) \ln z \right. \right. \\ & \left. \left. + \frac{188}{3z} - \frac{32}{3} - \frac{100}{3}z - \frac{32}{3}z^2 \right] L_M + \bar{c}_{T,g}^{(2)} \right], \quad (\text{A11}) \end{aligned}$$

$$\begin{aligned} \bar{c}_{T,g}^{(2)} = & C_F^2 \left[\left(\frac{16}{z} + 32 + 16z \right) (4S_{1,2}(-z) + 4 \ln(1+z) \text{Li}_2(-z) + 2 \ln z \ln^2(1+z) \right. \\ & - \ln^2 z \ln(1+z) + 2\zeta(2) \ln(1+z)) + \left(\frac{32}{z} - 192 + 32z \right) \text{Li}_3(-z) + \left(-\frac{160}{z} \right. \\ & + 240 - 120z \right) S_{1,2}(1-z) - \frac{16}{z} \text{Li}_3(1-z) + \left(\frac{48}{z} - 32 + 16z \right) \ln(1-z) \cdot \\ & \left. \cdot \text{Li}_2(1-z) + (48 - 24z) \ln z \text{Li}_2(1-z) + \left(-\frac{32}{z} + 64 - 32z \right) \ln z \text{Li}_2(-z) \right] \end{aligned}$$

$$\begin{aligned}
& + \left(\frac{40}{3z} - \frac{40}{3} + \frac{20}{3}z \right) \ln^3(1-z) + \left(\frac{44}{3} - \frac{22}{3}z \right) \ln^3 z + \left(\frac{48}{z} - 40 + 20z \right) \cdot \\
& \cdot \ln z \ln^2(1-z) + \left(\frac{32}{z} - 8 + 4z \right) \ln^2 z \ln(1-z) + \left(\frac{16}{z} - 48 + 24z \right) \cdot \\
& \cdot \zeta(2) \ln(1-z) + (-16 + 8z) \zeta(2) \ln z + \left(\frac{112}{z} - 208 + 40z \right) \zeta(3) + \left(-\frac{96}{z} \right. \\
& + 80 - 28z \text{Li}_2(1-z) + \left(-\frac{96}{z} + 80 - 12z \right) \ln z \ln(1-z) + \left(-\frac{64}{5z^2} \right. \\
& - 64 - 96z + \frac{16}{5}z^3 \text{Li}_2(-z) + \ln z \ln(1+z) \left. \right) + \left(-\frac{48}{z} + 56 - 14z \right) \cdot \\
& \cdot \ln^2(1-z) + \left(-32 + 83z - \frac{8}{5}z^3 \right) \ln^2 z + \left(\frac{96}{z} - 112 - 44z + \frac{16}{5}z^3 \right) \zeta(2) \\
& + \left(\frac{8}{z} - 24z \right) \ln(1-z) + \left(\frac{144}{5z} + \frac{418}{5} - \frac{262}{5}z - \frac{16}{5}z^2 \right) \ln z + \frac{316}{5z} - \frac{604}{5} \\
& + \frac{154}{5}z - \frac{16}{5}z^2 \left. \right] \\
& + C_A C_F \left[\left(\frac{16}{z} + 32 + 16z \right) \left(-2S_{1,2}(-z) - 2 \ln(1+z) \text{Li}_2(-z) \right. \right. \\
& + \ln z \text{Li}_2(-z) - \ln z \ln^2(1+z) - \zeta(2) \ln(1+z) \left. \right) + \left(\frac{32}{z} + 32 + 16z \right) \cdot \\
& \cdot \left(\text{Li}_3 \left(-\frac{1-z}{1+z} \right) - \text{Li}_3 \left(\frac{1-z}{1+z} \right) + \ln z \ln(1-z) \ln(1+z) + \ln(1-z) \cdot \right. \\
& \cdot \text{Li}_2(-z) \left. \right) + \left(\frac{48}{z} + 32 + 16z \right) \text{Li}_3(-z) + \left(-\frac{240}{z} - 160z \right) S_{1,2}(1-z) + \left(\frac{48}{z} \right. \\
& + 80 + 40z \text{Li}_3(1-z) - \left(\frac{48}{z} + 16 + 40z \right) \ln(1-z) \text{Li}_2(1-z) - \left(\frac{192}{z} + 32 \right. \\
& + 144z \ln z \text{Li}_2(1-z) + \left(\frac{8}{3z} - \frac{8}{3} + \frac{4}{3}z \right) \ln^3(1-z) - \left(\frac{160}{3z} + \frac{88}{3} \right. \\
& + \frac{124}{3}z \left. \right) \ln^3 z - \left(\frac{8}{z} + 24 + 12z \right) \ln z \ln^2(1-z) - \left(\frac{48}{z} + 64 + 48z \right) \cdot \\
& \cdot \ln^2 z \ln(1-z) + \left(\frac{16}{z} + 32 \right) \zeta(2) \ln(1-z) + \left(\frac{224}{z} - 96 + 128z \right) \zeta(2) \ln z \\
& + \left(\frac{40}{z} + 48 + 24z \right) \ln^2 z \ln(1+z) + \left(\frac{8}{z} + 40 + 12z \right) \zeta(3) + \left(-\frac{304}{3z} + 32 \right.
\end{aligned}$$

$$\begin{aligned}
& + 24z + \frac{32}{3}z^2) \text{Li}_2(1-z) + \left(-\frac{496}{3z} + 96 + 16z + \frac{32}{3}z^2\right) \ln z \ln(1-z) \\
& + \left(\frac{80}{3z} + 80 + 56z + \frac{32}{3}z^2\right) (\text{Li}_2(-z) + \ln z \ln(1+z)) + \left(-\frac{172}{3z} + 48 - 8z \right. \\
& + \frac{16}{3}z^2) \ln^2(1-z) + \left(-\frac{232}{3z} - 16 + 2z - \frac{16}{3}z^2\right) \ln^2 z + \left(\frac{136}{3z} + 40z \right. \\
& - \frac{32}{3}z^2) \zeta(2) + \left(\frac{356}{3z} - \frac{236}{3} - \frac{4}{3}z - \frac{32}{3}z^2\right) \ln(1-z) + \left(\frac{496}{3z} + \frac{772}{3} \right. \\
& \left. + \frac{172}{3}z + \frac{256}{9}z^2\right) \ln z + \frac{4438}{27z} - 36 - 106z - \frac{928}{27}z^2 \left. \right]. \quad (\text{A12})
\end{aligned}$$

Finally we also present the non-singlet longitudinal coefficient function (see also eq. (17) in [33])

$$\begin{aligned}
\overline{\mathbb{C}}_{L,q}^{\text{NS}} &= \frac{\alpha_s}{4\pi} C_F \left[2 \right] + \left(\frac{\alpha_s}{4\pi} \right)^2 \left[C_F^2 \left\{ (8 \ln(1-z) - 4 \ln z + 2 + 4z) L_M \right\} \right. \\
& \left. + C_A C_F \left\{ -\frac{22}{3} L_M \right\} + n_f C_F T_f \left\{ \frac{8}{3} L_M \right\} + \overline{c}_{L,q}^{\text{NS,(2),nid}} + \overline{c}_{L,q}^{\text{NS,(2),id}} \right], \quad (\text{A13})
\end{aligned}$$

$$\begin{aligned}
\overline{c}_{L,q}^{\text{NS,(2),nid}} &= C_F^2 \left\{ 16S_{1,2}(1-z) - 32\text{Li}_3(-z) + 16 \ln z \text{Li}_2(-z) - 16\zeta(2) \ln(1-z) \right. \\
& - 12\text{Li}_2(1-z) + 4 \ln z \ln(1-z) + 4 \ln^2(1-z) + (-10 + 8z + 4z^2 + \frac{8}{5}z^3) \cdot \\
& \cdot \ln^2 z + (24 - 16z - 8z^2 - \frac{16}{5}z^3) \zeta(2) + \left(\frac{24}{5z^2} + \frac{16}{z} - 16z - 8z^2 - \frac{16}{5}z^3\right) \cdot \\
& \cdot (\text{Li}_2(-z) + \ln z \ln(1+z)) + (14 + 4z) \ln(1-z) + \left(-\frac{24}{5z} - \frac{78}{5} + \frac{32}{5}z \right. \\
& \left. + \frac{16}{5}z^2\right) \ln z + \frac{24}{5z} - \frac{211}{5} + \frac{86}{5}z + \frac{16}{5}z^2 \left. \right\} \\
& + C_A C_F \left\{ -8S_{1,2}(1-z) + 16\text{Li}_3(-z) - 8 \ln z \text{Li}_2(-z) + 8\zeta(2) \ln(1-z) \right. \\
& + \left(-\frac{12}{5z^2} - \frac{8}{z} + 8z + 4z^2 + \frac{8}{5}z^3\right) (\text{Li}_2(-z) + \ln z \ln(1+z)) \\
& + (2 - 4z - 2z^2 - \frac{4}{5}z^3) (\ln^2 z - 2\zeta(2)) - \frac{46}{3} \ln(1-z) + \left(\frac{12}{5z} + \frac{22}{15} + \frac{4}{5}z \right. \\
& \left. - \frac{8}{5}z^2\right) \ln z - \frac{12}{5z} + \frac{2017}{45} - \frac{254}{15}z - \frac{8}{5}z^2 \left. \right\}
\end{aligned}$$

$$+n_f C_F T_f \left\{ \frac{8}{3}(\ln(1-z) + \ln z) - \frac{100}{9} + \frac{8}{3}z \right\}, \quad (\text{A14})$$

$$\begin{aligned} \bar{c}_{L,q}^{\text{NS,(2),id}} = & (C_F^2 - \frac{1}{2}C_A C_F) \left[32S_{1,2}(1-z) - 16\text{Li}_3(-z) + 32\ln(1+z)\text{Li}_2(-z) \right. \\ & + 16\zeta(2)\ln(1+z) + 16\ln z \ln^2(1+z) - 8\ln^2 z \ln(1+z) - 16\zeta(3) + \left(\frac{24}{5z^2} \right. \\ & - \frac{16}{z} - 16 - 16z + 8z^2 - \frac{16}{5}z^3)(\text{Li}_2(-z) + \ln z \ln(1+z)) + (4 + 8z - 4z^2 \\ & + \frac{8}{5}z^3)(\ln^2 z - 2\zeta(2)) + \left. \left(-\frac{24}{5z} + \frac{112}{5} - \frac{8}{5}z + \frac{16}{5}z^2 \right) \ln z + \frac{24}{5z} + \frac{64}{5} - \frac{104}{5}z \right. \\ & \left. + \frac{16}{5}z^2 \right]. \quad (\text{A15}) \end{aligned}$$

The remaining coefficient functions $\bar{\mathbb{C}}_{L,q}^{\text{PS}}$ and $\bar{\mathbb{C}}_{L,g}$ can be found in eqs. (19) and (20) respectively of [33].

Appendix B The coefficient functions in the annihilation scheme (A-scheme)

A glance at the coefficient functions in the A-scheme as presented in (4.52)-(4.57) reveals that they are all expressed into the $\overline{\text{MS}}$ -representation of the DGLAP splitting functions $P_{ij}^{(k)}$ and the longitudinal coefficients $\bar{c}_{L,p}^{(k)}$ ($p = q, g$). The longitudinal coefficient functions in the A-scheme are already given in eqs. (21)-(23) of [33] and we only add those formulae needed to construct the transverse coefficient functions $\mathbb{C}_{T,p}$ in the latter scheme. For $\mathbb{C}_{T,q}^{\text{NS}}$ (4.53) we have to compute the following convolutions

$$\begin{aligned} \frac{1}{2}(R^{(1)} \delta(1-z) - \bar{c}_{L,q}^{(1)}) \otimes P_{qq}^{(0)} = C_F^2 \left[12\mathcal{D}_0(z) + 9\delta(1-z) - 16 \ln(1-z) \right. \\ \left. + 8 \ln z - 10 - 14z \right], \end{aligned} \quad (\text{B1})$$

and

$$\begin{aligned} (R^{(1)} \delta(1-z) - \bar{c}_q^{(1)}) \otimes \bar{c}_{L,q}^{(1)} = C_F^2 \left[20\text{Li}_2(1-z) - 4 \ln^2(1-z) + 4 \ln z \ln(1-z) \right. \\ \left. + 4 \ln^2 z - 16\zeta(2) + (10 - 4z) \ln(1-z) + (4 - 8z) \ln z + 18 + 6z \right]. \end{aligned} \quad (\text{B2})$$

Note that apart from $R^{(1)}$, $R^{(2)}$ the non logarithmic (L_M) contributions to $\mathbb{C}_{L,q}^{\text{NS}}$ (4.52) and $\mathbb{C}_{T,q}^{\text{NS}}$ (4.53) have an opposite sign. The same observation holds for the coefficient functions $\mathbb{C}_{k,q}^{\text{PS}}$ (4.54), (4.55) and $\mathbb{C}_{k,g}$ (4.56), (4.57). For $\mathbb{C}_{k,g}$ we need the convolutions

$$\begin{aligned} P_{qq}^{(0)} \otimes \bar{c}_g^{(1)} = C_F^2 \left[\left(\frac{192}{z} - 160 + 80z \right) \text{Li}_2(1-z) + \left(\frac{64}{z} - 64 + 32z \right) \right. \\ \cdot \ln^2(1-z) + \left(\frac{128}{z} - 96 + 48z \right) \ln z \ln(1-z) + (32 - 16z) \ln^2 z \\ \left. + \left(-\frac{64}{z} + 64 - 32z \right) \zeta(2) + (32 - 8z) \ln(1-z) + (-64 + 32z) \ln z - \frac{80}{z} \right. \\ \left. + 96 - 16z \right], \end{aligned} \quad (\text{B3})$$

and

$$\begin{aligned} \bar{c}_g^{(1)} \otimes \bar{c}_{L,q}^{(1)} = C_F^2 \left[16\text{Li}_2(1-z) + 16 \ln^2 z + 16 \ln z \ln(1-z) + \left(\frac{16}{z} - 8 - 8z \right) \right. \\ \left. \cdot \ln(1-z) + \left(\frac{32}{z} + 16 - 16z \right) \ln z + \frac{32}{z} - 56 + 24z \right]. \end{aligned} \quad (\text{B4})$$

References

- [1] “QCD 20 years later”, vol. 1, Editors: P.M. Zerwas and H.A. Kastrup, World Scientific, Singapore 1992
- [2] J. Mnich, Phys. Rep **271** (1996) 181
- [3] T. Matsuura, R. Hamberg, and W.L. van Neerven, Nucl. Phys. **B345** (1990) 331
- [4] R. Hamberg, W.L. van Neerven, and T. Matsuura, Nucl. Phys. **B359** (1991) 343
- [5] W.L. van Neerven, and E.B. Zijlstra, Nucl. Phys. **B382** (1992) 11
- [6] E.B. Zijlstra, and W.L. van Neerven, Nucl. Phys. **B383** (1992) 525
- [7] E.B. Zijlstra, and W.L. van Neerven, Phys. Lett. **297B** (1992) 377
- [8] S.A. Larin and J.A.M. Vermaseren, Phys. Lett. **256B** (1991) 345
- [9] S.A. Larin, F.V. Tkachov and J.A.M. Vermaseren, Phys. Rev. Lett. **66** (1991) 862
- [10] S.A. Larin, T. van Ritbergen, and J.A.M. Vermaseren, Nucl. Phys. **B427** (1994) 41
- [11] S.G. Gorishni, A.L. Kataev, and S.A. Larin, Phys. Lett. **159B** (1991) 144
- [12] L.R. Surguladze, and M.A. Samuel, Phys. Rev. Lett. **66** (1991) 560, Erratum Phys. Rev. Lett. **66** (1991) 2416
- [13] K.G. Chetyrkin and O.V. Tarasov, Phys. Lett. **B327** (1994) 114
- [14] S.A. Larin, T. van Ritbergen, and J.A.M. Vermaseren, Phys. Lett. **B320** (1994) 159
- [15] S.A. Larin, T. van Ritbergen, and J.A.M. Vermaseren, Nucl. Phys. **B438** (1995) 278
- [16] K.G. Chetyrkin and F.V. Tkachov, Nucl. Phys. **B192** (1981) 159
- [17] D.I. Kazakov and A.B. Kotikov, Nucl. Phys. **B307** (1988) 721
- [18] Brandelik *et al.* (DASP Collaboration), Nucl. Phys. **B148** (1979) 189
- [19] H. Albrecht *et al.* (ARGUS), Z. Phys. **C44** (1989) 547
- [20] W. Braunschweig *et al.* (TASSO), Z. Phys. **C42** (1989) 189
- [21] W. Braunschweig *et al.* (TASSO), Z. Phys. **C47** (1990) 187
- [22] A. Peterson *et al.* (Mark II), Phys. Rev. **D37** (1988) 1
- [23] H. Aihara *et al.* (TPC/2 γ Collaboration), Phys. Rev. Lett. **61** (1988) 1263

- [24] O. Podobrin (CELLO), Ph. D. thesis, Universität Hamburg
- [25] T. Kumita *et al.* (AMY), Phys. Rev. **D42** (1990) 1339
- [26] Y.K. Li *et al.* (AMY), Phys. Rev. **D41** (1990) 2675
- [27] P. Abreu *et al.* (DELPHI), Phys. Lett. **B311** (1993) 408
- [28] D. Buskulic *et al.* (ALEPH), Phys. Lett. **B357** (1995) 487
- [29] D. Buskulic *et al.* (ALEPH), Z. Phys. **C66** (1995) 355
- [30] R. Akers *et al.* (OPAL), Z. Phys. **C58** (1993) 387
- [31] R. Akers *et al.* (OPAL), Z. Phys. **C63** (1994) 181
- [32] R. Akers *et al.* (OPAL), Z. Phys. **C68** (1995) 203
- [33] P.J. Rijken and W.L. van Neerven, INLO-PUB-4/96, hep-ph/9604436, to be published in Phys. Lett. B
- [34] V.N. Gribov and L.N. Lipatov, Sov. J. Nucl. Phys. **15** (1972) 675
- [35] G. Altarelli and G. Parisi, Nucl. Phys. **B126** (1977) 298
- [36] Yu.L. Dokshitzer, Sov. Phys. JETP **46** (1977) 641
- [37] K.E. Chetyrkin, A.L. Kataev, and F.V. Tkachov, Phys. Lett. **85B** (1979) 277
- [38] M. Dine, and J. Sapirstein, Phys. Rev. Lett. **43** (1979) 668
- [39] W. Celmaster, and R.J. Gonsalves, Phys. Rev. Lett. **44** (1980) 560
- [40] P. Nason, and B.R. Webber, Nucl. Phys. **B421** (1994) 473
- [41] B.R. Webber, Cavendish Laboratory Report Nos. Cavendish-HEP-94/17, hep-ph/9411384, 1994 (unpublished)
- [42] J.A.M. Vermaseren, FORM2, published by Computer Algebra Nederland (CAN), Kruislaan 413, 1089 SJ Amsterdam, The Netherlands
- [43] S.A. Larin, Phys. Lett. **303B** (1993) 113
- [44] R. Baier, and K. Fey, Z. Phys. **C2** (1979) 339
- [45] G. Altarelli, R.K. Ellis, G. Martinelli, and S.-Y. Pi, Nucl. Phys. **B160** (1979) 301
- [46] T. Matsuura, and W.L. van Neerven, Z. Phys. **C38** (1988) 623
- [47] T. Matsuura, S.C. van der Marck, and W.L. van Neerven, Nucl. Phys. **B319** (1989) 570

- [48] G. Kramer and B. Lampe, *Z. Phys.* **C34** (1987); Erratum **C42** (1989) 504
- [49] G. Pasarino and M. Veltman, *Nucl. Phys.* **B160** (1979) 151
- [50] W. Beenakker, Ph. D. thesis University of Leiden, The Netherlands (1989)
- [51] W. Beenakker, H. Kuijf, W.L. van Neerven, and J. Smith, *Phys. Rev.* **D40** (1989) 54
- [52] Erdélyi, Magnus, Oberhettinger, Tricomi, “Higher Transcendental functions”, Bateman Manuscript Project. Vol 1, McGraw-Hill 1953
- [53] G. Altarelli, R.K. Ellis, and G. Martinelli, *Nucl. Phys.* **B157** (1979) 461
- [54] B. Humpert, and W.L. Van Neerven, *Nucl. Phys.* **B184** (1981) 225
- [55] G. Curci, W. Furmanski, and R. Petronzio, *Nucl. Phys.* **B175** (1980) 27
- [56] W. Furmanski, and R. Petronzio, *Phys. Lett.* **97B** (1980) 437
- [57] W. Furmanski, and R. Petronzio, *Z. Phys.* **C11** (1982) 293
- [58] E.G. Floratos, C. Kounnas, and R. Lacaze, *Nucl. Phys.* **B192** (1981) 417
- [59] R. Barbieri, J.A. Mignaco, and E. Remiddi, *Nuovo Cim.* **11A** (1972) 824
- [60] L. Lewin, “Polylogarithms and Associated Functions” (North Holland, Amsterdam 1983)
- [61] A. Devoto, and D.W. Duke, *Riv. Nuovo Cim.* **7-6** (1984) 1
- [62] R. Mertig and W.L. van Neerven, *Z. Phys.* **C70** (1996) 637
- [63] J. Binnewies, B.A. Kniehl, and G. Kramer, *Z. Phys.* **C65** (1995) 471
- [64] J. Binnewies, B.A. Kniehl, and G. Kramer, *Phys. Rev.* **D52** (1995) 4947.

Figure captions

Fig. 1 Kinematics of the process $e^+e^- \rightarrow H + "X"$.

Fig. 2 Born contribution given by the subprocess $V \rightarrow "q" + \bar{q}$.

Fig. 3 One-loop correction to the subprocess $V \rightarrow "q" + \bar{q}$. Graphs with external self energies are omitted since they do not contribute in the case of massless quarks.

Fig. 4 Graphs contributing to the subprocess $V \rightarrow "q" + \bar{q} + g$ and $V \rightarrow "g" + q + \bar{q}$.

Fig. 5 Two-loop corrections to the subprocess $V \rightarrow "q" + \bar{q}$. Graphs with external self energies are omitted since they do not contribute in the case of massless quarks.

Fig. 6 One-loop corrections to the subprocesses $V \rightarrow "q" + \bar{q} + g$ and $V \rightarrow "g" + q + \bar{q}$. Graphs with external self energies are omitted since they do not contribute in the case of massless quarks and gluons.

Fig. 7 Graphs contributing to the subprocesses $V \rightarrow "q" + \bar{q} + g + g$ and $V \rightarrow "g" + q + \bar{q} + g$.

Fig. 8 Graphs contributing to the subprocess $V \rightarrow "q" + \bar{q}(1) + q + \bar{q}(2)$. The cross (\times) indicates that the process is exclusive with respect to the quark denoted by " q ". If $\bar{q}(1) \neq \bar{q}(2)$ only combinations A and C have to be considered. When $\bar{q}(1) = \bar{q}(2)$ combinations B and D have to be added to A and C.

Fig. 9 Cut diagrams obtained from the groups C and D in fig. 8 contributing to the process $V \rightarrow "q" + \bar{q}(1) + q + \bar{q}(2)$.

Fig. 10 Cut diagrams resulting from the combinations AD and BC in fig. 8 contributing to $V \rightarrow "q" + \bar{q}(1) + q + \bar{q}(2)$ in the case that $\bar{q}(1) = \bar{q}(2)$.

Fig. 11 The ratio $R_L = \sigma_T/\sigma_{\text{tot}}$. Dotted lines: R_L^{LO} ; solid lines: R_L^{NLO} . Lower curve: $R = 2Q$; middle curve: $R = Q$; upper curve: $R = Q/2$. The data point at $Q = M_Z$ is from OPAL [32].

Fig. 12 The ratio $R_L = \sigma_T/\sigma_{\text{tot}}$. Dotted lines: R_T^{NLO} ; R_T^{NNLO} . Lower curve: $R = 2Q$; middle curve: $R = Q$; upper curve: $R = Q/2$. The data point at $Q = M_Z$ is from OPAL [32].

Fig. 13 The longitudinal fragmentation function $F_L(x, Q^2)$ at $M = Q = M_Z$. Dotted line: F_L^{LO} ; solid line: F_L^{NLO} . The data are from ALEPH [28] and OPAL [32]. The fragmentation density set is BKK1 [63].

Fig. 14 The transverse fragmentation function $F_T(x, Q^2)$ at $M = Q = M_Z$. Dotted line: F_T^{NLO} ; solid line: F_T^{NNLO} . The data are from ALEPH [28] and OPAL [32]. The fragmentation density set is BKK1 [63].

Fig. 15 The ratio $K_L^H = F_L^{H,NLO}/F_L^{H,LO}$ with $H = \pi^+ + \pi^-$ at $M = Q$ for different

values of Q . Upper dotted line: $Q = 5.2$ GeV; solid line $Q = 10$ GeV; long dashed line: $Q = 29$ GeV; short dashed line: $Q = 35$ GeV; lower dotted line: $Q = 55$ GeV; dashed-dotted line: $Q = 91.2$ GeV. The fragmentation density set is BKK2 [64].

Fig. 16 The same as in fig. 19 but now for the ratio $K_T^H = F_T^{H,NNLO}/F_T^{H,NLO}$ with $H = \pi^+ + \pi^-$.

Fig. 17 The dependence of K_T on the fragmentation density sets at $M = Q = M_Z$. Dotted curve: set from [40]; solid curve: BKK1 [63]; dashed curve: BKK2 [64].

Fig. 18 The mass factorization scale dependence of F_L^{NLO} at $Q = M_Z$. Lower dotted curve: $M = 2Q$; middle dotted curve: $M = Q$; upper dotted curve: $M = Q/2$. The data are from ALEPH [28] and OPAL [32]. The fragmentation density set is BKK1 [63]

Fig. 19 Sensitivity of F_L^r ($r = LO, NLO$) to the mass factorization scale represented by Δ_L^r (5.14) at $Q = M_Z$. Dotted line: Δ_L^{LO} ; solid line: Δ_L^{NLO} . The fragmentation density set is BKK1 [63].

Fig. 20 The same as in fig. 18 but now for F_T^{NLO} . Also presented is the curve for F_T^{NNLO} (solid line).

Fig. 21 The same as in fig. 19 but now for Δ_T^r (5.14). Also shown is Δ_T^{NNLO} (dashed line).

Fig. 22 The mass factorization scale dependence of the total fragmentation function $F^{H,NLO}$ with $H = \pi^+ + \pi^-$ at $Q = 29$ GeV. Lower dotted curve: $M = 2Q$; middle dotted curve: $M = Q$; upper dotted curve: $M = Q/2$; solid line: $F_T^{H,NNLO}$. The data are from TPC/2 γ [23]. The fragmentation density set is BKK2 [64].

Fig. 23 Sensitivity of $F^{H,r}$ ($r = LO, NLO, NNLO$) to the mass factorization scale represented by $\Delta^{H,r}$ with $H = \pi^+ + \pi^-$ at $Q = 29$ GeV. Dotted line: $\Delta^{H,LO}$; solid line: $\Delta^{H,NLO}$; dashed line: $\Delta^{H,NNLO}$. The fragmentation density set is BKK2 [64].

Table 1
List of parton subprocesses in e^+e^- annihilation up to order α_s^2 .

figure	Parton subprocesses	
2	$\alpha_s^0: V \rightarrow q + \bar{q}$	
3	$\alpha_s^1: V \rightarrow q + \bar{q}$	(one loop correction)
4	$V \rightarrow "q" + \bar{q} + g$	
4	$V \rightarrow q + \bar{q} + "g"$	
5	$\alpha_s^2: V \rightarrow q + \bar{q}$	(two loop correction)
6	$V \rightarrow "q" + \bar{q} + g$	(one loop correction)
7	$V \rightarrow "q" + \bar{q} + g + g$	
6	$V \rightarrow q + \bar{q} + "g"$	(one loop correction)
7	$V \rightarrow q + \bar{q} + "g" + g$	
8	$V \rightarrow "q" + \bar{q} + q' + \bar{q}'$	

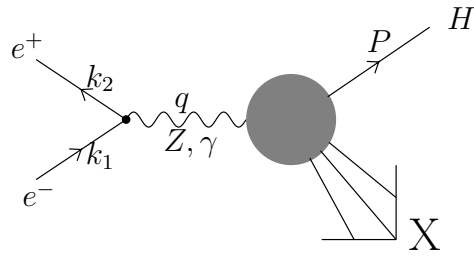


Fig. 1

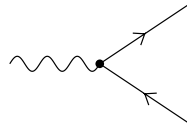


Fig. 2

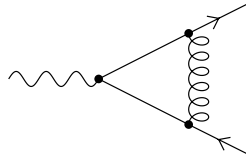


Fig. 3

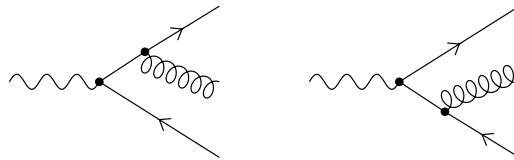


Fig. 4

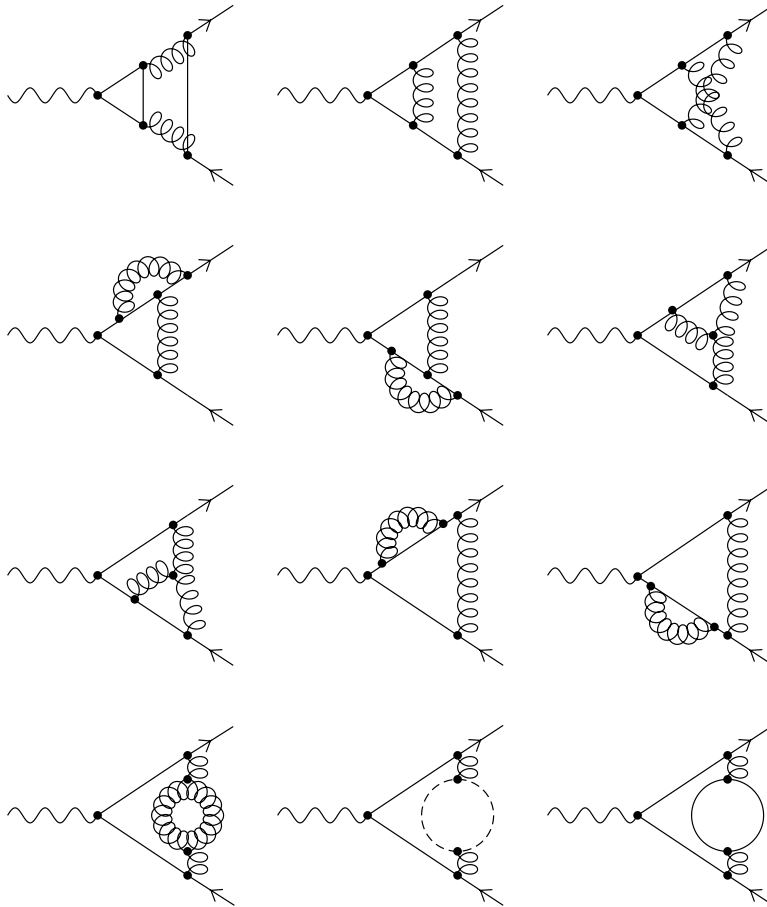


Fig. 5

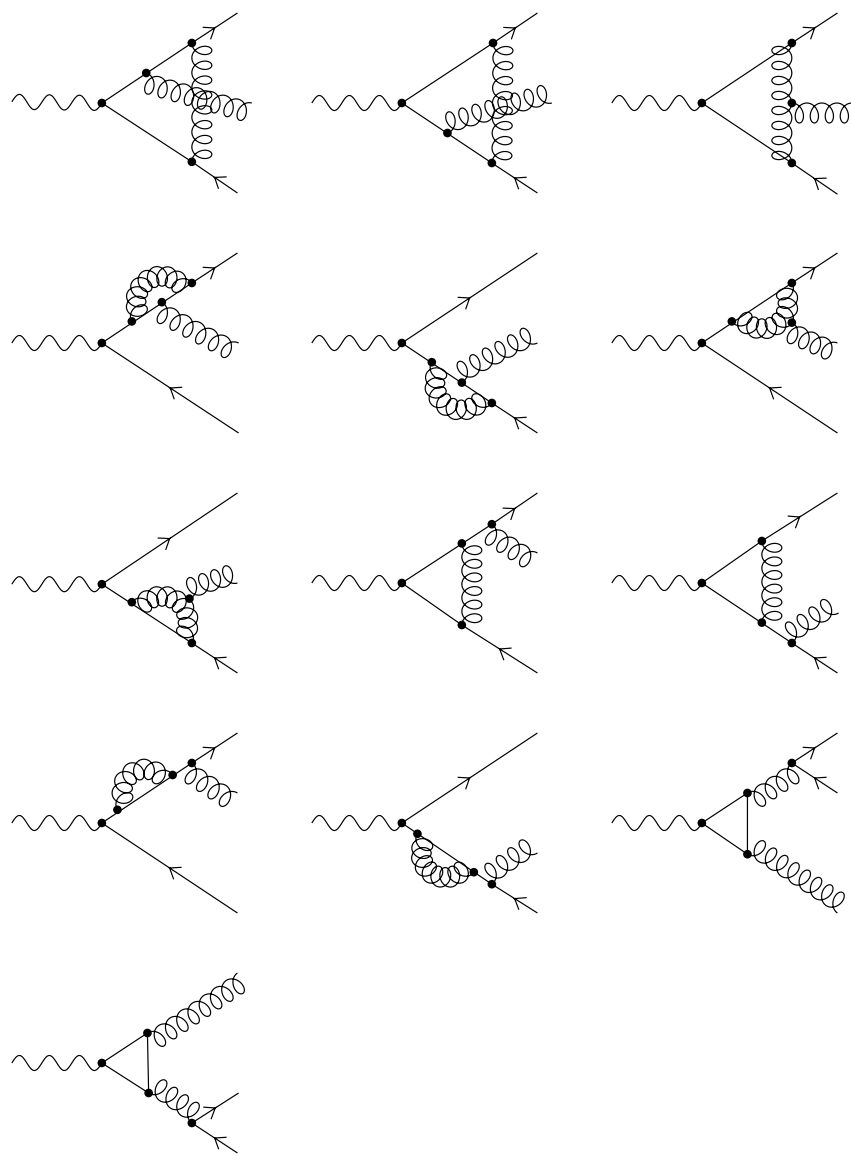


Fig. 6

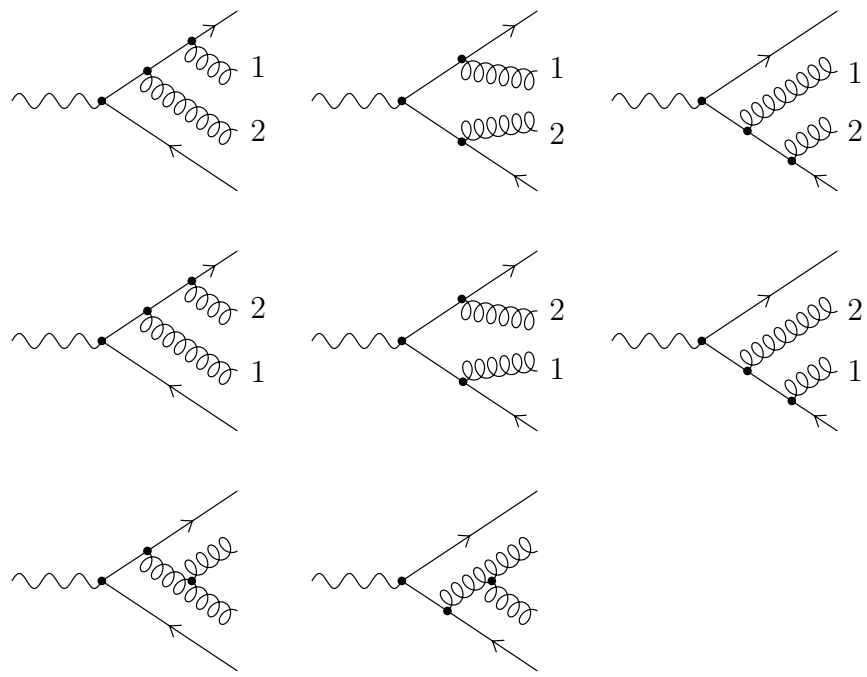


Fig. 7

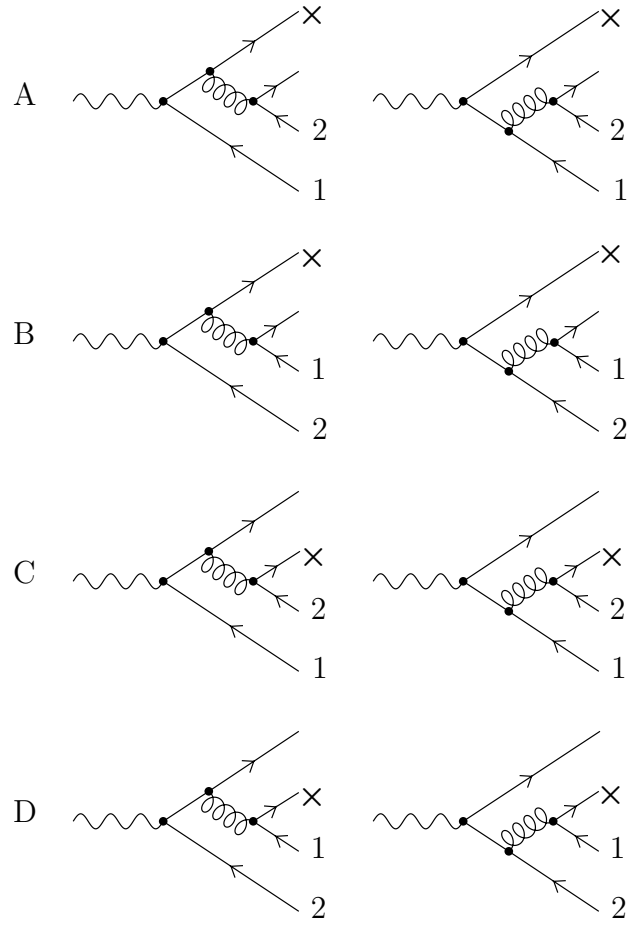


Fig. 8

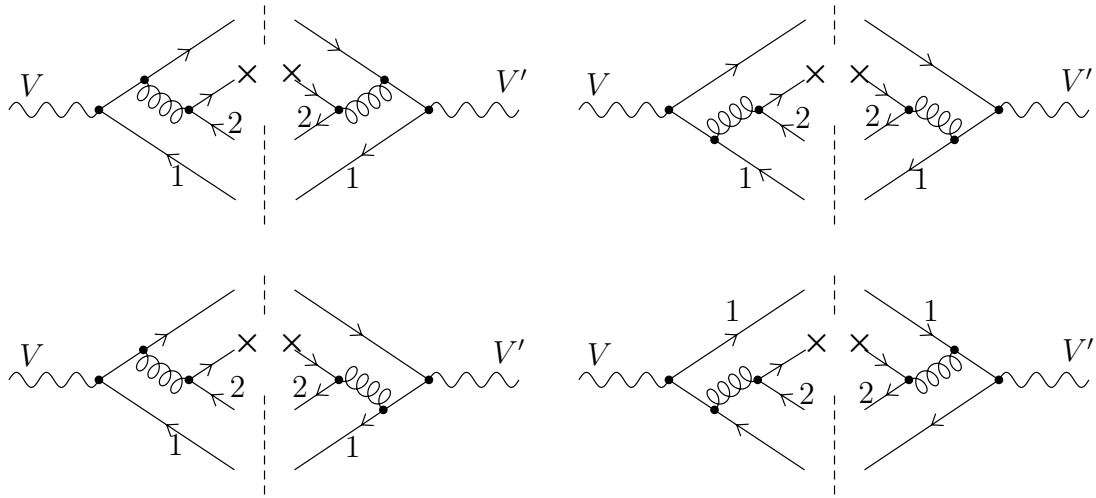


Fig. 9

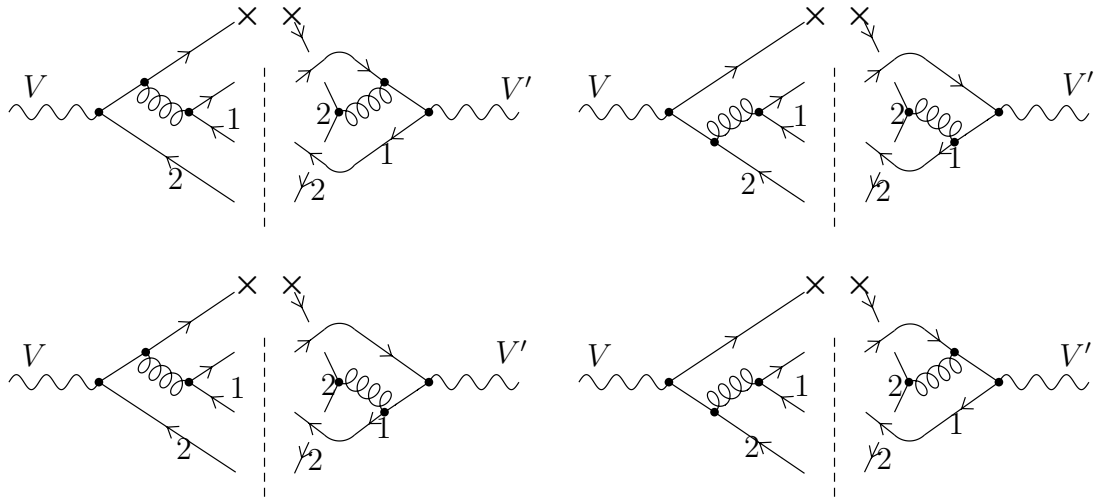


Fig. 10

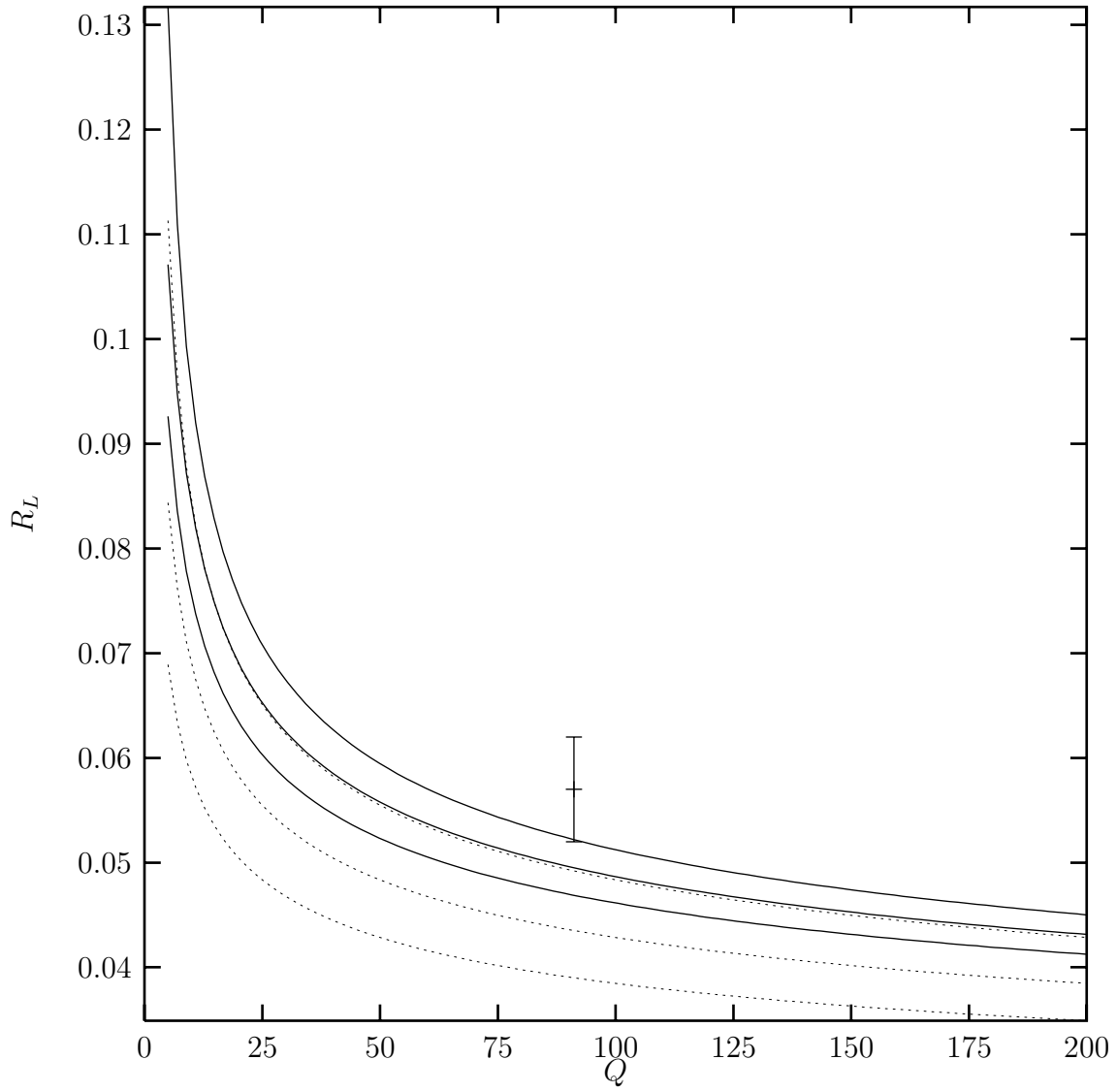


Fig. 11

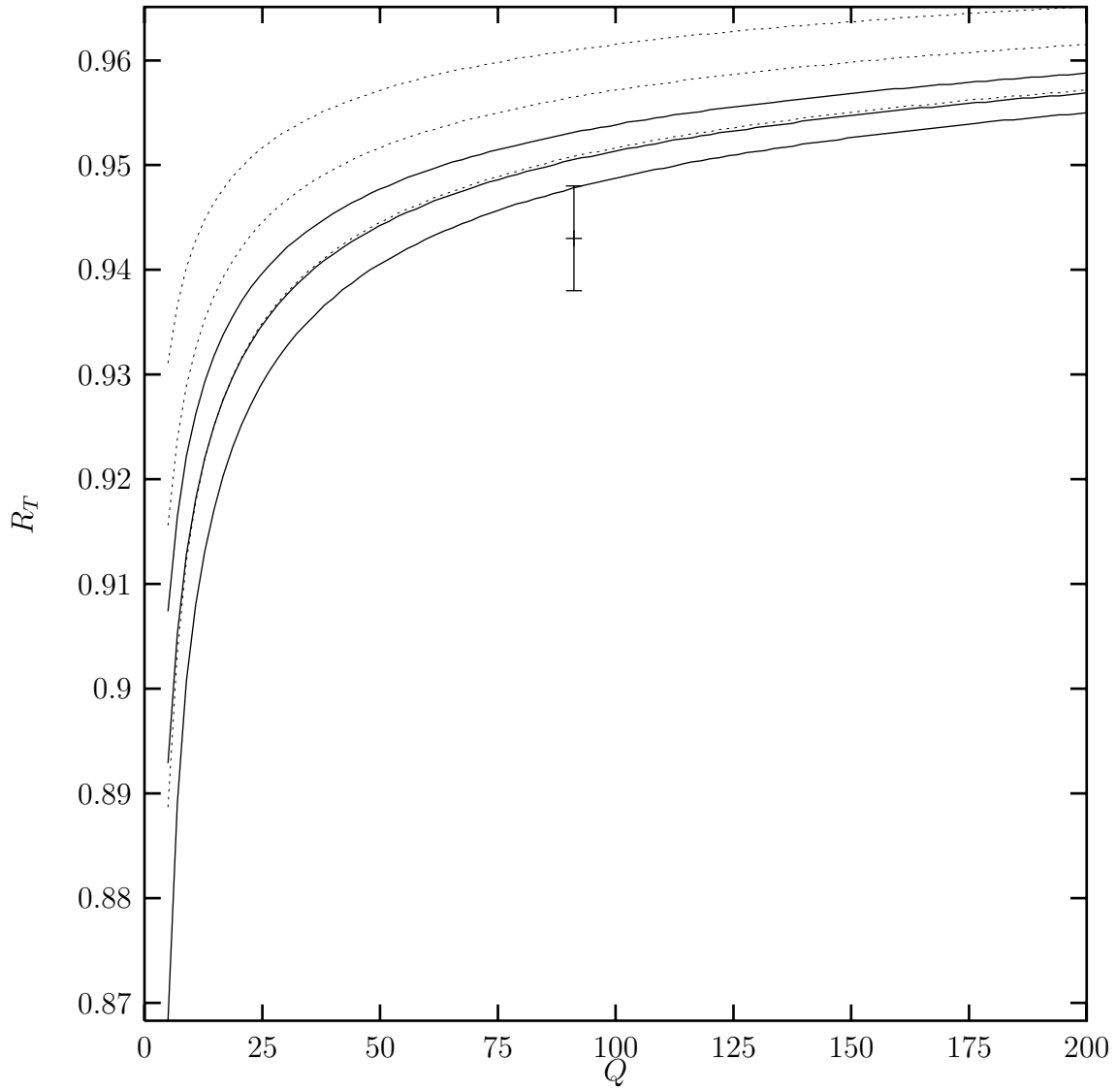


Fig. 12

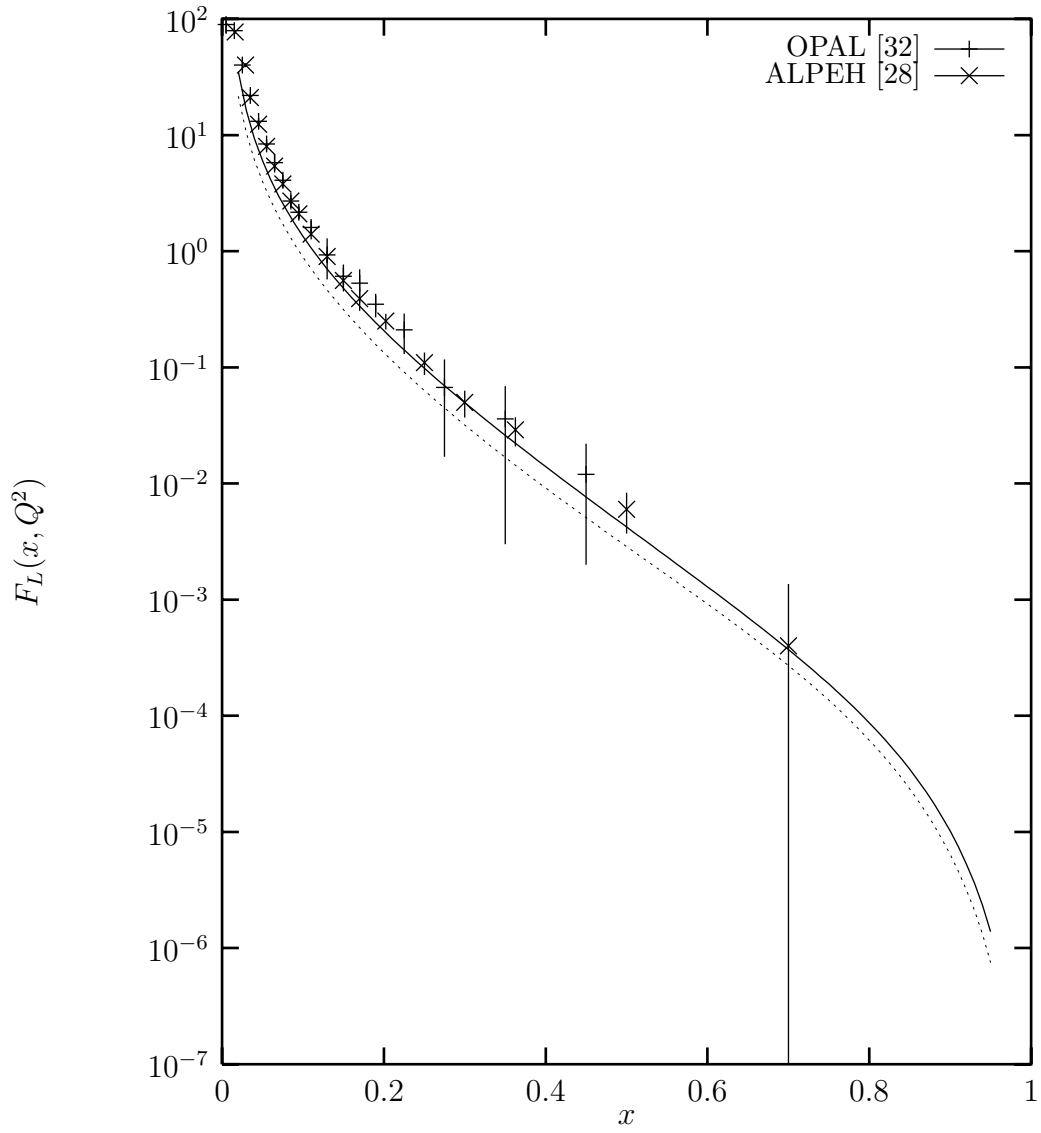


Fig. 13

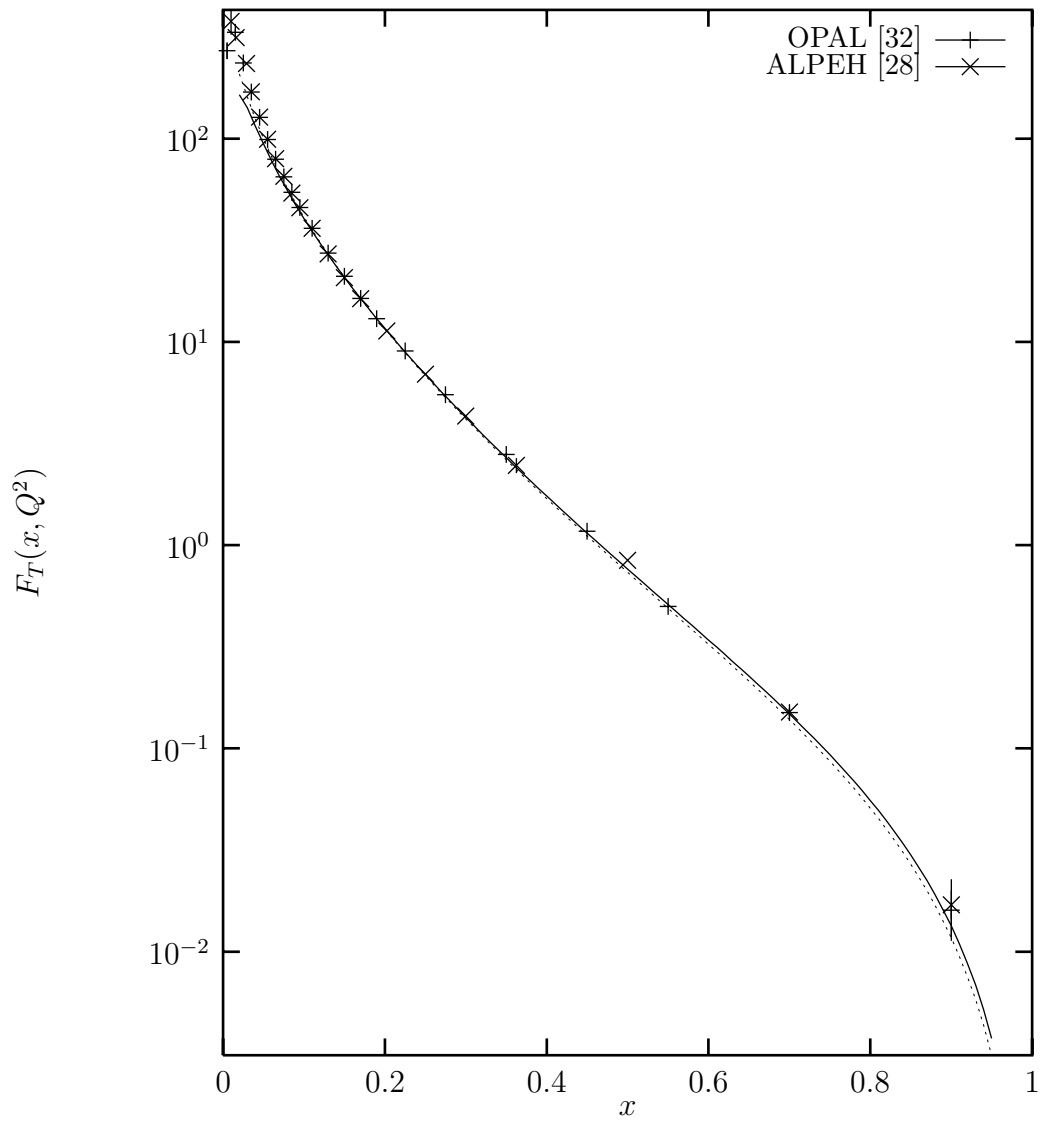


Fig. 14

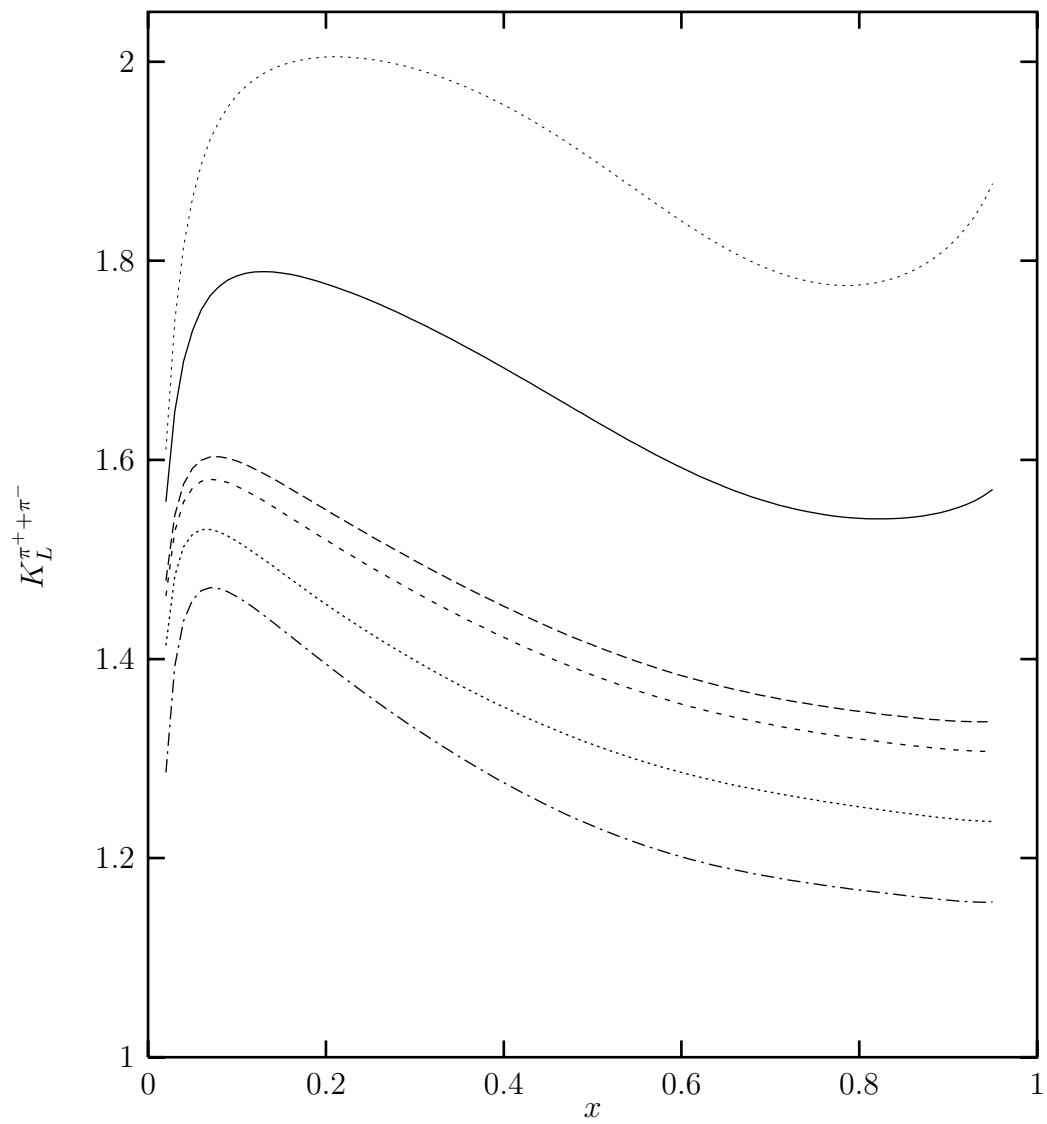


Fig. 15

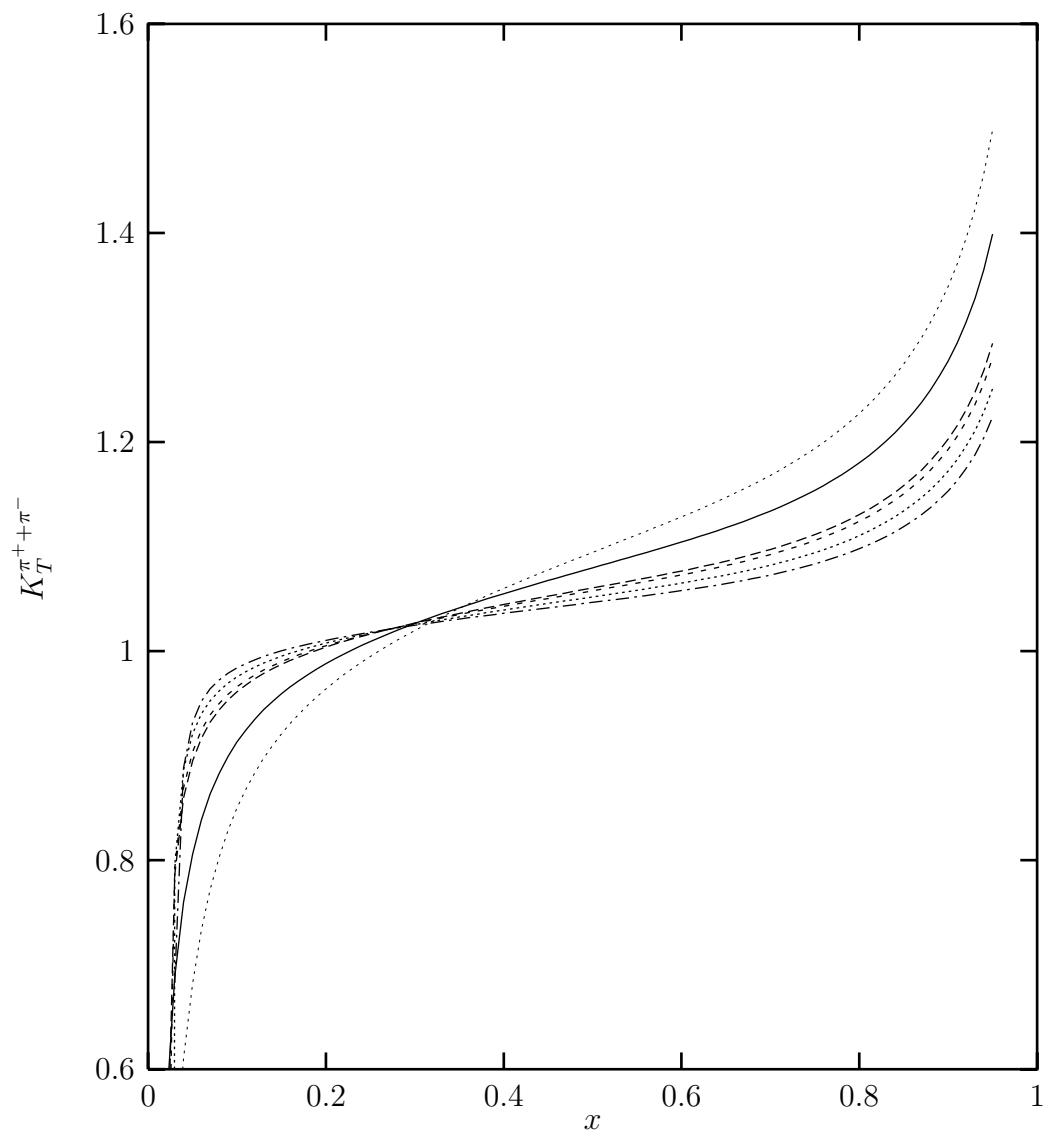


Fig. 16

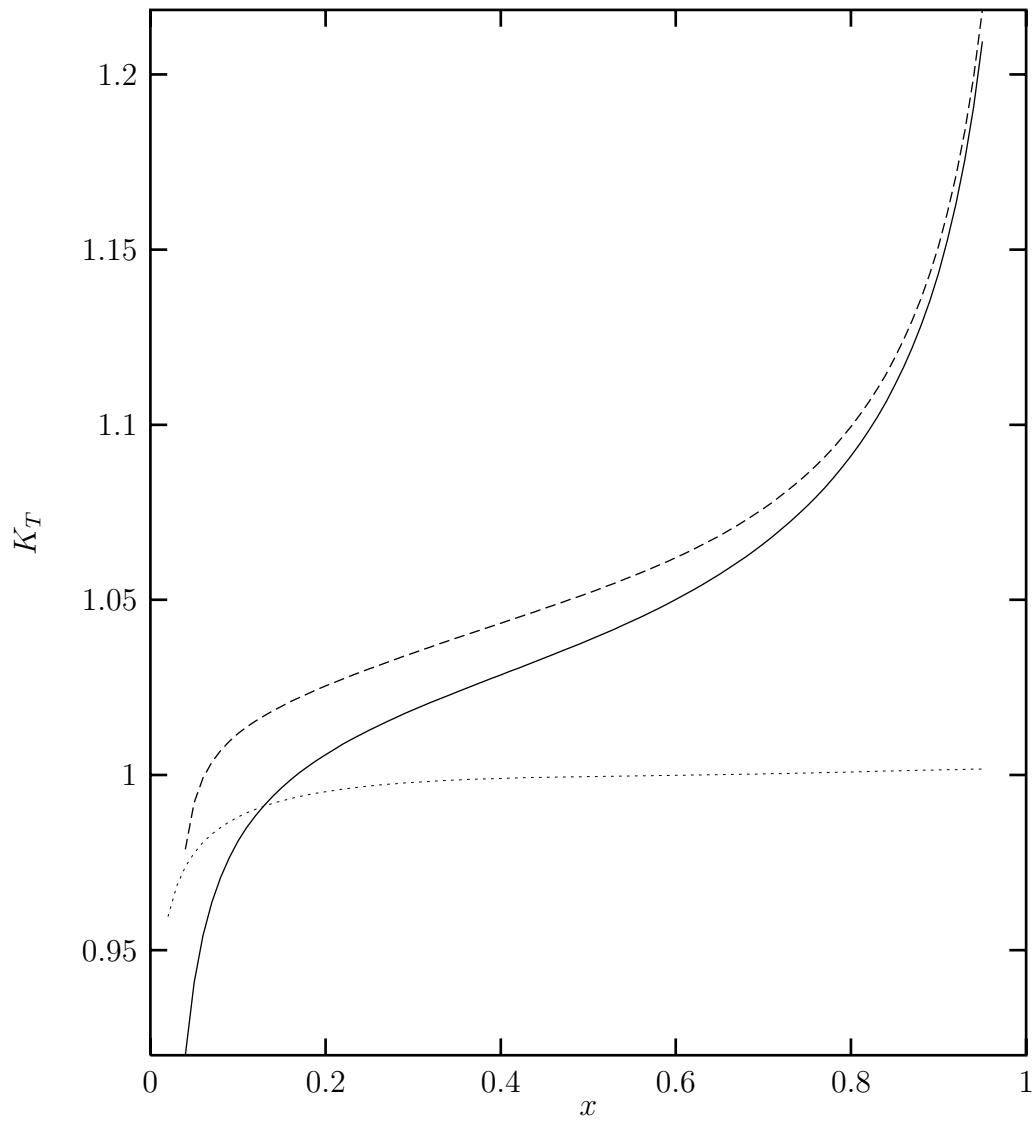


Fig. 17

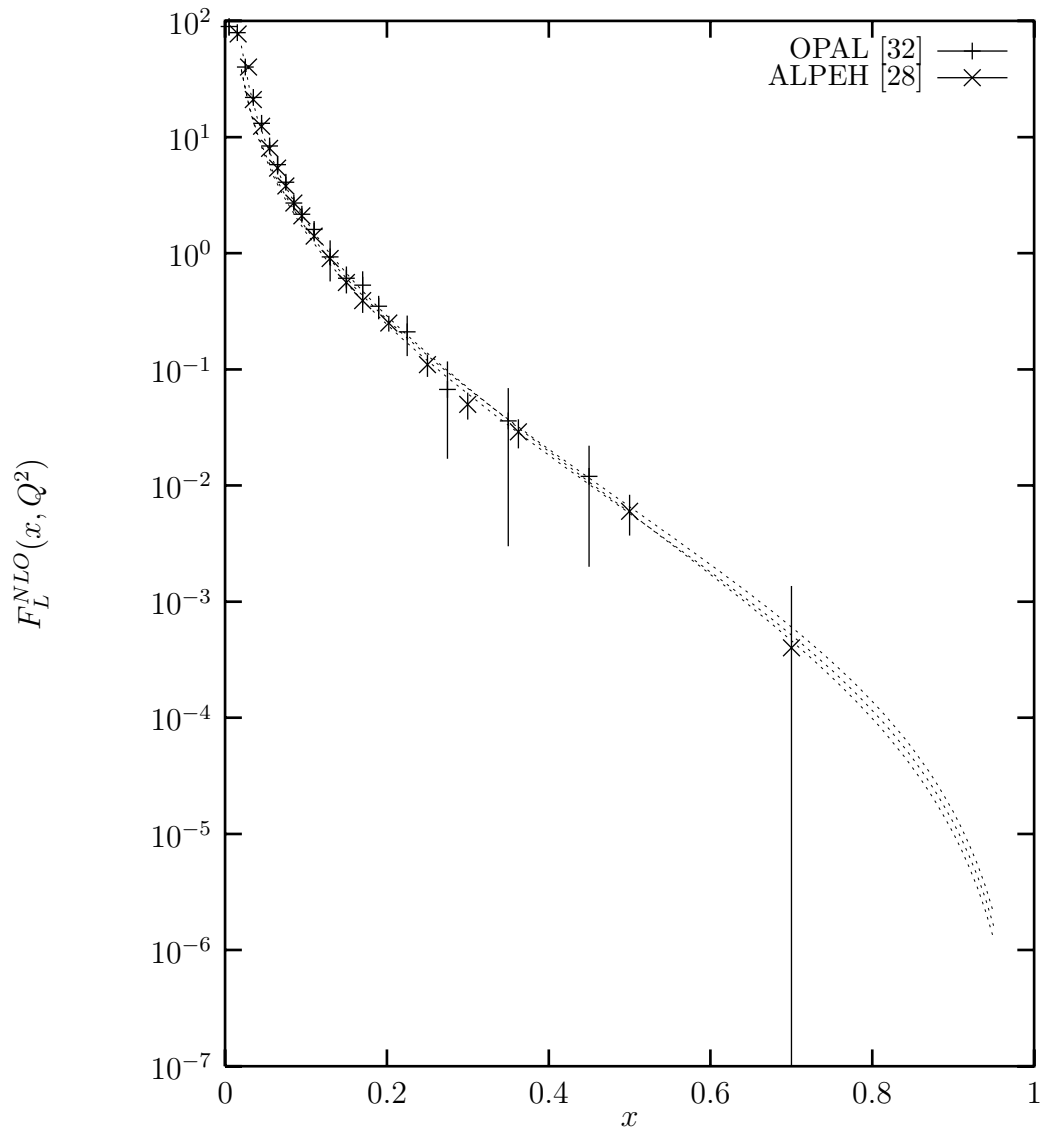


Fig. 18

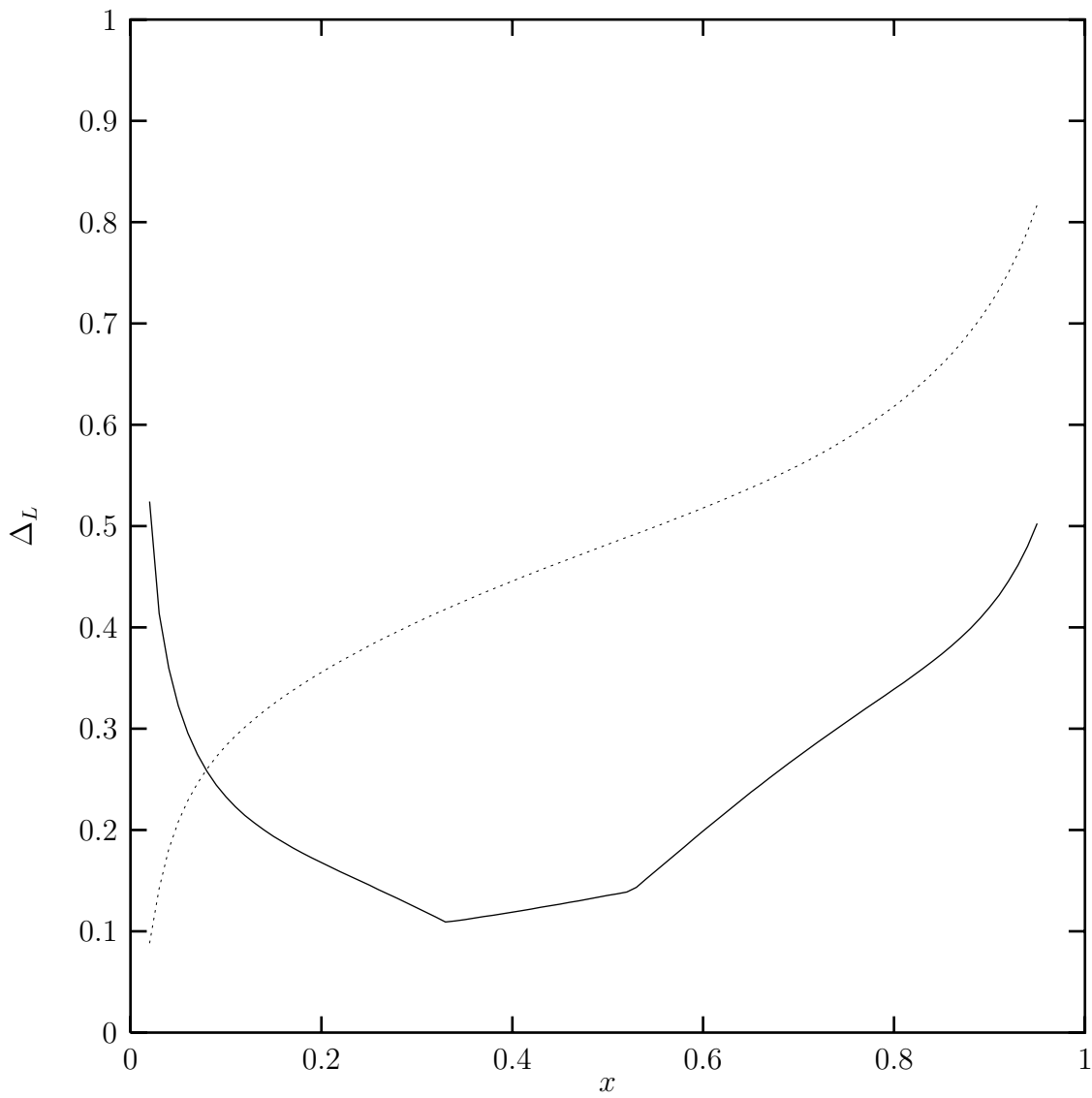


Fig. 19

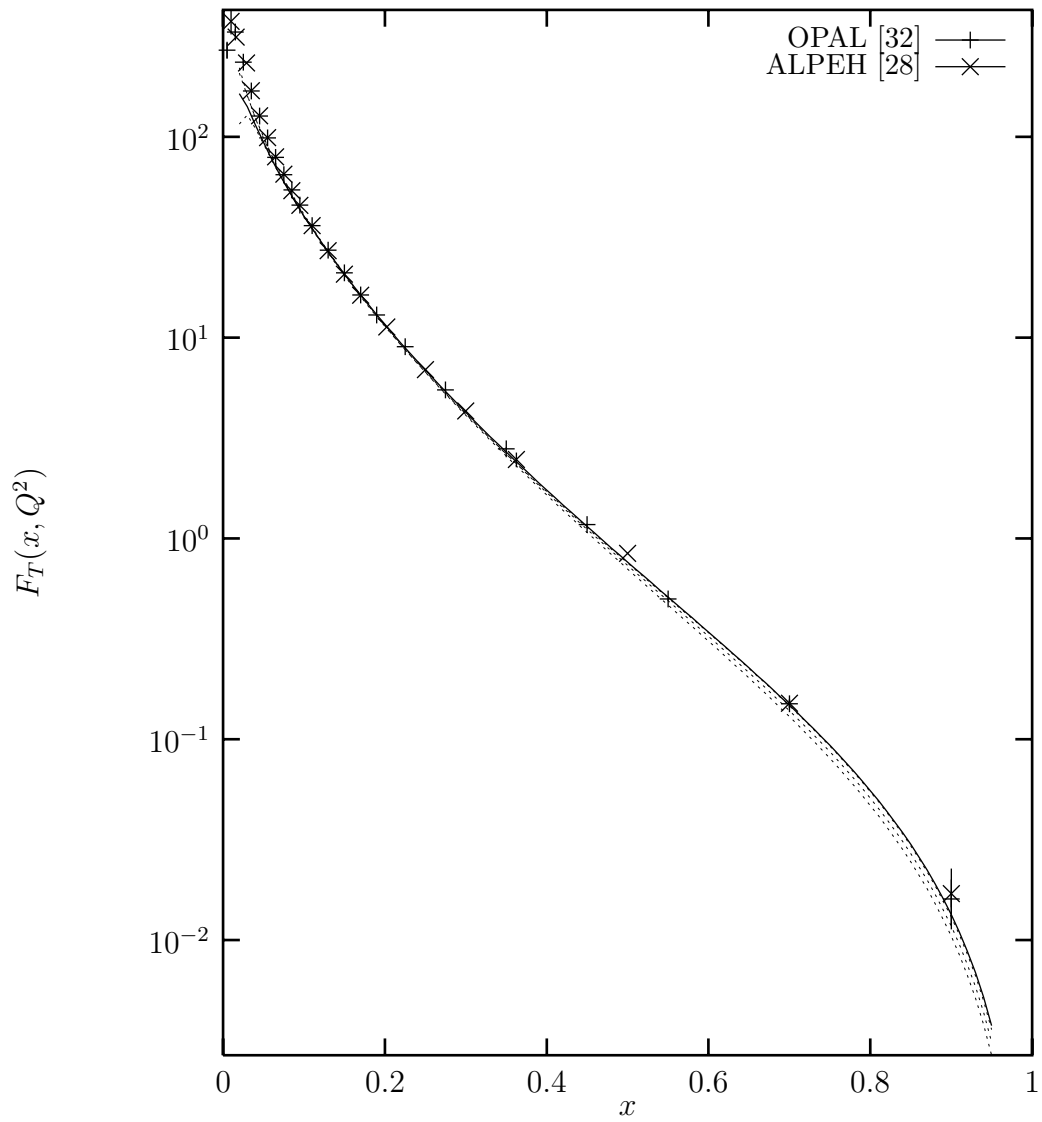


Fig. 20

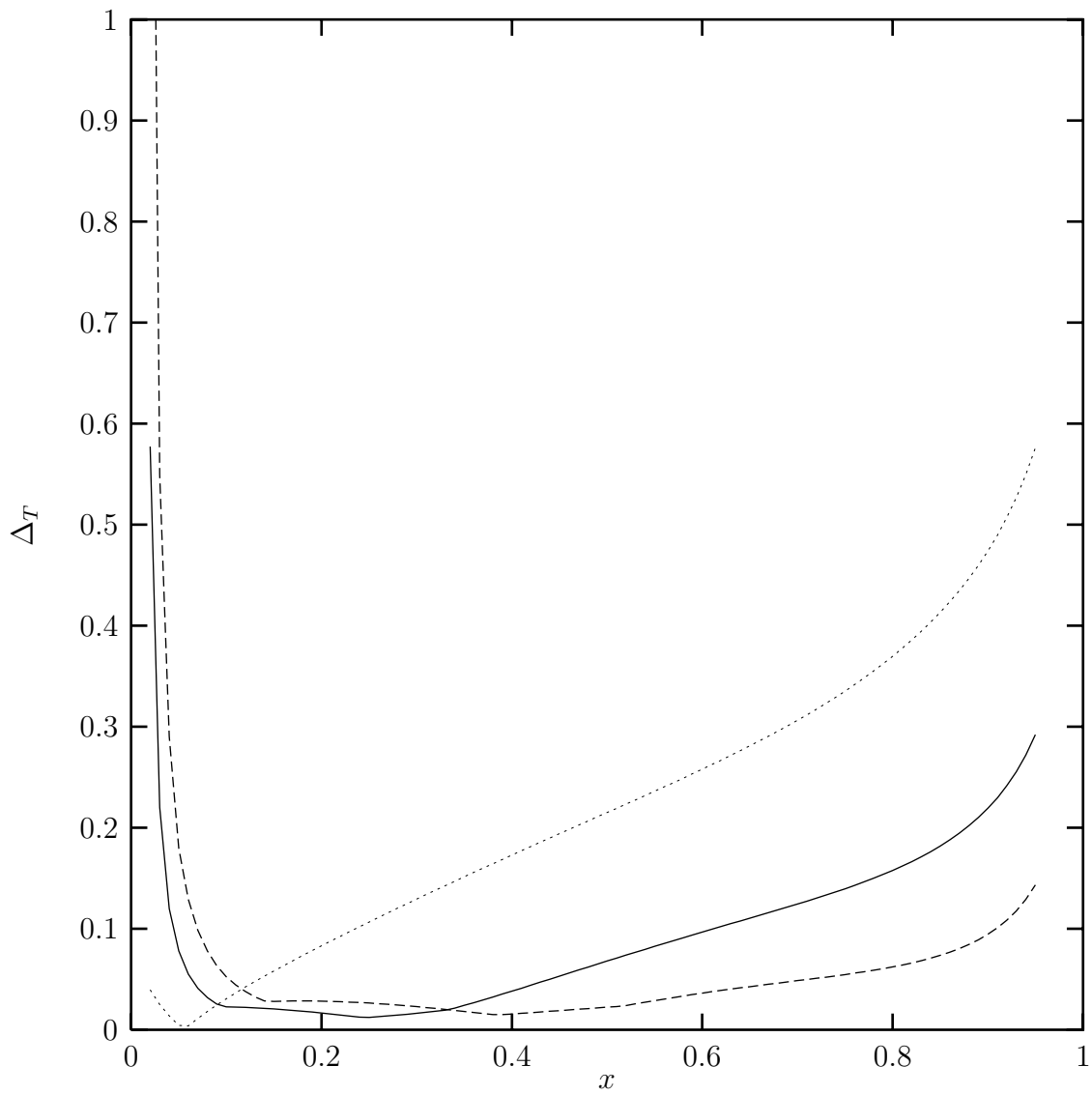


Fig. 21

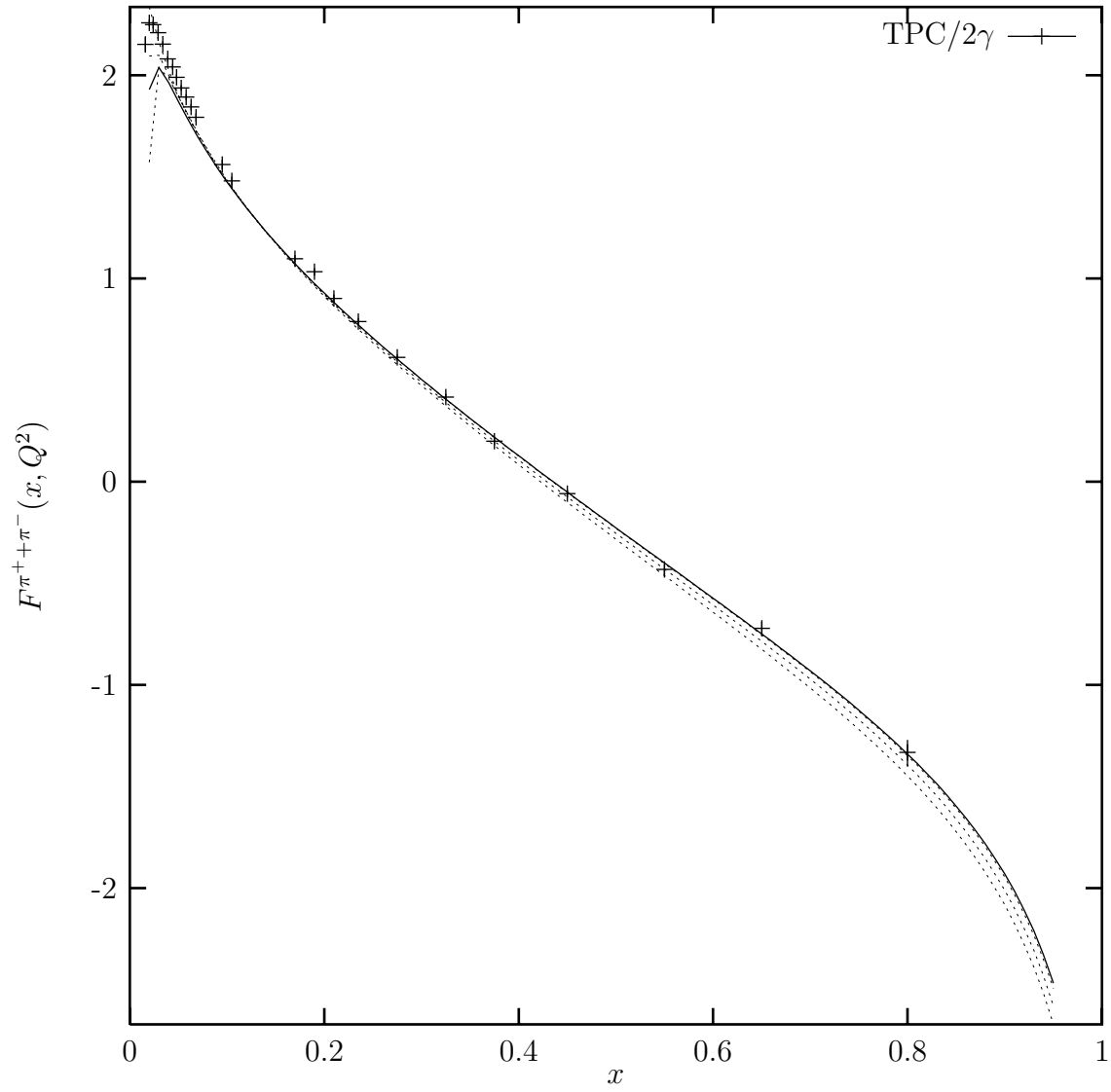


Fig. 22

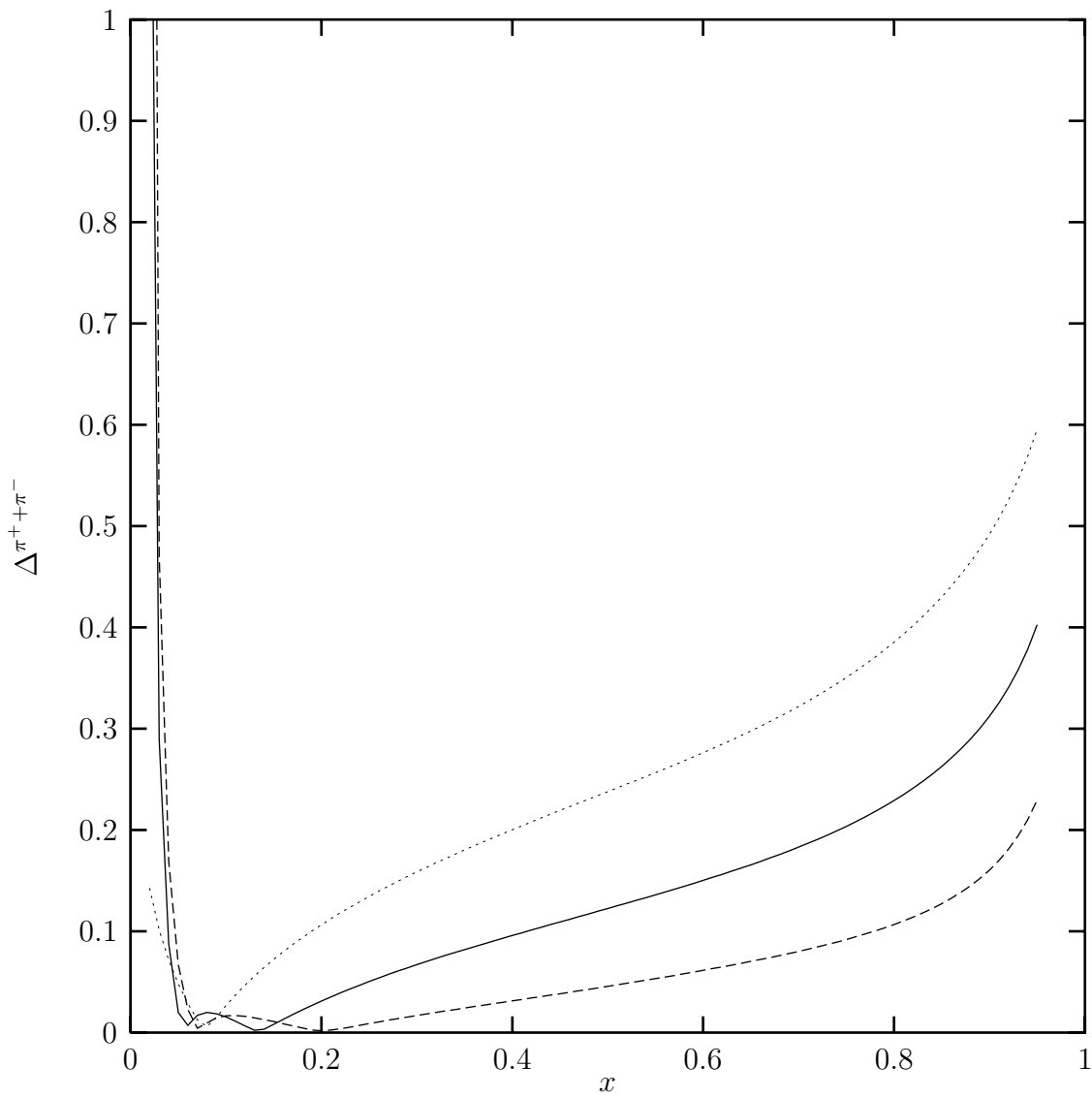


Fig. 23